2011

Nanoscale Drug Delivery Vehicles Based on Poly(ester amide)s

Gregory J. Zilinskas

Nanoscale Drug Delivery Vehicles Based on Poly(ester amide)s

(Spine title: Nanoscale Drug Delivery Vehicles Based on Poly(ester amide)s)
(Thesis Format: Integrated Article)

By

Gregory J. Žilinskas

Graduate Program in Biomedical Engineering

Submitted in partial fulfillment
of the requirements for the degree of
Master of Engineering Science

The School of Graduate and Postdoctoral Studies
University of Western Ontario
London, Ontario, Canada

October, 2011

THE UNIVERSITY OF WESTERN ONTARIO
SCHOOL OF GRADUATE AND POSTDOCTORAL STUDIES

CERTIFICATE OF EXAMINATION

Supervisor

Dr. Elizabeth R. Gillies

Supervisory Committee

Dr. Kibret Mequanint

Dr. Jesse Zhu

Examiners

Dr. Kibret Mequanint

Dr. Mel Usselman

Dr. Jin Zhang

The thesis by

Gregory J. Žilinskas

entitled:

Nanoscale Drug Delivery Vehicles Based on Poly(ester amide)s

is accepted in partial fulfillment of the
requirements for the degree of
Master of Engineering Science

Date

Chair of the Thesis Examination Board

Abstract

Poly(ester amide)s (PEA)s offer several properties superior to currently used systems such as fewer acidic degradation products and functional handles for the conjugation of bioactive molecules. Herein, two novel PEA based drug delivery systems were developed and evaluated. The first utilizes PEAs containing pendant carboxylic acid functional groups and was evaluated with respect to its ability to control the release of a model drug, a Rhodamine B derivative. The drug exhibited sustained release without a burst phase, demonstrating the utility of the carboxylic functional handles. A second drug delivery system was prepared utilizing novel poly(ethylene oxide)-PEA copolymers which formed into micelles. The resulting system was capable of encapsulating and releasing Nile Red, a model hydrophobic drug, on a pharmacologically relevant time scale. Overall, these results suggest that PEAs are excellent biomaterials, capable of delivering therapeutics and have the potential to overcome many of the deficiencies found in current delivery systems.

Key Words

Poly(ester amide), drug delivery vehicle, nanoparticle, sustained release, micelle

Table of Contents

CERTIFICATE OF EXAMINATION ..... **II**
ABSTRACT ..... **III**
TABLE OF CONTENTS ..... **IV**
LIST OF FIGURES ..... **VII**
LIST OF SCHEMES ..... **VIII**
LIST OF TABLES ..... **VIII**
LIST OF ABBREVIATIONS ..... **IX**
CHAPTER ONE: INTRODUCTION **1**
1.1 DRUG DELIVERY 1
1.2 RENAL CLEARANCE 2
1.3 RETICULOENDOTHELIAL SYSTEM 3
1.4 TARGETING 4
1.4.1 Passive Targeting 4
1.4.2 Active Targeting 5
1.5 REVIEW OF CURRENT DRUG DELIVERY SYSTEMS 9
1.5.1 Polymeric nanoparticles 10
1.5.2 Micellar drug delivery systems 16
1.6 POLY(ESTER AMIDE)S 19
1.6.1 Biomedical Uses of Poly(ester amide)s 23
1.7 THESIS GOALS 25
1.8 REFERENCES 28
CHAPTER TWO: COVALENT IMMOBILIZATION OF DRUG MOLECULES IN POLY(ESTER AMIDE) NANOPARTICLES **36**
2.1 INTRODUCTION 36
2.2 RESULTS AND DISCUSSION 39
2.2.1 Synthesis of Polymers without Pendant Functional Groups 39
2.2.2 Optimization of the Nanoparticle Preparation Procedure 40
2.2.3 Synthesis of Polymers with Pendant Functional Groups 44
2.2.4 Preparation of Nanoparticles Containing Covalently Immobilized Model Drug 45
2.2.5 Characterization and Application of the Nanoparticles 48
2.3 CONCLUSIONS 52
2.4 EXPERIMENTAL 53
2.4.0 General Procedure and Methods 53
2.4.1 Procedure for Solution Polymerizations of Poly(ester amide)s without Pendant Functional Groups 54

2.4.2 Procedure for Interfacial Polymerizations of Poly(ester amide)s without Pendant Functional Groups 54
2.4.3 Procedure for Solution Polymerizations of Functional Poly(ester amide)s 56
2.4.4 Procedure for Interfacial Polymerizations of Functional Poly(ester amide)s 57
2.4.5 General Procedure for Rhodamine Derivative Coupling to PEAs 58
2.4.6 Nanoparticle Formation Procedure 60
2.4.7 Determination of Dye Loading 60
2.4.8 Covalently Immobilized Nanoparticle Release Study Procedure 61
2.4.9 Physically Encapsulated Nanoparticle Release Study Procedure 61
2.5 REFERENCES 62

CHAPTER THREE: DEVELOPMENT OF POLY(ETHYLENE OXIDE)-POLY(ESTER AMIDE) GRAFT COPOLYMERS FOR MICELLAR DRUG DELIVERY VEHICLES 64

3.1 INTRODUCTION 64
3.2 RESULTS AND DISCUSSION 66
3.2.1 Synthesis of PEO-PEA graft copolymers 66
3.2.2 Preparation of micelles 73
3.2.3 Effect of PEO Loading on Micelle Formation 74
3.2.4 Further Characterization and Release 77
3.3 CONCLUSIONS 82
3.4 EXPERIMENTAL 83
3.4.0 General Procedure and Methods 83
3.4.1 Synthesis of Polymer **4** 84
3.4.2 Synthesis of Polymer **5** 85
3.4.3 Synthesis of Activated Poly(ethylene oxide) (MW=5,000 g/mol) **6** 85
3.4.4 Synthesis of Activated Poly(ethylene oxide) (MW=2000 g/mol) **7** 86
3.4.5 Synthesis of PEO-PEA Copolymer **8** 86
3.4.6 Synthesis of PEO-PEA Copolymer **9** 87
3.4.7 Poly(ester amide)-co-poly(ethylene glycol) using 3.0 eq of 5000 g/mol PEG, **10** 88
3.4.8 Poly(ester amide)-co-poly(ethylene glycol) using 1.2 eq of 2000g/mol PEG, **11** 89
3.4.9 Micelle Formation 90
3.4.10 Determination of CAC 90
3.4.11 MTT Procedure 91
3.4.12 Encapsulation and Release of Nile Red 91
3.4.13 Hydrolytic Degradation of Micelles 92
3.4.14 TEM Sample Preparation 93
3.5 REFERENCES 94

CHAPTER FOUR: CONCLUSION 95

4.1 THESIS SUMMARY 95
4.2 FUTURE WORK 97

4.2.1 Covalent Immobilization of Drug Molecules in Poly(ester amide) Nanoparticles 97
4.2.2 Development of Poly(ethylene oxide)-Poly(ester amide) Graft Copolymers for Micellar Drug Delivery Vehicles 98
4.2.3 Combination of Projects 98
4.3 REFERENCES 99
CURRICULUM VITAE 100

List of Figures

Figure 1.1: Encapsulation can keep drug concentrations within the therapeutic range while reducing the number of injections relative to traditional free drug delivery methods. 2
Figure 1.2: General structure of the poly(ester amide). 21
Figure 1.3: Two Approaches to PEA Drug Delivery Vehicles. 26
Figure 2.1: Diagram of covalently immobilized PEA drug delivery system. 38
Figure 2.2: Structures of PEAs without pendant functional groups. 39
Figure 2.3: General oil in water nanoparticle formation procedure. 40
Figure 2.4: An investigation of the effect of [PEA] on particle diameter shows that the particles are smaller at lower [PEA]. However, at very low concentrations no particles are formed. 41
Figure 2.5: An investigation of the effect of [PVA] on particle diameter shows that as the [PVA] is increased, the particle size decreases. 42
Figure 2.6: An investigation of the effect of oil/water ratio on particle diameter does not show an effect on particle size. Note that particles do not form at higher ratios. 43
Figure 2.7: DLS trace of NP from polymer 6. Note that the x axis is in a logarithmic scale. 44
Figure 2.8: Structures of functionalized PEAs. Each PEA contains approximately 10 mol% of the aspartic acid unit randomly distributed throughout the polymer backbone. 45
Figure 2.9: Structure of the chosen model drug, an alcohol functionalized Rhodamine B derivative. 46
Figure 2.10: DLS trace of NP formed from dye-conjugated polymer 6. Note that the x axis is in a logarithmic scale. 46
Figure 2.11: Effect of polymer choice on release rates of covalently immobilized Rhodamine. 48
Figure 2.13: Long time frame release of covalently immobilized Rhodamine. 50
Figure 2.14: DLS trace showing no change in particle diameter after lyophilization and reconstitution. Note that the x axis is in a ogarithmic scale. 51
Figure 2.15: MTT assay displaying low PEA NP toxicity. 52
Figure 3.1: Structure of PEA with pendant amines. 66
Figure 3.2: GPC trace of polymer 9 after dialysis. PEO visible as longer elution time side peak. 71
Figure 3.3: GPC trace of copolymer 9 after preparative GPC displaying effective removal of PEO. 72
Figure 3.4: DLS traces for self assemblies formed from copolymers 8 to 11. 75
Figure 3.5: TEM images for self assemblies formed from copolymer 8 to 11. 76
Figure 3.6: Structure of the chosen model drug, Nile Red. 78
Figure 3.7: Graph displaying results of CAC experiment. Florescence was observed at all concentrations. 79
Figure 3.8: MTT cell viability study showing no cell toxicity. 80

Figure 3.9: Comparing Nile Red release from micelles at varying pHs. 81
Figure 3.10: GPC micelle degradation study indicating that the copolymer breaks down under physiological conditions. 82

List of Schemes

Scheme 3.1: Interfacial polymerization reaction conditions 67
Scheme 3.2: Deprotection of PEA. 68
Scheme 3.3: Activating PEO with 4-nitrophenyl chloroformate 69
Scheme 3.4: Synthesis of PEO-PEA graft copolymers 70

List of Tables

Table 3.1: Effect of PEO loading on polymer 73
Table 3.2: Effect of PEO loading on micelles 74

List of Abbreviations

MTT	3-(4,5-Dimethylthiazol-2-yl)-2,5-diphenyltetrazolium bromide
TAM	4-amino-2,2,6,6-tetramethylpiperidine-1-oxy
DMAP	4-dimethylaminopyridine
AmB	amphotericin B
CAC	critical aggregation concentration
DHT	dihydrotestosterone
DIPEA	diisopropylethylamine
DMSO	dimethylsulfoxide
DOX	doxorubicin
DLS	dynamic Light Scattering
EPR	enhanced permeability and retention
EGFR	epidermal growth factor receptor
EGCG	epigallocatechin gallate
FR	folate receptor
GPC	gel permeation chromatography
HER-2	human epidermal receptor-2
HER	human epidermal receptors
IR	infrared
MMP	matrix metalloproteinase receptor
MW	molecular weight
MWCO	molecular weight cut off
MDR	multidrug resistance
DCC	N,N'-Dicyclohexylcarbodiimide
DMA	N,N-dimethylacetamide
NP	nanoparticle
NMR	nuclear magnetic resonance
PEO	poly(ethylene oxide)
PEO 2K	poly(ethylene oxide) of molecular weight 2000 g/mol
PEO 5K	poly(ethylene oxide) of molecular weight 5000 g/mol
P-gp	p-glycoprotein
PAA	poly(acrylic acid)
PCL	poly(caprolactone)
PEA	poly(ester amide)
PEG	poly(ethylene glycol)
PEO	poly(ethylene oxide)
PLA	poly(lactic acid)
PLGA	poly(lactic-co-glycolic acid)
PPO	poly(propylene oxide)
PVA	poly(vinyl alcohol)
PCL	poly(caprolactone)
PDI	polydispersity index
RES	reticuloendothelial system

SEM	scanning electron microscopy
siRNA	small interfering ribonucleic acid
TPP	sodium tripolyphosphate
TPGS	tocopheryll poly(ethylene glycol) succinate
TEM	transmission electron microscopy
UV-Vis	ultraviolet-visible
VCAM-1	vascular cell adhesion molecule-1
VEGFR	vascular endothelial growth factor receptor

Chapter One:

Introduction

1.1 Drug Delivery

Recently the pharmaceutical and biotechnology industries have developed a wide array of drug candidates. While many of these therapeutics have remarkable potential, they remain ineffective unless they can be successfully delivered. The successful clinical application of these formulations requires an engineering approach, which addresses drug stability, administration, absorption, metabolism and bioavailability at the target site, however, many currently used systems are inadequate in one or more of these factors.[1] Problems such as low drug solubility[2] and rapid renal clearance[3] affect bioavailability, while the harsh *in vivo* conditions may cause loss of bioactivity.[4] Some therapeutics, such as protein drugs, are particularly susceptible to many of these factors, making them difficult to deliver via oral administration,[3,5] the most convenient mode of drug delivery, due to its ease of use and high patient compliance.[6] In order to maintain bioactivity of these susceptible drugs, administration via the parenteral route may be necessary.[7] An attractive method to minimizing discomfort and improving patient compliance is to develop sustained-release formulations with well defined release kinetics. A slower release rate will reduce the number of injections a patient will require, as long as stability is unaffected, and delivery of drugs with narrow therapeutic windows is safer and more convenient when delivered through a system with well defined kinetics. As seen in Figure 1.1, when delivering via a traditional free drug approach, the concentration of drug within the blood may vary significantly over time. The concentration can fall above or below the

therapeutic range due to issues such as poor patient compliance. In contrast, by employing a sustained release vehicle, the rate of drug release can be optimized to stay within the therapeutic range and less frequent dosing is required. Another benefit of using a delivery system is the potential to target certain tissues. Particles circulating for extended periods can accumulate in cancerous tissues while particles decorated with targeting moieties may greatly increase local concentrations of drugs while having minimal effect on other tissues.[6] Nanoscale systems offer a promising means of overcoming many issues arising in drug delivery which are discussed in detail below.

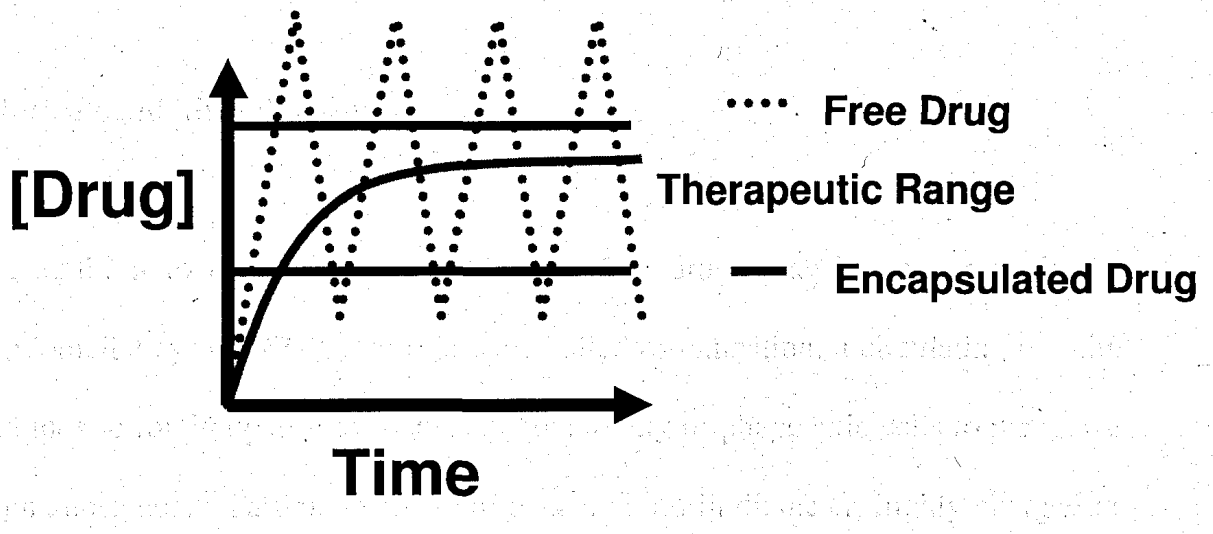

Figure 1.1: Encapsulation can keep drug concentrations within the therapeutic range while reducing the number of injections relative to traditional free drug delivery methods.

1.2 Renal Clearance

As blood circulates, it passes through the kidneys where the glomerulus filters out solutes, waste products, and excess water.[8] The epithelial cell coating of the glomerulus

contains pores ranging in size from 4 nm to 14 nm; thus, circulating macromolecules with hydrodynamic radii smaller than the glomerular pores will permeate the membrane and be excreted. Polymers with hydrodynamic radii small enough to permeate, tend to have molecular weights (MW)s between 30000 and 50000 g/mol[9] though this range is an estimate as shape, flexibility and polymer chemistry can have a large effect on hydrodynamic radius. Many current pharmaceuticals are well below this MW range and are readily excreted, reducing their circulation time and biological activity. By encapsulating a drug within a nanoparticle (NP), renal clearance can be avoided, greatly enhancing the drug's circulation time and thus potentially the therapeutic efficacy.[8]

1.3 Reticuloendothelial System

In addition to clearance by the kidneys, free drugs may be removed via the reticuloendothelial system (RES). In a process called opsonization, a circulating protein, opsonin, binds to foreign particles, increasing the ability of phagocytic cells to recognize the foreign substance.[10] Particles which are over 200 nm in diameter, highly charged or hydrophobic particles are highly susceptible to opsonin binding and removal via the RES. Once bound by opsonin, the liver and spleen can more effectively remove these circulating particles or phagocytic cells can break them down to be removed by the lymphatic system.[9]

1.4 Targeting

Nanoscale drug delivery systems can achieve tumour targeting through two mechanisms: passive and active targeting. Passive targeting involves the prolonged circulation of the carrier and its preferential accumulation in cancerous tissue. In contrast, active targeting requires incorporated ligands on the nanocarrier surface which bind specifically to receptors on a certain cell type's surface, thereby promoting nanocarrier-cell interaction and cellular internalization. The two methods of targeting are described in detail below.

1.4.1 Passive Targeting

Cancerous tissue requires an ever-increasing supply of nutrition and oxygen to meet the requirements of its rapid growth. As a result, the neovasculature of cancerous tissue greatly differs from that found in healthy tissue- a dichotomy which is visible through variation in shape, excessive dilation, poor alignment, disorganization and the presence of large fenestrations.[9] In addition, perivascular cells and the basement membrane in the vascular wall tend to be either absent or abnormal in cancerous tissue. These anatomical defects present in the tumor vasculature promote extensive leakage of circulating blood components into the tumor. Along with this blood, circulating macromolecules in the size range of 20 nm to 200 nm have been shown to preferentially extravasate into the cancerous tissue.[1,9,11,12] Once macromolecules have permeated into

the interstitium, the ill-defined lymphatic network in the tumor is unable to effectively remove them, causing the local concentration to rise by as much as 50 times.[9] The abnormally high levels of extravasation, coupled with the below average venous return and poor lymphatic clearance, result in the accumulation of macromolecules within the tumor interstitium. This phenomenon has been termed the enhanced permeability and retention (EPR) effect. It is important to note that the EPR effect does not apply to free drugs with low molecular weights because they diffuse rapidly back into the circulating blood and are highly affected by renal filtration, which removes them from the blood before they have time to accumulate.

1.4.2 Active Targeting

As there is no direct interaction between a nanoscale delivery system and cancerous tissue during the passive targeting of the EPR effect, the penetration of the carrier is limited.[13] In order to increase cell penetration, attaching targeting ligands to the carrier surface is an attractive option. The practice of active targeting is based primarily on:[13]

i) the overexpression of specific antigenic receptors on the surface of cancer cells relative to cells in normal tissues,

ii) the specificity and high binding affinity of targeting ligands to receptors,

iii) the intracellular delivery possible by cell mediated endocytosis via the ligand-receptor interaction.

Although targeting of cancer cells is a wide field, with a variety of different approaches, two of the most important targeting modalities are angiogenesis and uncontrolled cell proliferation.

Angiogenesis is characterized by the invasion, migration and proliferation of smooth muscle and endothelial cells.[14] These cells then degrade the basement membrane and form a new lumen structure. Tumour cells infiltrate the newly developed lumen structure and secrete a variety of proangiogenic factors[15] and once adequately vascularized, the cancer may translate into a metastatic form and spread to other parts of the body.[16] By attacking the growth of the blood supply, the abnormally high blood requirement can be exploited to limit the metastatic capabilities and size of tumours.[17] This angiogenic approach offers many advantages over traditional therapies:[13,18]

i) destroying the vasculature decreases the growth and metastatic capabilities of the tumour,

ii) neovascular endothelial cells are less able to undergo phenotypic variations, diminishing secondarily acquired drug resistance found in conventional cancer therapies,

iii) the tumour vasculature is not specific for the type of cancer.

The main angiogenic targets explored by NP systems for therapeutic benefit include: the vascular endothelial growth factor receptors (VEGFR)s,[19] $\alpha v\beta 3$ integrins,[13] matrix metalloproteinase receptors (MMP)s,[20] and vascular cell adhesion molecule-1 (VCAM-1).[21]

Alternately, cell proliferation markers are excellent targets for cancer therapeutics as many are over-expressed on tumour cells. NPs can be actively targeted by the incorporation of monoclonal antibodies to target cell proliferation receptors.[22] The four basic targeting criteria of monoclonal antibodies for cancer therapeutic application are:[13]

i) the antigen of interest is over-expressed by tumour cells,

ii) the antigen participates as a principle component in the progression of the disease,

iii) the antigen is stable in its present form upon the tumour cell surface,

iv) the antigen is expressed by a large percentage of tumour cells and a large variety of tumours.

Uncontrolled cell proliferation targets tend to be used more regularly by actively targeting NPs. The most established targets include: human epidermal receptors (HER), transferrin receptors, and folate receptors.

The HER family of receptor tyrosine kinases contains two highly upregulated targets on tumour cell surfaces, epidermal growth factor receptor (EGFR) and human epidermal receptor-2 (HER-2). Both are known to mediate a cell signaling pathway for growth and proliferation in response to the binding of the growth factor ligand and are among the most heavily researched proliferation targets.[23] Clinical studies using monoclonal antibody blockade and EGFR tyrosine kinase inhibitors have suggested that EGFR blockade is a well-tolerated and effective treatment strategy.[24-27]

Both metastatic and drug resistant cells have an elevated number of transferrin receptors relative to healthy cells, making it a pertinent target for cancer therapeutics.[28] Transferrin is a serum, non-heme, iron-binding glycoprotein that helps transport iron to proliferating cells.[28] In order to dissociate the iron, transferrin binds to the transferrin receptors on the cell surface, becomes endocytosed and iron is released due to the lower pH inside the cell. The transferrin receptor is overexpressed in malignant cells due to the increased iron requirement to fuel the uncontrolled growth of cancerous tissue.[29] Transferrin receptor targeting for cancer therapeutics has been successfully used in human clinical trials with adriamycin,[30] cisplatin,[31] and diphtheria toxin.[32]

The folate receptor (FR) is a 38 kDa glycoprotein and is one of the most highly researched targets for cancer treatment.[33-36] Folic acid, also known as vitamin B9, is necessary for the synthesis of biologically important molecules such as purines and pyrimidines[37] and since mammalian cells are unable to synthesize this vitamin, it must be internalized.[38] For non-malignant cells, the reduced-folate carrier is highly specific for reduced forms of this vitamin, such as 5-methyl-tetrahydrofolate[39] but there remains debate regarding the specificity of the transport of other folate conjugates.[13,40-42] It is possible to design folate-linked pharmaceuticals that only enter cells via an alternative route, the FR, which is highly expressed in cancer cells, activated macrophages, the placenta, and the apical surfaces of some polarized epithelia.[40,43,44] Fortunately, the FR is significantly upregulated on many cancer cells, in some cases by two orders of magnitude relative to healthy tissue.[38] In addition, folate ligands are attractive because they are inexpensive, non-toxic, non-immunogenic, relatively easy to conjugate to carriers, retain high binding affinity, and are relatively stable in both storage and circulation.[38]

Another advantage of active targeting is the potential to suppress the multidrug resistance (MDR) condition in which tumours develop resistance to a range of anticancer chemotherapeutics.[45] It has been shown that one method through which breast and ovarian tumours develop resistance is the overexpression of the p-glycoprotein (P-gp) transporter efflux pumps.[45] This adenosine triphosphate-dependant efflux pump removes chemotherapeutic agents from the cell, greatly decreasing the therapeutic efficacy of the treatment.[46] A wide selection of commonly used drugs such as: paclitaxel, doxorubicin (DOX), and vinblastine are removed from cells by these pumps.[12] However, the route of entry into a cell by an actively targeted nanocarrier is receptor-mediated endocytosis which will circumvent the P-gp efflux, thereby increasing overall therapeutic efficacy.[47,48]

1.5 Review of Current Drug Delivery Systems

The utility of nanocarriers may be seen by their potential to improve the therapeutic index of their payloads by increasing drug efficacy, lowering drug toxicity, and achieving steady state therapeutic levels of drugs over an extended period of time.[49] They can also improve drug solubility and drug stability, which allows for the development of new drugs that could not have been used previously due to pharmacokinetic or biochemical constraints. To date, the most commonly researched nanoscale delivery devices include: polymeric NPs,[50-55] dendrimers,[56-67] nanoshells,[68-72] liposomes,[28,33,34,47,48,73-75] micelles,[76-79] nucleic acid-based NPs,[80-83] magnetic NPs,[66,84-88] and viral NPs.[89-91] The utility of these nanotechnologies is becoming increasingly

recognized and several examples of first generation nanocarriers have been approved by the Food and Drug Administration for therapeutic and diagnostic applications. Of particular note are: Abraxane, an albumin-bound particle form of paclitaxel,[92] Doxil, a PEGylated liposome carrier for DOX,[93] DaunoXome, a liposomal formulation of daunorubicin[94] and Feridex, a superparamagnetic iron oxide magnetic resonance imaging contrast agent.[95] As the utility of these approved therapeutic and diagnostic tools becomes more evident, and more research is done in optimizing their properties, new tools will emerge and become approved for use in vivo.

1.5.1 Polymeric nanoparticles

One of the most influential works on polymer NPs written by Langer et al., was published in Science in 1994 and has been cited almost 1,200 times.[96] This article outlines the desired features of nanoscale carrier including: (i) that the agent to be encapsulated comprises a reasonably high weight fraction (loading) of the total carrier system (for example, more than 30%), (ii) that the amount of agent used in the first step of the encapsulation process is incorporated into the final carrier (entrapment efficiency) at a reasonably high level (for example, more than 80%), (iii) the ability to be freeze-dried and reconstituted in solution without aggregation, (iv) biodegradability, (v) small size (less than 5 μm), and (vi) characteristics to prevent rapid clearance of the particles from the bloodstream. The particles they created to meet all these criteria were core-shell NPs made from either poly(lactic-co-glycolic acid) (PLGA), poly(caprolactone) (PCL), and copolymers of these two. The chemical composition and polymer molecular weight

were varied and degradation time and release kinetics were varied accordingly. The shell material for all particles studied was poly(ethylene glycol) (PEG). Particles were made by forming an oil in water emulsion with subsequent solvent evaporation. The resulting particles could be stored, without preservatives, by lyophilization and later redispersed. Characterization by atomic force microscopy and quasi-elastic light scattering revealed monodisperse, spherical particles of mean diameter 140 nm. In vivo studies showed that decreasing PEG loading significantly reduced the circulation time. A model drug lidocaine, a local anesthetic known to block sodium channels in axons,[97] was shown to have a loading of 45% and an entrapment efficiency of over 95%. An important discovery came from the realization that high drug loadings actually produced slower release rates. This is counter-intuitive as a higher concentration gradient should cause a more rapid release. The group hypothesized that higher loadings induced drug crystallization within the NP. The phase separation requires drug dissolution and then subsequent diffusion from the particle. The hypothesis was supported by calorimetric and x-ray diffraction studies. It was proposed that possible uses for the NPs include: transferrin coupling to allow for endocytosis of a particle containing DNA, antibody coupling to the PEG end group forming highly specific, targetable entities to desired tissues, as well as the ubiquitous drug delivery and medical imaging applications.

Since Langer et al.'s article, much interest has been generated for PLGA due to its biocompatibility and commercial availability in different molecular weights and copolymer compositions that allow for precise tailoring of release properties and degradation.[98-101] The degradation products of PLGA are non-toxic as the polymer degrades first into its monomers, lactic and glycolic acid, which enter the Krebs' cycle,

are metabolized, and are subsequently eliminated from the body as carbon dioxide and water;[99] however, large accumulations of acidic species have been shown to cause tissue inflammation and the acidic degradation of the particles may damage the therapeutic payload.[102] Despite this drawback PLGA has been successfully implemented as a nanocarrier for anti-cancer agents (paclitaxel and DOX),[103,104] sex hormones (estradiol),[105,106] anti-leishmanial agents (amphotericin B),[107] immunosuppressants (cyclosporine),[108] and hyperlipidemia treatments (atorvastatin, sold under the name Lipitor).[109] In addition, PLGA has been shown to effectively encapsulate antioxidants such as coenzyme Q10,[110] curcumin,[111] epigallocatechin gallate (EGCG).[112] Combining drug and antioxidant payloads may help treat co-existing disease states and reduce drug induced toxicity.[113,114] Grama et al. created a library of PLGA NPs by encapsulating a wide variety of drugs, hormones and antioxidants. It was shown that the emulsion–diffusion–evaporation NP formation procedure was highly versatile and able to encapsulate all payloads under study with the exception of amphotericin B which was achieved by nanoprecipitation and DOX and EGCG where the double emulsion method was adopted.[115] It was also found that the entrapment of bioactives in NPs resulted in significantly higher bioavailability in all compounds compared to their respective conventional forms. One particular example was estradiol which demonstrated 1014% relative oral bioavailability compared to its simple suspension.[115] Additionally, the nanoparticulate formulation was able to sustain release over 192 h, in spite of the short half-life of parent molecule.[106]

Another traditionally used drug delivery platform is chitosan, a natural polysaccharide composed of β(1 → 4)-linked glucosamine units together with some

proportion of N-acetylglucosamine units. Chitosan occurs rarely in nature, but it is generally obtained by extensive deacetylation of chitin.[116] It exhibits excellent qualities for drug delivery applications such as biocompatibility, biodegradability, non-toxicity, mucoadhesivity and the important capacity to increase the penetration of drugs across mucosal barriers.[116] This penetration is beneficial for designing non-invasive routes of drug administration, such as oral, mucosal (nasal, pulmonary) and ocular routes. Several methods for obtaining chitosan NPs have been developed, and some of them, such as ionotropic gelation and complex coacervation, involve very mild preparation conditions. Ionotropic gelation consists of the ionic crosslinking of chitosan with multivalent counter-ions such as $Fe(CN)_6^{-4}$, $Fe(CN)_6^{-3}$, citrate and sodium tripolyphosphate (TPP). The NPs are obtained by the addition of a dilute chitosan acid solution to a solution of TPP with stirring. The size of the particles can be controlled by both chitosan and TPP concentrations and no organic solvents are needed.[117] This procedure has been frequently reported in the literature for the preparation of drug-loaded chitosan NPs. Chitosan particles prepared via ionotropic gelation have been shown to effectively deliver ammonium glycyrrhizinate,[118] proteins,[119] insulin,[120] and DOX.[121] The gelation process does have drawbacks as the dilute solutions required are inconvenient for scale up and poor time-stability of the resulting colloidal dispersion may require the addition of stabilizers. An alternate method, complex coacervation is achieved by mixing two oppositely charged polyelectrolytes. The polyelectrolyte complex separates into a polymer-rich phase that coexists with a very dilute phase. The polyelectrolyte complex produced forms an insoluble film or barrier that covers the particles. Hu et al. prepared chitosan–poly(acrylic acid) (PAA) NPs by the dropwise addition of dilute chitosan

solutions (0.02 wt%) into 0.002 wt% PAA aqueous solutions under magnetic stirring.[122] Hu et al. also prepared chitosan–PAA NPs by template polymerization of PAA in a chitosan solution at 70 °C using K2S2O8 as an initiator. After polymerization, aggregates were separated by filtration and the NPs in the supernatant solution were characterized. The hollow nanospheres obtained by this procedure were crosslinked with glutaraldehyde and loaded with DOX.[123] It was found that the drug-loading content was up to 4.3% and the particles were 118 nm in diameter. The NPs were also able to maintain DOX concentration in the blood for a longer time period relative to free drug. It has also been shown that chitosan NPs can encapsulate small interfering ribonucleic acid (siRNA) through complex coacervation of chitosan and polyguluronate. Encapsulation of siRNA is essential due to its rapid degradation and low intracellular association in vitro and in vivo. The siRNA-loaded chitosan-based NPs had mean diameters between 110 and 430 nm, and the diameter could be controlled depending on the weight ratio of chitosan and polyguluronate. The NPs showed low cytotoxicity and were useful in delivering siRNA to HEK 293FT and HeLa cells, effectively inhibiting the induction of targeting mRNA.[124]

It can be concluded that, both ionotropic gelation and complex coacervation are mild and useful procedures for obtaining NPs. It is necessary to start with very dilute solutions and to control the pH carefully during preparation, purification and storage to avoid aggregation.[116] The particles are versatile and biocompatible making them effective delivery vehicles although they are still hampered by acidic degradation products and a lack of functional handles.

Although targeted polymeric NPs remain a challenge, it is possible achieve selective delivery. Allémann *et al.* have investigated tumour delivery using Trastuzumab

targeted poly(lactic acid) NP and have found that they specifically and efficiently bind to cancer cells.[125] Similarly, Pan and Feng showed increased cell internalization with folate receptor-targeted paclitaxel-loaded NPs made with blends of poly(lactic acid)-co-tocopheryll poly(ethylene glycol) succinate (TPGS) and carboxylic acid-terminated TPGS on MCF-7 and C6 glioma cells.[126]

Although their size precludes them from the class of NPs, Guo *et al.* have developed microspheres of amino acid based poly(ester amide)s (PEAs) via an oil in water emulsion/solvent evaporation technique.[55] The effects of PEA polymer concentration, poly(vinyl alcohol) (PVA) emulsifier concentration, and the homogenizer speed on the size and morphology of final PEA microspheres were examined by analyzing their SEM images. It is found that a low PEA concentration, a high PVA concentration, and a high homogenizer speed are the optimal conditions for minimizing particle diameter. This method produced microspheres of approximately one micrometer diameter. The biodegradation behaviours of these microspheres were investigated and it was found that the degradation was largely based on surface erosion. The particles were also capable of encapsulating paclitaxel with high efficiency; however, the large particle size means they will be readily cleared by the RES and the lack of functional handles limits the possible uses of this system.

Unfortunately, one of the common limitations of many polymeric drug delivery systems is that they have burst release kinetics.[127-129] This burst effect is in most cases an undesirable effect where a large percentage of the drug is released in a short time period. The burst release tends to be unpredictable and may induce local toxicity. The short half-life of resulting drugs *in vivo* results in a loss of activity. Releasing too much drug at once

is economically and therapeutically wasteful, and the shortened release profile requires more frequent dosing. In some cases, such as flavours in the food industry and pulsatile delivery devices, burst may be desirable, but even in these cases the amount of drug released in the burst is hard to model and control.[130,131]

In order to address the burst release effect, several approaches have been taken. The most common approach has been to covalently immobilize the drug molecule within the particle via a biodegradable linkage to the polymer. One example of such a linkage is the covalent immobilization of DOX onto the terminal group of PLGA performed by Yoo *et al.*[129] The resulting conjugate could be formed into 350 nm nanospheres in a single oil in water emulsion and it was shown the particles released the DOX payload over the course of one month.[129] A novel method of removing the burst effect was undertaken by Tong and Cheng by using the drug-initiated, controlled, living polymerization of cyclic esters.[128] The hydroxyl groups on paclitaxel were incorporated into poly(lactide) via the site-specific polymerization of lactide mediated by either a zinc or magnesium complex. NP with diameters of less than 100 nm and low PDIs were formed through nanoprecipitation. The burst release was removed and the release of paclitaxel was significantly slowed. Unconjugated drug exhibited 75% release in one day and the conjugated system required six days to achieve the same release.

1.5.2 Micellar drug delivery systems

The use of block copolymers in drug delivery was first proposed by Ringsdorf et al. in the early 1980s.[132] The basis of these systems is that block copolymers with large

solubility differences between hydrophilic and hydrophobic segments will assemble in aqueous media into polymeric micelles with a nanoscopic size range with fairly narrow size distributions.[76,133-135] These micelles are characterized by their unique core–shell architecture where hydrophobic segments are segregated from the aqueous exterior to form an inner core surrounded by hydrophilic segments. Hydrophobic payloads can be encapsulated within this core and will be slowly released by diffusion. The encapsulation and slow diffusion out of micelles can be utilized for drug delivery applications; however, it is imperative that the drug delivery carrier be formed from a biocompatible polymer.[136] The selection of core-forming blocks tends to be limited to a few polymers such as poly(propylene oxide) (PPO),[137] poly (γ-benzyl-L-glutamate) (PBLG),[138] poly(caprolactone) (PCL),[138,139] poly(lactic acid) (PLA),[140,141] and poly (D,L-lactide) (PDLLA).[142] The encapsulation efficiency of the micelle system is strongly dependent on the payload/core interaction and increasing the number of available polymers will increase the variety and effectiveness of nanocarrier delivery systems. Although therapeutically useful as discussed below, these commonly used core-forming polymers lack functional handles, which limits their utility.

One core-forming polymer that has shown particular utility is PCL, in part due to possessing relatively more hydrophobic character than other core forming polymers.[143] This utility was exemplified by Allen et al. by encapsulating FK506, otherwise known as tacrolimus, and L-685,818 which had been previously difficult to deliver. These neurotrophic agents are used in the treatment of neurodegenerative diseases. The degree of neurite-like outgrowth achieved in cell cultures investigated was less than that obtained when the cells were treated with free FK506 or L-685,81, meaning that work

still must be undertaken in order to optimize this delivery system. In addition, large aggregates formed during micellation, necessitating filtering prior to use. In a separate publication, Allen et al. made use of a stronger payload/core interaction and formed a very effective delivery system for dihydrotestosterone (DHT) using poly(caprolactone)-b-poly(ethylene oxide) micelles.[144] The release profile of the drug from the micelle solution was found to be a slow steady release, which continued over a one-month period. The biological activity of the micelle-incorporated DHT was found to be fully retained and the drug loading was an impressive 240%.

Another commonly used class of polymers for micelle formation are poloxamers (trade name Pluronics). Poloxamers are non-ionic, triblock copolymers formed from a hydrophobic PPO block flanked by two poly(ethylene oxide) (PEO) blocks. This class of polymers self-assemble without additional surfactants since the PEO blocks are already incorporated. Variation of the molecular characteristics such as PPO/PEO ratio and molecular weight of the copolymers allows for fine control over the physical properties of the system. As a result, poloxamers are an important class of surfactants which have found widespread industrial applications in detergency, dispersion stabilization, foaming, emulsification, and lubrication[145] along with more specialized applications in pharmaceutics, bioprocessing, and separations.[146-149] Poloxamers have shown promise in avoiding multidrug resistance as well as the potential to cross the blood brain barrier.[150] The versatility of this system has been well established by encapsulating a range of therapeutics into poloxamers of varying MW. For example P105 has been shown to effectively encapsulate ruboxyl,[151] and DOX[151,152] while P85 displayed similar results[153,154] with daunorubicin, DOX, vinblastine, mitomycin C, cisplatin, and taxol.

Another class of versatile polymers used in micelle preparations are the poly(ethylene oxide)-b-poly(L-amino acid)s. Physical encapsulation is one means of loading this class of polymer as seen in Lavasanifar et al.'s work were poly(ethylene oxide)-b-poly(N-hexylstearate-L-aspartamide) micelles physically entrapped amphotericin B (AmB), a potent antifungal agent.[153] The 20 nm micelles resulted in reduced hemolytic activity compared with free AmB. The drug loading was only 1%; however, the authors claim that this loading is clinically relevant for use in humans for systemic fungal diseases. In addition to physical encapsulation, poly(ethylene oxide)-b-poly(L-amino acid)s are appealing as they may facilitate chemical modification post-polymerization through the repeating amino acid, as exemplified by Yokoyama et al. conjugating DOX to a poly(ethylene oxide)-poly(aspartic acid) block copolymer.[154] This class of polymers is relatively non-toxic and may biodegrade through hydrolysis and/or enzymatic degradation, though the extent of biodegradability remains to be established.[150]

1.6 Poly(ester amide)s

PEAs are a class of polymers characterized by both amide and ester bonds in the polymer backbone. PEAs emulate poly(esters) in that they offer a degree of control over both the mechanical and thermal properties as well as their rates of degradation. The incorporation of amide linkages increases the ability to tune the chemical and physical properties and along with the esters allow for the possibility of enzymatic degradation. PEAs offer a variety of advantages over traditional systems such as poly(glycolic acid) or poly(lactic acid) as these tend to produce potentially harmful acidic byproducts. Although

the glycolic and lactic acids generated during the hydrolysis of these traditionally used polymers are present in natural human metabolic pathways, a large accumulation of these acidic species has been demonstrated to result in tissue inflammation.[155,156] The susceptibility of the poly(ester amide)s to enzymatic degradation should enhance surface degradation, thereby limiting the possibility of a large accumulation of acidic species in tissues.[157] Conversely, the commonly used poly(amino acid)s require relatively unstable and expensive N-carboxyanhydride monomers for synthesis[158] and have been found to be immunogenic under some circumstances.[159]

While there are several classes of PEAs, the PEAs derived from α-amino acids, diols, and diacids (Figure 1.2) are of particular interest for the current work, as they have been demonstrated to undergo hydrolytic and enzymatic degradation at physiological pH[160] and the monomer components of the polymer can be chosen from metabolic intermediates (natural amino acids and diacids) allowing for the degradation products to also be non-toxic. In addition, by intelligent design of the backbone, the polymer's chemical functionality and properties including solubility, crystallinity, biocompatibility, and degradation rate can be readily tuned.[161] Finally, traditional systems tend to be hampered by a lack of functional handles.[1] These PEAs offer a multitude of avenues to introduce functionality into the polymer backbone via the incorporation of amino acids with side chain functional groups.[160,161] For example, the pendant functional groups on lysine or aspartic acid units offer the means to covalently attach drugs, targeting moieties, or other functional molecules into the PEA.

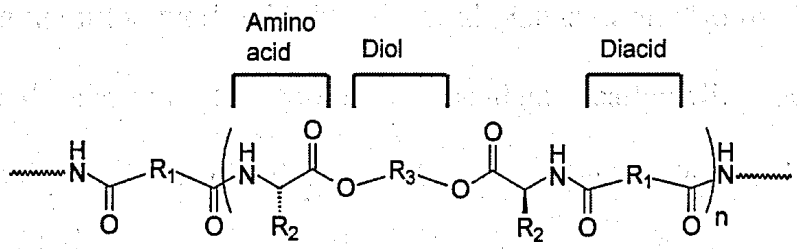

Figure 1.2: General structure of the poly(ester amide).

R1 is generally linear aliphatic or aromatic, R2 is the side chain of an amino acid and R3 is generally linear aliphatic

Although poly(ester amide)s have appeared in the literature as early as the 1960s[162,163] for use as model systems for proteins, it is only until recently that their full utility has been realized. In order to exploit this utility, a variety of PEAs, with varying monomer units and hence different properties have been synthesized. To date, PEAs have been synthesized containing alanine,[160,161] phenylalanine,[160,161,164] leucine,[165] aspartic acid,[161] lysine,[157,160] serine,[166] and arginine.[167-169] Unsaturated PEAs have also been synthesized mainly through the use of allyglycine,[170-172] fumaric acid,[173] and maleic acid.[174,175]

Recently, the incorporation of functional groups along the backbone of PEAs using α-amino acids has become an important area of research. For example, Jokhadze et al. formed a benzyl ester to protect the carboxylic acid group of lysine and performed a solution polycondensation using the α and ε amino groups as the diamine.[176] Following the polymerization, the lysine benzyl ester was selectively cleaved via hydrogenolysis yielding pendant carboxylic acid groups. These free carboxylic acids were further functionalized with 4-amino-2,2,6,6-tetramethylpiperidine-1-oxy (TAM), a biomedically useful cell growth inhibitor.

Building upon the work of Jokhadze et al., Guan et al. also used a benzyl ester which was hydrogenated to yield a pendant carboxylic acid; however, dimethylolpropionic acid, a diamine derived from hexanediol and glycine, was conjugated instead.[177]

Our group in collaboration with the Mequanint group at the University of Western Ontario, recently developed synthetic procedures where the protected, functional amino acids carboxybenzyl-lysine-(t-butoxycarbonyl)-OH[160] or carboxybenzyl-aspartic acid-(t-butyl ester)-OH[161] were converted into diamine-based polymerization monomers through N,N'-Dicyclohexylcarbodiimide (DCC) couplings with butanediol. These monomers were then combined with other monomers of varying structures in solution based polymerization methods to demonstrate the synthetic versatility of the method and to arrive at polymers with varying physical properties. Recently, we also compared this solution phase method to an interfacial polycondensation and found that higher molecular weights were produced with the interfacial method.[157] In addition, interfacial polymerization is generally more attractive than solution polycondensation because it is faster and less influenced by impurities.[178]

Alternately, Pang and Chu have recently incorporated DL-2-allylglycine as the functional amino acid into a solution polycondensation. The utility of DL-2-allylglycine stems from the double bond that allowed the authors to further derivatize the polymer. For example, reaction of the alkene with 3-mercaptopropionic acid was shown to yield a pendant carboxylic acid, while 2-aminoethanethiol hydrochloride produced a pendant amine and sodium-3-mercapto-1-propanesulfonate yielded a pendant sulfonate group. The authors also claim that if not derivatized, the double bond could also be crosslinked

with PEG diacrylate to produce a hydrogel.[179] While attractive, the DL-2-allylglycine monomer is quite expensive to prepare and results in some loss of the biomimicry of the polymers as it is not a natural amino acid.

1.6.1 Biomedical Uses of Poly(ester amide)s

Jokhadze et al. used PEAs to immobilize TAM, which is a nitric oxide mimic shown to suppress the proliferation of human smooth muscle cells in vitro.[176] The suppression effect is ideal for the mediation of certain clinical conditions such as restenosis of vascular stents.[180] The physical and biological properties of the polymers, as well as the ability to conjugate bioactive molecules, make PEAs a very attractive option for biomaterials.

In recent work, Knight *et al.* have shown that certain PEAs may be effective tissue engineering scaffolds as the glass transition temperatures are below or within the physiological range, ensuring proper pliability. Human coronary artery smooth muscle cell attachment and spreading was observed up to 7 days of culture and immunostaining of cells illustrated strong vinculin expression on all surfaces; however, smooth muscle α-actin expression was not abundant, suggesting a proliferative, rather than a contractile, smooth muscle cell phenotype. These results suggest that PEAs could be used in vascular tissue engineering applications.

Del Valle et al. investigated the use of a biodegradable PEA to create a drug delivery scaffold. The scaffold was made through a compression-molding/particulate-leaching method and showed good cell viability and supported cell growth. Ibuprofen

was loaded onto the scaffold and was found to release quickly. The release rate could be slowed by the addition of PCL to the immersion medium allowing for control over the release rate.181

Chu et al. have shown that hydrogels based on PEAs can be used as sustained release systems.[171,182,183] In other work, PEAs have been used by Liu et al. as non-viral gene delivery vehicles with a high plasmid deoxyribonucleic acid binding capacity.[184] In addition, Defife et al. has found that PEA coated cardiovascular stents promote a more natural healing response.[185,186]

Currently, there are very few examples of particle-based drug delivery systems comprising PEAs. For example, Guo *et al.* developed microspheres of amino acid based PEAs via an oil in water emulsion/solvent evaporation technique.[55] The effects of PEA polymer concentration, PVA emulsifier concentration, and the homogenizer speed on the size and morphology of final PEA microspheres were examined by analyzing their scanning electron microscopy (SEM) images. It was found that a low PEA concentration, a high PVA concentration, and a high homogenizer speed were the optimal conditions for obtaining particles one micrometer in diameter. The biodegradation behaviours of these microspheres were investigated and it was found that the degradation was largely based on surface erosion. The particles were also capable of encapsulating paclitaxel with high efficiency, approximately 95%; however, the particles are microsized, meaning they will be readily cleared by the RES and the lack of functional handles limits the possible uses of this system. While PEA based NP delivery systems of antibiotics and paclitaxel have been reported,[187,188] currently, to the best of our knowledge, there are no micellar drug carriers based on PEAs.

1.7 Thesis Goals

Having developed a synthetic method for the incorporation of pendant amine and carboxylic acid functional handles onto the PEA backbone,[157,160,161] and with the Mequanint group, demonstrated the potential utility of these PEAs in vascular tissue engineering applications,[157] the goal of this thesis was to explore the potential utility of these functional handles in the development of enhanced drug delivery systems based on PEAs. The thesis involves two different, but related applications of these functional groups.

In Chapter 2, the use of pendant carboxylic acid groups of aspartic acid moieties along the PEA backbone to covalently immobilize drug molecules by degradable ester linkages is explored (Figure 1.3a). The aim of this work is to address the burst release problem commonly observed for polymer NP based drug delivery systems as described above.[130,131] After synthesizing a model drug-PEA conjugate complex, the resulting conjugate is converted into surfactant-stabilized NPs via an oil in water emulsion. Over time, the ester bond between the polymer and the drug will slowly hydrolyze, releasing the drug. The appeal of this system is that the release of the drug will be limited by the hydrolysis kinetics, not diffusion. Therefore, the release will be more controlled[56] and the system will be less likely to release its payload before accumulating in the target tissue.[63] In addition, unlike the previously described PEA particles,[55,189] the size of these particles is optimized to be less than 200 nm in diameter, thus potentially allowing them to circulate in the vascular without rapid removal by the reticuloendothelial system.

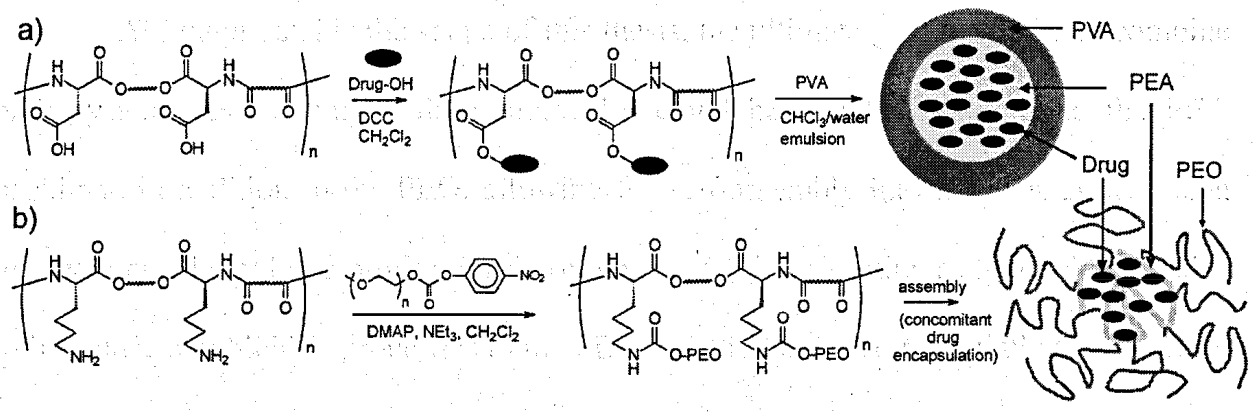

Figure 1.3: Two Approaches to PEA Drug Delivery Vehicles.

a) Polymer nanoparticles with covalently bound drugs that will not exhibit a burst release
b) PEO grafted PEAs self assemblies that can physically entrap drugs

While promising for drug delivery applications, in the course of this thesis research, some limitations to the surfactant stabilized NPs described above were encountered. For example, large quantities of PVA were required to obtain nanosized particles. While PVA has been approved by the Food and Drug Administration for many applications, coating of the NP surface may mask the properties of the PEA, slow the particle's biodegradation, and prevent the conjugation of targeting moieties to the PEA's pendant functional groups. In addition, it was found that some model drugs interacted with the PVA surfactant, resulting in their non-specific binding to the particle surface. To address these issues, as described in Chapter 3, amphiphilic properties can be imparted to the PEA itself through the conjugation of hydrophilic PEO to the pendant lysine moieties of a hydrophobic PEA backbone (Figure 1.3b). The PEO-PEA graft copolymers are then shown to self-assemble into micelles that can encapsulate model hydrophobic drugs in the micelle interior. These micelles do not require additional surfactant loading and the assemblies are smaller, which may lead to an extended circulation time *in vivo*.[2,6,9,11]

Although outside the scope of this thesis, the ultimate goal would be to combine both systems. For example, drug molecules could be covalently bound to the PEA backbone in addition to the PEO, allowing for self-assembly into micelles as well as a highly controlled release profile. Furthermore, in addition to acting as hydrophilic chains to introduce amphiphilic properties to the PEA, the PEO can also potentially function as a linker for the addition of targeting ligands. Towards this longer term goal, this thesis describes the independent development of both the NP and micelle systems using model drug molecules to illustrate the concepts.

1.8 References

(1) Hoffman, A.; Stayton, P.; Press, O.; Murthy, N.; Lackey, C.; Cheung, C.; Black, F.; Campbell, J.; Fausto, N.; Kyriakides, T.; Bornstein, P. *Biotechnol. Bioprocess Eng.* **2001**, *6*, 205.

(2) Liversidge, G. G.; Cundy, K. C. *Int. J. Pharm.* **1995**, *125*, 91.

(3) Yoshida, F.; Topliss, J. G. *J. Med. Chem.* **2000**, *43*, 2575.

(4) Hong, J.; Shah, J. C.; McGonagle, M. D. *J. Pharm. Sci.* **2011**, *100*, 2703.

(5) Koren, E.; Apte, A.; Sawant, R. R.; Grunwald, J.; Torchilin, V. P. *Drug Delivery* **2011**, *18*, 377.

(6) Yeo, Y.; Baek, N.; Park, K. *Biotechnol. Bioprocess Eng.* **2001**, *6*, 213.

(7) Feng, F. F.; Zheng, D. D.; Zhang, D. R.; Duan, C. X.; Wang, Y. C.; Jia, L. J.; Wang, F. H.; Liu, Y.; Gao, Q.; Zhang, Q. *J. Microencapsulation* **2011**, *28*, 280.

(8) Tencer, J.; Frick, I. M.; Oquist, B. W.; Alm, P.; Rippe, B. *Kidney Int.* **1998**, *53*, 709.

(9) Iyer, A. K.; Khaled, G.; Fang, J.; Maeda, H. *Drug Discov. Today* **2006**, *11*, 812.

(10) Patel, H. M. *Crit. Rev. Ther. Drug Carrier Syst.* **1992**, *9*, 39.

(11) Sandhiya, S.; Dkhar, S. A.; Surendiran, A. *Fundam. Clin. Pharmacol.* **2009**, *23*, 263.

(12) Shi, M.; Lu, J.; Shoichet, M. S. *J. Mater. Chem.* **2009**, *19*, 5485.

(13) Byrne, J. D.; Betancourt, T.; Brannon-Peppas, L. *Adv. Drug Delivery Rev.* **2008**, *60*, 1615.

(14) Shen, W.; Shi, H.-M.; Fan, W.-H.; Luo, X.-P.; Jin, B.; Li, Y. *Mol. Biol. Rep.* **2011**, *38*.

(15) *Drugs* **2007**, *67*, 2045.

(16) Romero, D.; O'Neill, C.; Terzic, A.; Contois, L.; Young, K.; Conley, B. A.; Bergan, R. C.; Brooks, P. C.; Vary, C. P. H. *Cancer Res.* **2011**, *71*, 3482.

(17) Folkman, J. *Sci. Am.* **1996**, *275*, 150.

(18) Kumar, S.; Li, C. G. *Trends Immunol.* **2001**, *22*, 129.

(19) Cao, Z. X.; Zheng, R. L.; Lin, H. J.; Luo, S. D.; Zhou, Y.; Xu, Y. Z.; Zeng, X. X.; Wang, Z.; Zhou, L. N.; Mao, Y. Q.; Yang, L.; Wei, Y. Q.; Yu, L. T.; Yang, S. Y.; Zhao, Y. L. *Cell. Physiol. Biochem.* **2011**, *27*, 565.

(20) Kamino, M.; Kishida, M.; Kibe, T.; Ikoma, K.; Iijima, M.; Hirano, H.; Tokudome, M.; Chen, L.; Koriyama, C.; Yamada, K.; Arita, K.; Kishida, S. *Cancer Sci.* **2011**, *102*, 540.

(21) Gosk, S.; Moos, T.; Gottstein, C.; Bendas, G. *Biochim. Biophys. Acta-Biomembr.* **2008**, *1778*, 854.

(22) Filpula, D. *Biomol. Eng.* **2007**, *24*, 201.

(23) Laskin, J. J.; Sandler, A. B. *Cancer Treat. Rev.* **2004**, *30*, 1.

(24) Ciardiello, F.; Caputo, R.; Bianco, R.; Damiano, V.; Fentanini, G.; Cuccato, S.; De Placido, S.; Bianco, A. R.; Tortora, G. *Clin. Cancer Res.* **2001**, *7*, 1459.

(25) Droller, M. J. *J. Urol.* **2000**, *164*, 594.

(26) Karashima, T.; Sweeney, P.; Slaton, J. W.; Kim, S. J.; Kedar, D.; Izawa, J. I.; Fan, Z.; Pettaway, C.; Hicklin, D. J.; Shuin, T.; Dinney, C. P. N. *Clin. Cancer Res.* **2002**, *8*, 1253.

(27) Petit, A.; Rak, J.; Hung, M.; Rockwell, P.; Goldstein, N.; Fendly, B.; Kerbel, R. *Am. J. Pathol.* **1997**, *151*, 1523.

(28) Singh, M. *ChemInform* **1999**, *30*, no.

(29) Gatter, K. C.; Brown, G.; Trowbridge, I. S.; Woolston, R. E.; Mason, D. Y. *J. Clin. Pathol.* **1983**, *36*, 539.

(30) Faulk, W. P.; Taylor, C. G.; Yeh C-J, G.; McIntyre, J. A. *Mol. Biother.* **1990**, *2*, 57.

(31) Head, J. F.; Wang, F.; Elliott, R. L. *Adv Enzyme Regul* **1997**, *37*, 147.

(32) Rainov, N. G.; Soling, A. *Curr. Opin. Mol. Ther.* **2005**, *7*, 483.

(33) Lee, R. J.; Low, P. S. *Biochim. Biophys. Acta-Biomembr.* **1995**, *1233*, 134.

(34) Pan, X. Q.; Zheng, X.; Shi, G. F.; Wang, H. Q.; Ratnam, M.; Lee, R. J. *Blood* **2002**, *100*, 594.

(35) Sudimack, J.; Lee, R. J. *Adv. Drug Delivery Rev.* **2000**, *41*, 147.

(36) Zhao, X. B. B.; Lee, R. J. *Adv. Drug Delivery Rev.* **2004**, *56*, 1193.

(37) Beaudin, A. E.; Abarinov, E. V.; Noden, D. M.; Perry, C. A.; Chu, S.; Stabler, S. P.; Allen, R. H.; Stover, P. J. *Am. J. Clin. Nutr.* **2011**, *93*, 789.

(38) Low, P. S.; Antony, A. C. *Adv. Drug Delivery Rev.* **2004**, *56*, 1055.

(39) Witt, T. L.; Stapels, S. E.; Matherly, L. H. *J. Biol. Chem.* **2004**, *279*, 46755.

(40) Lu, J. Y.; Lowe, D. A.; Kennedy, M. D.; Low, P. S. *J. Drug Targeting* **1999**, *7*, 43.

(41) Matherly, L. H.; Diop-Bove, N.; Goldman, I. D. *Targeted Drug Strategies for Cancer and Inflammation* **2011**, 1.

(42) Matherly, L. H.; Gangjee, A. *Discovery of Novel Antifolate Inhibitors of De Novo Purine Nucleotide Biosynthesis with Selectivity for High Affinity Folate Receptors and the Proton-Coupled Folate Transporter Over the Reduced Folate Carrier for Cellular Entry*; Springer, 2011.

(43) Antony, A. C. *Blood* **1992**, *79*, 2807.

(44) Jackman, A. L.; Jansen, G.; Ng, M. *Folate Receptor Targeted Thymidylate Synthase Inhibitors*; Springer, 2011.

(45) Abbasi, M.; Lavasanifar, A.; Berthiaume, L. G.; Weinfeld, M.; Uludag, H. *Cancer* **2010**, *116*, 5544.

(46) Gottesman, M. M.; Fojo, T.; Bates, S. E. *Nat. Rev. Cancer* **2002**, *2*, 48.

(47) Goren, D.; Horowitz, A. T.; Tzemach, D.; Tarshish, M.; Zalipsky, S.; Gabizon, A. *Clin. Cancer Res.* **2000**, *6*, 1949.

(48) Kobayashi, T.; Ishida, T.; Okada, Y.; Ise, S.; Harashima, H.; Kiwada, H. *Int. J. Pharm.* **2007**, *329*, 94.

(49) Alexis, F.; Rhee, J.-W.; Richie, J. P.; Radovic-Moreno, A. F.; Langer, R.; Farokhzad, O. C. *Urologic Oncology: Seminars and Original Investigations*, *26*, 74.

(50) Cheng, D.; Hong, G.; Wang, W.; Yuan, R.; Ai, H.; Shen, J.; Liang, B.; Gao, J.; Shuai, X. *J. Mater. Chem.* **2011**, *21*, 4796.

(51) Lim, K. J.; Bisht, S.; Bar, E. E.; Maitra, A.; Eberhart, C. G. *Cancer Biol. Ther.* **2011**, *11*, 464.

(52) Sun, H.; Almdal, K.; Andresen, T. L. *Chem. Commun.* **2011**, *47*, 5268.

(53) Yao, H.; Ng, S. S.; Huo, L.-F.; Chow, B. K. C.; Shen, Z.; Yang, M.; Sze, J.; Ko, O.; Li, M.; Yue, A.; Lu, L.-W.; Bian, X.-W.; Kung, H.-F.; Lin, M. C. *Mol. Cancer Ther.* **2011**, *10*, 1082.

(54) Yin, B.; Hakkarainen, M. *J. Mater. Chem.* **2011**, *21*, 8670.

(55) Guo, K.; Chu, C. C. *J. Biomed. Mater. Res. B Appl. Biomater.* **2009**, *89B*, 491.

(56) Cheng, Y. Y.; Xu, T. W. *Eur. J. Med. Chem.* **2008**, *43*, 2291.

(57) Gillies, E. R.; Frechet, J. M. J. *Drug Discov. Today* **2005**, *10*, 35.

(58) Kelly, C. V.; Liroff, M. G.; Triplett, L. D.; Leroueil, P. R.; Mullen, D. G.; Wallace, J. M.; Meshinchi, S.; Baker, J. R.; Orr, B. G.; Holl, M. M. B. *ACS Nano* **2009**, *3*, 1886.

(59) Lee, C. C.; Gillies, E. R.; Fox, M. E.; Guillaudeu, S. J.; Frechet, J. M. J.; Dy, E. E.; Szoka, F. C. *Proc. Natl. Acad. Sci. U. S. A.* **2006**, *103*, 16649.

(60) McNerny, D. Q.; Leroueil, P. R.; Baker, J. R. *Wiley Interdiscip Rev Nanomed Nanobiotechnol.* **2010**, *2*, 249.

(61) Mullen, D. G.; McNerny, D. Q.; Desai, A.; Cheng, X. M.; DiMaggio, S. C.; Kotlyar, A.; Zhong, Y.; Qin, S.; Kelly, C. V.; Thomas, T. P.; Majoros, I.; Orr, B. G.; Baker, J. R.; Holl, M. M. B. *Bioconjugate Chem.* **2011**, *22*, 679.

(62) Myc, A.; Patri, A. K.; Baker, J. R. *Biomacromolecules* **2007**, *8*, 2986.

(63) Patri, A. K.; Kukowska-Latallo, J. F.; Baker, J. R. *Adv. Drug Delivery Rev.* **2005**, *57*, 2203.

(64) Shi, X. Y.; Thomas, T. P.; Myc, L. A.; Kotlyar, A.; Baker, J. R. *Phys. Chem. Chem. Phys.* **2007**, *9*, 5712.

(65) Shukla, R.; Hill, E.; Shi, X. Y.; Kim, J.; Muniz, M. C.; Sun, K.; Baker, J. R. *Soft Matter* **2008**, *4*, 2160.

(66) Swanson, S. D.; Kukowska-Latallo, J. F.; Patri, A. K.; Chen, C. Y.; Ge, S.; Cao, Z. Y.; Kotlyar, A.; East, A. T.; Baker, J. R. *Int. J. Nanomedicine* **2008**, *3*, 201.

(67) Zhang, Y. H.; Thomas, T. P.; Desai, A.; Zong, H.; Leroueil, P. R.; Majoros, I. J.; Baker, J. R. *Bioconjugate Chem.* **2010**, *21*, 489.

(68) Kartseva, M. E.; Dement'eva, O. V.; Filippenko, M. A.; Rudoy, V. M. *Colloid J.* **2011**, *73*, 340.

(69) Klimavicz, C.; Bennett, G.; Barnes, P. W. *Abstr. Pap. Am. Chem. Soc.* **2011**, *241*.

(70) Mahmoud, W. E.; Al-Ghamdi, A. A. *Polym. Adv. Technol.* **2011**, *22*, 877.

(71) Waldman, S. A.; Fortina, P.; Surrey, S.; Hyslop, T.; Kricka, L. J.; Graves, D. J. *Future oncology (London, England)* **2006**, *2*, 705.

(72) Xi, L.; Wang, Z.; Zuo, Y.; Shi, X. *Nanotechnology* **2011**, *22*.

(73) Banerjee, R.; Tyagi, P.; Li, S.; Huang, L. *Int. J. Cancer* **2004**, *112*, 693.

(74) Manjappa, A. S.; Chaudhari, K. R.; Venkataraju, M. P.; Dantuluri, P.; Nanda, B.; Sidda, C.; Sawant, K. K.; Murthy, R. S. R. *J. Controlled Release* **2011**, *150*, 2.

(75) Sakakibara, T.; Chen, F. A.; Kida, H.; Kunieda, K.; Cuenca, R. E.; Martin, F. J.; Bankert, R. B. *Cancer Res.* **1996**, *56*, 3743.

(76) Gillies, E. R.; Frechet, J. M. J. *Chem. Commun.* **2003**, 1640.

(77) Gillies, E. R.; Frechet, J. M. J. *Pure Appl. Chem.* **2004**, *76*, 1295.

(78) Gillies, E. R.; Frechet, J. M. J. *Bioconjugate Chem.* **2005**, *16*, 361.

(79) Gillies, E. R.; Goodwin, A. P.; Frechet, J. M. J. *Bioconjugate Chem.* **2004**, *15*, 1254.

(80) Abdelmawla, S.; Guo, S.; Zhang, L.; Pulukuri, S. M.; Patankar, P.; Conley, P.; Trebley, J.; Guo, P.; Li, Q.-X. *Mol. Ther.* **2011**, *19*, 1312.

(81) Guo, P. *Methods* **2011**, *54*, 201.

(82) Shu, Y.; Cinier, M.; Shu, D.; Guo, P. *Methods* **2011**, *54*, 204.

(83) Zhou, J.; Shu, Y.; Guo, P.; Smith, D. D.; Rossi, J. J. *Methods* **2011**, *54*, 284.

(84) Landmark, K. J.; DiMaggio, S.; Ward, J.; Kelly, C. V.; Vogt, S.; Hong, S.; Kotlyar, A.; Myc, A.; Thomas, T. P.; Penner-Hahn, J. E.; Baker, J. R.; Holl, M. M. B.; Orr, B. G. *ACS Nano* **2008**, *2*, 773.

(85) Leuschner, C.; Kumar, C. S. S. R.; Hansel, W.; Soboyejo, W.; Zhou, J.; Hormes, J. *Breast Cancer Res. Treat.* **2006**, *99*, 163.

(86) Plouffe, B. D.; Nagesha, D. K.; DiPietro, R. S.; Sridhar, S.; Heiman, D.; Murthy, S. K.; Lewis, L. H. *J. Magn. Magn. Mater.* **2011**, *323*, 2310.

(87) Teste, B.; Kanoufi, F.; Descroix, S.; Poncet, P.; Georgelin, T.; Siaugue, J.-M.; Petr, J.; Varenne, A.; Hennion, M.-C. *Anal. Bioanal. Chem.* **2011**, *400*, 3395.

(88) Zhu, R.; Luo, K.; Xu, X.; Wu, Y.; He, B.; Gu, Z. *Acta Polymerica Sinica* **2011**, 679.

(89) Aljabali, A. A. A.; Shah, S. N.; Evans-Gowing, R.; Lomonossoff, G. P.; Evans, D. J. *Integr. Biol.* **2011**, *3*, 119.

(90) Franzen, S.; Lockney, D. M.; Wang, R.; Lommel, S.; Hauck, M. *Abstr. Pap. Am. Chem. Soc.* **2011**, *241*.

(91) Lockney, D. M.; Guenther, R. N.; Loo, L.; Overton, W.; Antonelli, R.; Clark, J.; Hu, M.; Luft, C.; Lommel, S. A.; Franzen, S. *Bioconjugate Chem.* **2011**, *22*, 67.

(92) Green, M. R.; Manikhas, G. M.; Orlov, S.; Afanasyev, B.; Makhson, A. M.; Bhar, P.; Hawkins, M. J. *Ann. Oncol.* **2006**, *17*, 1263.

(93) Ellerhorst, J. A.; Bedikian, A.; Ring, S.; Buzaid, A. C.; Eton, O.; Legha, S. S. *Oncol. Rep.* **1999**, *6*, 1097.

(94) Fassas, A.; Anagnostopoulos, A. *Leuk. Lymphoma* **2005**, *46*, 795.

(95) Wang, Y. X. J.; Hussain, S. M.; Krestin, G. P. *Eur. Radiol.* **2001**, *11*, 2319.

(96) Gref, R.; Minamitake, Y.; Peracchia, M. T.; Trubetskoy, V.; Torchilin, V.; Langer, R. *Science* **1994**, *263*, 1600.

(97) Strichar.Gr *J. Gen. Physiol.* **1973**, *62*, 37.

(98) Anderson, J. M.; Shive, M. S. *Adv. Drug Delivery Rev.* **1997**, *28*, 5.

(99) Bala, I.; Hariharan, S.; Kumar, M. *Crit. Rev. Ther. Drug Carrier Syst.* **2004**, *21*, 387.

(100) Kumari, A.; Yadav, S. K.; Yadav, S. C. *COLLOID SURFACE B* **2010**, *75*, 1.

(101) Mohamed, F.; van der Walle, C. F. *J. Pharm. Sci.* **2008**, *97*, 71.

(102) Estey, T.; Kang, J.; Schwendeman, S. P.; Carpenter, J. F. *J. Pharm. Sci.* **2006**, *95*, 1626.

(103) Bhardwaj, V.; Ankola, D. D.; Gupta, S. C.; Schneider, M.; Lehr, C. M.; Kumar, M. N. V. R. *Pharm. Res.* **2009**, *26*, 2495.

(104) Kalaria, D. R.; Sharma, G.; Beniwal, V.; Kumar, M. N. V. R. *Pharm. Res.* **2009**, *26*, 492.

(105) Hariharan, S.; Bhardwaj, V.; Bala, I.; Sitterberg, J.; Bakowsky, U.; Kumar, M. *Pharm. Res.* **2006**, *23*, 184.

(106) Mittal, G.; Sahana, D. K.; Bhardwaj, V.; Kumar, M. N. V. R. *J. Controlled Release* **2007**, *119*, 77.

(107) Italia, J. L.; Yahya, M. M.; Singh, D.; Kumar, M. N. V. R. *Pharm. Res.* **2009**, *26*, 1324.

(108) Italia, J. L.; Bhatt, D. K.; Bhardwaj, V.; Tikoo, K.; Kumar, M. N. V. R. *J. Controlled Release* **2007**, *119*, 197.

(109) Meena, A. K.; Ratnam, D. V.; Chandraiah, G.; Ankola, D. D.; Rao, P. R.; Kumar, M. N. V. R. *Lipids* **2008**, *43*, 231.

(110) Ankola, D. D.; Viswanad, B.; Bhardwa, V.; Ramarao, P.; Kumar, M. N. V. R. *Eur. J. Pharm. Biopharm.* **2007**, *67*, 361.

(111) Shaikh, J.; Ankola, D. D.; Beniwal, V.; Singh, D.; Kumar, M. N. V. R. *Eur. J. Pharm. Sci.* **2009**, *37*, 223.

(112) Italia, J. L.; Datta, P.; Ankola, D. D.; Kumar, M. N. V. R. *J. Biomed. Nanotechnol.* **2008**, *4*, 304.

(113) Galli, F.; Azzi, A. *BioFactors (Oxford, England)* **2010**, *36*, 33.

(114) van Vugt, R. M.; Rijken, P. J.; Rietveld, A. G.; van Vugt, A. C.; Dijkmans, B. A. C. *Clin. Rheumatol.* **2008**, *27*, 771.

(115) Grama, C. N.; Ankola, D. D.; Kumar, M. N. V. R. *Curr. Opin. Colloid Interface Sci.* **2011**, *16*, 238.

(116) Peniche, H.; Peniche, C. *Polym. Int.* **2011**, *60*, 883.

(117) Calvo, P.; RemunanLopez, C.; VilaJato, J. L.; Alonso, M. J. *Pharm. Res.* **1997**, *14*, 1431.

(118) Wu, Y.; Yang, W. L.; Wang, C. C.; Hu, J. H.; Fu, S. K. *Int. J. Pharm.* **2005**, *295*, 235.

(119) Colonna, C.; Conti, B.; Perugini, P.; Pavanetto, F.; Modena, T.; Dorati, R.; Genta, I. *J. Microencapsulation* **2007**, *24*, 553.

(120) Ma, Z. S.; Yeoh, H. H.; Lim, L. Y. *J. Pharm. Sci.* **2002**, *91*, 1396.

(121) Janes, K. A.; Fresneau, M. P.; Marazuela, A.; Fabra, A.; Alonso, M. J. *J. Controlled Release* **2001**, *73*, 255.

(122) Hu, Y.; Jiang, X. Q.; Ding, Y.; Ge, H. X.; Yuan, Y. Y.; Yang, C. Z. *Biomaterials* **2002**, *23*, 3193.

(123) Hu, Y.; Ding, Y.; Ding, D.; Sun, M.; Zhang, L.; Jiang, X.; Yang, C. *Biomacromolecules* **2007**, *8*, 1069.

(124) Lee, D. W.; Yun, K.-S.; Ban, H.-S.; Choe, W.; Lee, S. K.; Lee, K. Y. *J. Controlled Release* **2009**, *139*, 146.

(125) Nobs, L.; Buchegger, F.; Gurny, R.; Allemann, E. *Bioconjugate Chem.* **2006**, *17*, 139.

(126) Pan, J.; Feng, S.-S. *Biomaterials* **2008**, *29*, 2663.

(127) Bae, Y.; Fukushima, S.; Harada, A.; Kataoka, K. *Angew. Chem., Int. Ed.* **2003**, *42*, 4640.

(128) Tong, R.; Cheng, J. *Angew. Chem., Int. Ed.* **2008**, *47*, 4830.

(129) Yoo, H. S.; Oh, J. E.; Lee, K. H.; Park, T. G. *Pharm. Res.* **1999**, *16*, 1114.

(130) Huang, X.; Brazel, C. S. *J. Controlled Release* **2001**, *73*, 121.

(131) Rizi, K.; Green, R. J.; Khutoryanskaya, O.; Donaldson, M.; Williams, A. C. *J. Pharm. Pharmacol.* **2011**, *63*, 1141.

(132) Bader, H.; Ringsdorf, H.; Schmidt, B. *Angew. Makromol. Chem.* **1984**, *123*, 457.

(133) Blanco, E.; Hsiao, A.; Mann, A. P.; Landry, M. G.; Meric-Bernstam, F.; Ferrari, M. *Cancer Sci.* **2011**, *102*, 1247.

(134) Park, J.; Moon, M.; Seo, M.; Choi, H.; Kim, S. Y. *Macromolecules* **2010**, *43*, 8304.

(135) Tong, R.; Christian, D. A.; Tang, L.; Cabral, H.; Baker, J. R.; Kataoka, K.; Discher, D. E.; Cheng, J. J. *Mrs Bulletin* **2009**, *34*, 422.

(136) Soo, P. L.; Luo, L. B.; Maysinger, D.; Eisenberg, A. *Langmuir* **2002**, *18*, 9996.

(137) Kabanov, A. V.; Nazarova, I. R.; Astafieva, I. V.; Batrakova, E. V.; Alakhov, V. Y.; Yaroslavov, A. A.; Kabanov, V. A. *Macromolecules* **1995**, *28*, 2303.

(138) Jeong, Y. I.; Nah, J. W.; Lee, H. C.; Kim, S. H.; Cho, C. S. *Int. J. Pharm.* **1999**, *188*, 49.

(139) Gan, Z. H.; Jim, T. F.; Li, M.; Yuer, Z.; Wang, S. G.; Wu, C. *Macromolecules* **1999**, *32*, 590.

(140) Yasugi, K.; Nagasaki, Y.; Kato, M.; Kataoka, K. *J. Controlled Release* **1999**, *62*, 89.

(141) Riley, T.; Stolnik, S.; Heald, C. R.; Xiong, C. D.; Garnett, M. C.; Illum, L.; Davis, S. S.; Purkiss, S. C.; Barlow, R. J.; Gellert, P. R. *Langmuir* **2001**, *17*, 3168.

(142) Du, L.; Jin, Y.; Zhou, W.; Zhao, J. *Ultrasound Med. Biol.* **2011**, *37*, 1252.

(143) Allen, C.; Yu, Y. S.; Maysinger, D.; Eisenberg, A. *Bioconjugate Chem.* **1998**, *9*, 564.

(144) Allen, C.; Han, J.; Yu, Y.; Maysinger, D.; Eisenberg, A. *J. Controlled Release* **2000**, *63*, 275.

(145) Alexandridis, P.; Holzwarth, J. F.; Hatton, T. A. *Macromolecules* **1994**, *27*, 2414.

(146) Zhang, W.; Shi, Y.; Chen, Y.; Hao, J.; Sha, X.; Fang, X. *Biomaterials* **2011**, *32*, 5934.

(147) Antunes, F. E.; Gentile, L.; Rossi, C. O.; Tavano, L.; Ranieri, G. A. *COLLOID SURFACE B* **2011**, *87*, 42.

(148) Lin, S. Y.; Kawashima, Y. *Pharm. Acta Helv.* **1985**, *60*, 339.

(149) Lin, S. Y.; Kawashima, Y. *Pharm. Acta Helv.* **1985**, *60*, 345.

(150) Adams, M. L.; Lavasanifar, A.; Kwon, G. S. *J. Pharm. Sci.* **2003**, *92*, 1343.

(151) Rapoport, N. Y.; Herron, J. N.; Pitt, W. G.; Pitina, L. *J. Controlled Release* **1999**, *58*, 153.

(152) Marin, A.; Muniruzzaman, M.; Rapoport, N. *J. Controlled Release* **2001**, *71*, 239.

(153) Lavasanifar, A.; Samuel, J.; Kwon, G. S. *J. Controlled Release* **2001**, *77*, 155.

(154) Yokoyama, M.; Okano, T.; Sakurai, Y.; Kataoka, K. *J. Controlled Release* **1994**, *32*, 269.

(155) Bergsma, J. E.; Debruijn, W. C.; Rozema, F. R.; Bos, R. R. M.; Boering, G. *Biomaterials* **1995**, *16*, 25.

(156) Moroni, L.; De Wijn, J. R.; Van Blitterswijk, C. A. *J. Biomater. Sci., Polym. Ed.* **2008**, *19*, 543.

(157) Knight, D. K.; Gillies, E. R.; Mequanint, K. *Biomacromolecules* **2011**, *12*, 2475.

(158) Lu, H.; Cheng, J. *J. Am. Chem. Soc.* **2008**, *130*, 12562.

(159) Vermeersch, H.; Remon, J. P. *J. Controlled Release* **1994**, *32*, 225.

(160) De Wit, M. A.; Wang, Z. X.; Atkins, K. M.; Mequanint, K.; Gillies, E. R. *J. Polym. Sci., Part A: Polym. Chem.* **2008**, *46*, 6376.

(161) Atkins, K. M.; Lopez, D.; Knight, D. K.; Mequanint, K.; Gillies, E. R. *J. Polym. Sci., Part A: Polym. Chem.* **2009**, *47*, 3757.

(162) Bradbury, E. M.; Carpente.Bg; Stephens, R. M. *Biopolymers* **1968**, *6*, 905.

(163) Krull, H. H.; Wall, J. S.; Zobel, H.; Dimler, R. J. *Biochemistry* **1965**, *4*, 626.

(164) Guo, K.; Chu, C. C. *J. Appl. Polym. Sci.* **2010**, *117*, 3386.

(165) Chkhaidze, E.; Tugushi, D.; Kharadze, D.; Gomurashvili, Z.; Chu, C. C.; Katsarava, R. *J MACROMOL SCI A* . **2011**, *48*, 544.

(166) Deng, M. X.; Wu, J.; Reinhart-King, C. A.; Chu, C. C. *Acta Biomater.* **2011**, *7*, 1504.

(167) Pang, X. A.; Wu, J.; Reinhart-King, C.; Chu, C. C. *J. Polym. Sci., Part A: Polym. Chem.* **2010**, *48*, 3758.

(168) Wu, J.; Mutschler, M. A.; Chu, C. C. *J. Mater. Sci. Mater. Med.* **2011**, *22*, 469.

(169) Yamanouchi, D.; Wu, J.; Lazar, A. N.; Kent, K. C.; Chu, C. C.; Liu, B. *Biomaterials* **2008**, *29*, 3269.

(170) Guo, K.; Chu, C. C. *J. Polym. Sci., Part A: Polym. Chem.* **2007**, *45*, 1595.

(171) Guo, K.; Chu, C. C. *Biomaterials* **2007**, *28*, 3284.

(172) Guo, K.; Chu, C. C. *J. Appl. Polym. Sci.* **2008**, *110*, 1858.

(173) Chkhaidze, E.; Tugushi, D.; Kharadze, D.; Gomurashvili, Z.; Chu, C.-C.; Katsarava, R. *J MACROMOL SCI A* . **2011**, *48*, 544.

(174) Ai, Y. P.; Jiang, F.; Xie, S. K.; Yi, R. X. *J. Appl. Polym. Sci.* **2009**, *114*, 1208.

(175) Pedron, S.; Peinado, C.; Bosch, P.; Anseth, K. S. *Acta Biomater.* **2010**, *6*, 4189.

(176) Jokhadze, G.; Machaidze, M.; Panosyan, H.; Chu, C. C.; Katsarava, R. *J. Biomater. Sci., Polym. Ed.* **2007**, *18*, 411.

(177) Guan, H. L.; Deng, C.; Xu, X. Y.; Liang, Q. Z.; Chen, X. S.; Jing, X. B. *J. Polym. Sci., Part A: Polym. Chem.* **2005**, *43*, 1144.

(178) Wittbecker, E. L.; Morgan, P. W. *J. Polym. Sci., Part A: Polym. Chem.* **1996**, *34*, 521.

(179) Pang, X.; Chu, C.-C. *Biomaterials* **2010**, *31*, 3745.

(180) Lee, K.-H.; Chu, C.-C.; Quimby, F.; Klaessig, S. *Macromol. Symp.* **1998**, *130*, 71.

(181) Del Valle, L. J.; Roca, D.; Franco, L.; Puiggalí, J.; Rodríguez-Galán, A. *J. Appl. Polym. Sci.* **2011**, *122*, 1953.

(182) Guo, K.; Chu, C. C. *J. Biomater. Sci., Polym. Ed.* **2007**, *18*, 489.

(183) Pang, X. A.; Chu, C. C. *Polymer* **2010**, *51*, 4200.

(184) Yamanouchi, D.; Wu, J.; Lazar, A. N.; Kent, K. C.; Chu, C. C.; Liu, B. *Biomaterials* **2008**, *29*, 3269.

(185) DeFife, K. M.; Grako, K.; Cruz-Aranda, G.; Price, S.; Chantung, R.; Macpherson, K.; Khoshabeh, R.; Gopalan, S.; Turnell, A. G. *J. Biomater. Sci., Polym. Ed.* **2009**, *20*, 1495.

(186) Lee, S. H.; Szinai, I.; Carpenter, K.; Katsarava, R.; Jokhadze, G.; Chu, C.-C.; Huang, Y.; Verbeken, E.; Bramwell, O.; De Scheerder, I.; Hong, M. K. *Coron. Artery Dis.* **2002**, *13*, 237.

(187) Guo, K.; Chu, C. C. *J. Biomed. Mater. Res., Part B: Appl. Biomater.* **2009**, *89*, 491.

(188) Kartvelishvili, T.; Tsitlanadze, G.; Edilashvili, L.; Japaridze, N.; Katsarava, R. *Macromol. Chem. Phys.* **1997**, *198*, 1921.

(189) Vera, M.; Puiggali, J.; Coudane, J. *J. Microencapsulation* **2006**, *23*, 686.

Chapter Two:

Covalent Immobilization of Drug Molecules in Poly(ester amide) Nanoparticles

2.1 Introduction

Nanotechnology pertains to synthetic, engineerable objects that are on the order of 100 nm in one dimension, leading to unique properties due to the material's large surface area to volume ratio and its nanoscopic size.[1,2] One of the most important applications of these unique properties is the creation of nanoparticle (NP) based drug delivery vectors that can overcome a host of pharmaceutical and physiological barriers in order to enhance the delivery of drug molecules to a biological target. Towards this end, a wide range of polymer based nanoparticles have been developed. Perhaps the most common example is poly(lactic-co-glycolic acid) (PLGA) which has been shown to encapsulate anti-cancer agents (paclitaxel and doxorubicin),[3,4] sex hormones (estradiol),[5,6] anti-leishmanial agents (amphotericin B),[7] immunosuppressants (cyclosporine)[8] and hyperlipidemia treatments (atorvastatin, sold under the name Lipitor).[9] All of these NP systems displayed higher bioactivity relative to free drug as well as an increased in vivo circulation time. Other examples of nanoscale, polymeric delivery systems include chitosan to deliver ammonium glycyrrhizinate,[10] proteins,[11] insulin,[12] and doxorubicin[13] or poly(caprolactone) (PCL) to deliver tamoxifen,[14] mixnoxidil,[15] and octyl methoxycinnamate.[16]

Overall, polymer nanoparticles have been successful in enhancing the effective solubility of hydrophobic drugs[1,17,18], preventing enzymatic degradation[19], and avoiding sequestration by phagocytes of the reticuloendothelial system (RES).[20,21] Despite their promise, there still remains a series of challenges for polymer nanoparticles, one of which is the commonly observed burst release effect.[22,23] It occurs when a large percentage of the drug is released in a short time period and is in most cases undesirable. The burst release tends to be unpredictable, may induce local toxicity, and may result in a loss of activity if the drug has a short half-life.[22] In addition, releasing too much drug at once is economically and therapeutically wasteful, and the shortened release profile requires more frequent dosing. In some cases, such as flavours in the food industry or pulsatile delivery devices, burst may be desirable, but even in these cases, the amount of drug released in the burst is relatively hard to model and control.[22,23]

While there are relatively few examples, it has recently been demonstrated that the covalent immobilization of drug molecules within polymer nanoparticles may be an effective way to slow and better control their release rates.[24] While it has been shown that many drug/polymer complexes display promise *in vitro,* in particles targeted to cancerous tissue *in vivo*, covalent immobilization may greatly increase therapeutic efficacy since the drug is not released prematurely under physiological conditions.[25]

Overall, one of the key properties desirable in a polymer nanoparticle delivery system is the biodegradability of the polymer. While many different biodegradable polymers are potentially available, in recent years poly(ester amide)s (PEAs) based on amino acids, diols, and dicarboxylic acids have emerged as promising materials for a wide range of biomedical applications such as drug eluting stents,[26,27] tissue engineering

scaffolds,[28] and drug delivery vehicles such as scaffolds,[29] hydrogels,[30-32] and microspheres.[33,34] Currently there are only two examples of drug delivery particles based on this class of PEAs,[33,34] but these report particle diameters of approximately 1 μm and 4.5 μm respectively. It has been shown that particles with a diameter greater than 200 nm are easily removed by the reticuloendothelial system, while smaller particles will circulate longer in the body.[35-37] It has also been shown that particles in the range of 2-200 nm tend to accumulate in cancerous tissue due to the enhanced permeability and retention effect.[35-37] Therefore, the NP systems described in previous work may not be useful for many drug delivery applications such as tumour targeting. Recently, our group has reported versatile approaches for the incorporation of pendant functional groups into PEA backbones by the copolymerization of protected aspartic acid or lysine moieties with other monomers. Here we explore the use of these pendant functional groups for the covalent immobilization of drug molecules in order to develop enhanced drug delivery nanoparticle systems based on PEAs (Figure 2.1). In addition, we report for the first time PEA nanoparticles with diameters less than 200 nm that could be able to circulate in the blood.

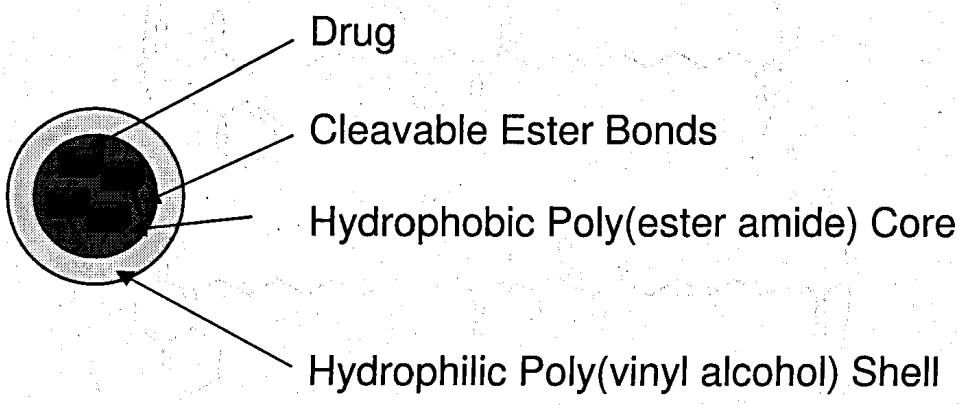

Figure 2.1: Diagram of covalently immobilized PEA drug delivery system.

2.2 Results and Discussion

2.2.1 Synthesis of Polymers without Pendant Functional Groups

In order to optimize the nanoparticle preparation procedure, polymers without functional handles, **1-4**, were used as they can be more easily synthesized relative to the analogous polymers containing functional handles (Figure 2.2). These polymers were prepared by the previously reported methods[28,38] and were characterized by ^{1}H nuclear magnetic resonance (NMR) spectroscopy as well as gel permeation chromatography (GPC). The characterization data agreed with those previously reported.

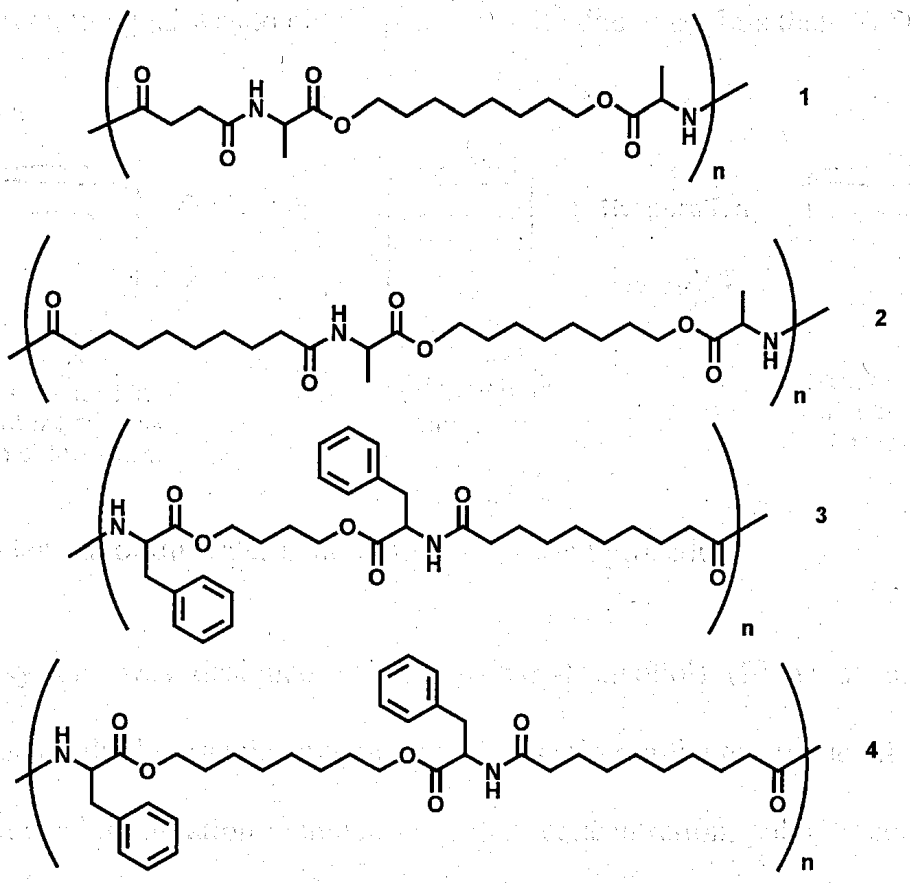

Figure 2.2: Structures of PEAs without pendant functional groups.

2.2.2 *Optimization of the Nanoparticle Preparation Procedure*

With polymers in hand, a procedure to form nanoparticles was required. An oil in water solvent evaporation method was chosen based on the solubility of PEAs, its general effectiveness, and its ease of use.[19] As seen in Figure 2.3, the procedure involves the formation of an emulsion between an aqueous surfactant and the polymer of interest in a volatile organic solvent. As the solvent evaporates, the polymer forms nanosized particles that remain suspended in the aqueous phase due to the presence of a surfactant shell. Using procedures for similar systems found in literature, a procedure for PEAs was optimized to produce the smallest particles with the narrowest polydispersities.[19,39] As described above, the goal was to obtain particles with diameters less than 200 nm.

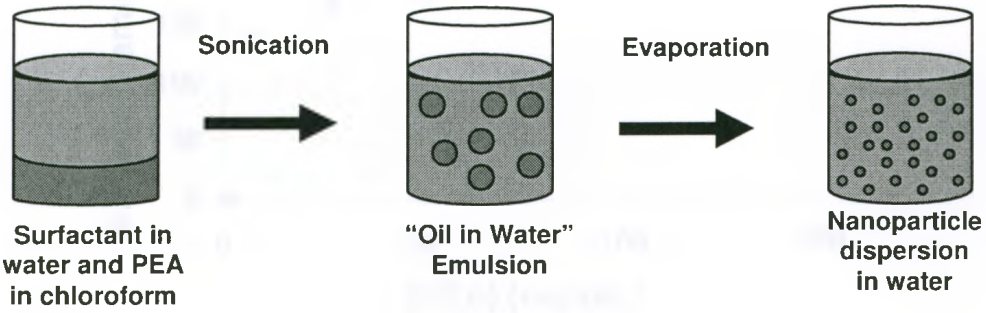

Figure 2.3: General oil in water nanoparticle formation procedure.

The system was designed using poly(vinyl alcohol) (PVA) as a surfactant, chloroform as a volatile organic solvent and a sonication probe to produce the emulsion. Parameters under investigation included surfactant concentration, polymer concentration, oil/water volume ratio, probe height, and sonication time. Dialysis, ultrafiltration and centrifugation were evaluated for the removal of free PVA and ultrafiltration was chosen

as the preferred method as dialysis membranes did not have a high enough molecular weight cut-off and our centrifuge was not powerful enough to isolate the NPs since the particles produced were much smaller than those previously reported.[33,34]

To produce smaller particles several parameters of the NP formation procedure were tuned. First, the concentration of PEA in the oil phase was varied while keeping the concentration of surfactant and oil/water ratio constant. As shown in Figure 2.4, it was found that decreasing the concentration of the oil phase decreased particle diameter. However, there was a limit where a too dilute solution failed to produce particles. It was found that 5 mg/mL was an optimal concentration for minimum diameter.

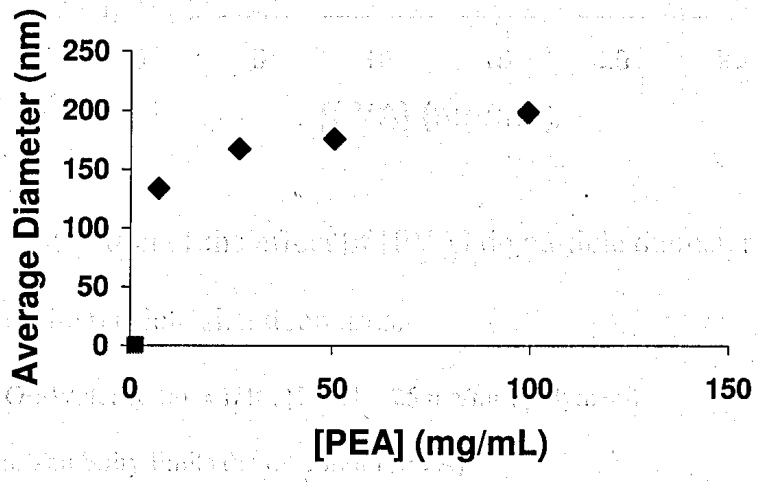

Figure 2.4: An investigation of the effect of [PEA] on particle diameter shows that the particles are smaller at lower [PEA]. However, at very low concentrations no particles are formed.

Parameters: Oil/Water Ratio = 1/10, [PVA] = 20 mg/mL, polymer **4**

Next, the concentration of surfactant was varied while the concentration of PEA and oil/water ratio was held constant. As shown in Figure 2.5, it was found that increasing the concentration of PVA decreased particle diameter; however, the concentration is limited by the aqueous solubility. Therefore, a saturated solution of 20 mg/mL was used in the optimum procedure.

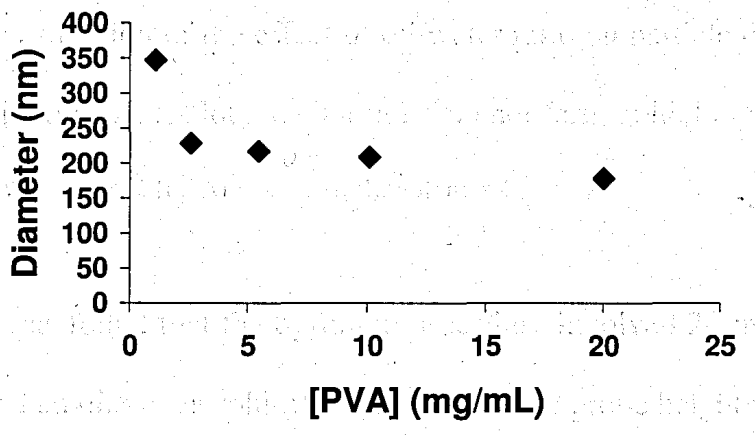

Figure 2.5: An investigation of the effect of [PVA] on particle diameter shows that as the [PVA] is increased, the particle size decreases.

Parameters: Oil/Water Ratio = 1/10, [PEA] = 25 mg/mL, polymer **4**

Note: aqueous solubility limits the maximum [PVA]

Finally, the oil/water volume ratio was varied while keeping the concentration of PVA and PEA constant. As shown in Figure 2.6, it was found that the minimum diameter occurred at a ratio of 0.05.

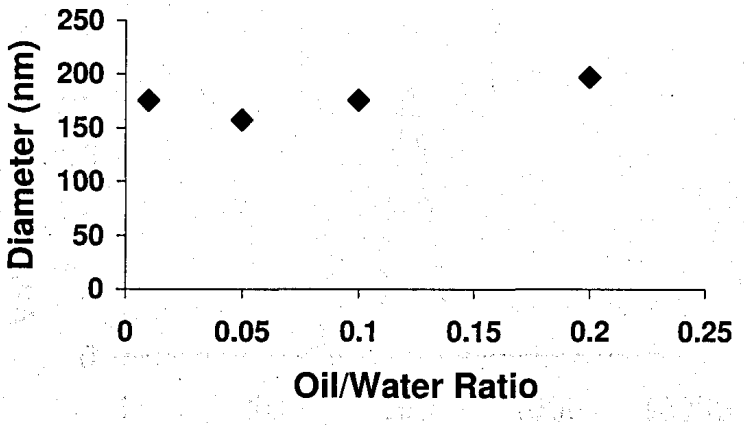

Figure 2.6: An investigation of the effect of oil/water ratio on particle diameter does not show an effect on particle size. Note that particles do not form at higher ratios.

Parameters: [PVA] = 11.5 mg/mL, [PEA] = 25 mg/mL, polymer 4

Overall, it was found that the optimum procedure involved 20 mg/mL of PVA, 5 mg/mL of PEA, and an oil/water volume ratio of 0.05. The probe height was set at 1.5 cm and the volume of water used was 10 mL. According to dynamic light scattering (DLS), the diameter of particles produced was approximately 120 nm (Figure 2.7) which is an order of magnitude smaller than previously reported.[33] The PDI of the particles was also very low, only 0.041, indicating the particles are nearly uniform in size, a necessity if the system will be used clinically. The procedure was repeated for a variety of PEAs, all producing similar results. Therefore, the general procedure is versatile with respect to polymer composition and can be extended to other systems.

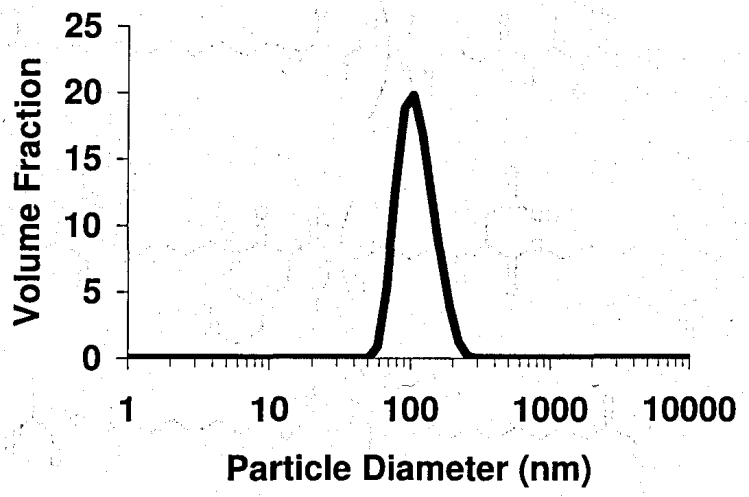

Figure 2.7: DLS trace of NP from polymer **6**. Note that the x axis is in a logarithmic scale.

D = 118.4 nm, PDI = 0.041

2.2.3 Synthesis of Polymers with Pendant Functional Groups

Functional polymers were synthesized according to published procedures.[40] PEAs of various diols, diacids, and amino acids were synthesized in order to assess a range of possible applications for the polymers. The materials were characterized by ^{1}H NMR and GPC and four unique PEAs, polymers **5-8**, shown in Figure 2.8, were isolated for testing as potential drug delivery vehicles. Polymers **5** and **6** were made using a solution polymerization technique due to the short chain length of succinic acid while polymers **7** and **8** which used sebacic acid were made using an interfacial technique. Both methods produce random copolymers with repeating ester and amide bonds.

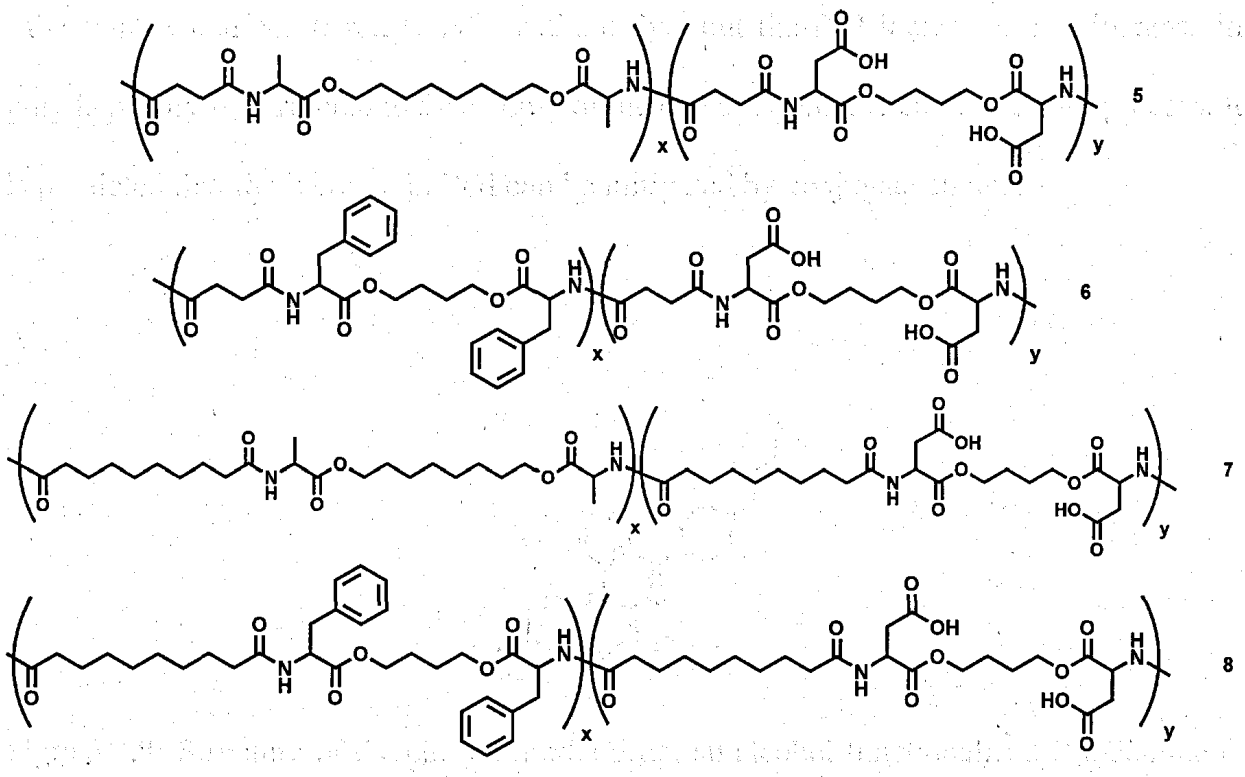

Figure 2.8: Structures of functionalized PEAs. Each PEA contains approximately 10 mol% of the aspartic acid unit randomly distributed throughout the polymer backbone.

2.2.4 Preparation of Nanoparticles Containing Covalently Immobilized Model Drug

Alcohol functionalized Rhodamine B was used as a model drug in order to assess the loading ability of the nanoparticles. This Rhodamine B derivative, shown in Figure 2.9, is highly absorbent and fluorescent, making it an ideal model for a drug molecule. The dye was bonded to the aspartic acid using dicyclohexylcarbodiimide (DCC) to form a hydrolyzable ester linkage prior to particle formation. The dye/polymer complex was characterized by ultraviolet-visible (UV-Vis) spectroscopy prior to particle formation, and then formed into nanoparticles using the aforementioned procedure. Figure 2.10 displays the DLS results for the resulting nanoparticles. The average diameter remains

the same when compared to NPs without dye, but the PDI increases. The increase in polydispersity is attributed to π-stacking of the dye affecting the emulsification process. It is predicted that the increase in PDI can be mitigated by conjugate choice.

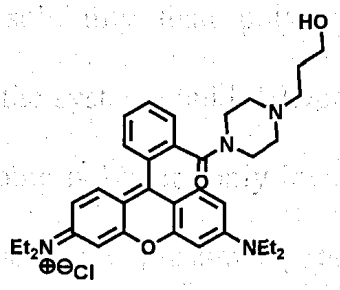

Figure 2.9: Structure of the chosen model drug, an alcohol functionalized Rhodamine B derivative.

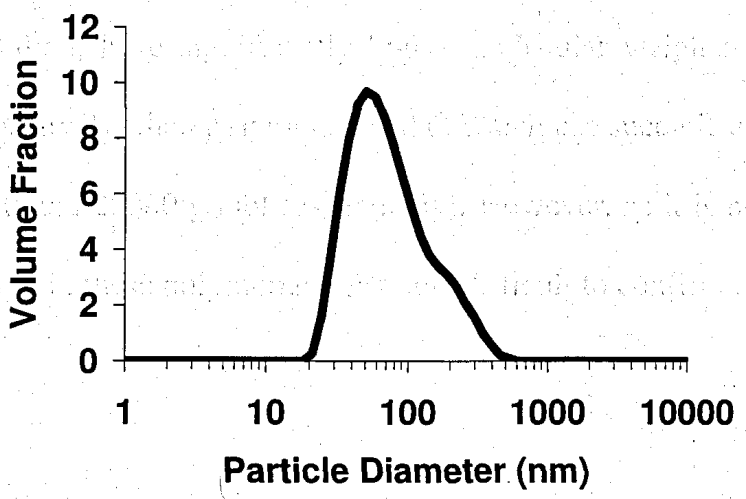

Figure 2.10: DLS trace of NP formed from dye-conjugated polymer **6**. Note that the x axis is in a logarithmic scale.

D = 116.4 nm, PDI = 0.261

Preliminary degradation studies were performed on a series of NPs from the different functional polymers having covalently immobilized dye to determine the one with the best degradation kinetics. As shown in Figure 2.11, the release rate can be engineered by monomer choice, creating a family of PEA drug delivery vehicles with varying pharmacokinetics. Polymer **6** was chosen for further study as it had the fastest release and had much better solubility than polymer **5,** facilitating synthesis and expanding the list of candidates the system could deliver. Interestingly, the nanoparticles composed of the more hydrophobic polymers only release negligible quantities of drug over the time scale of this experiment, presumably due to poor water access to the nanoparticle core, resulting in very slow ester hydrolysis rates. However, it should also be noted that the polymer molecular weights vary with monomer selection and the lack of release can possibly be attributed to molecular weight effects rather than increased hydrophobicity. Polymers **7** and **8**, which used sebacic acid and the interfacial polymerization method, have significantly higher molecular weights (M_w= 32000 and 101000 g/mol respectively) than polymers **5** and **6**, which use succinic acid and a solution method (M_w= 7700 and 20000 g/mol respectively). However, as it is not easy to control the molecular weight in these polymerizations, it is difficult to confirm this.

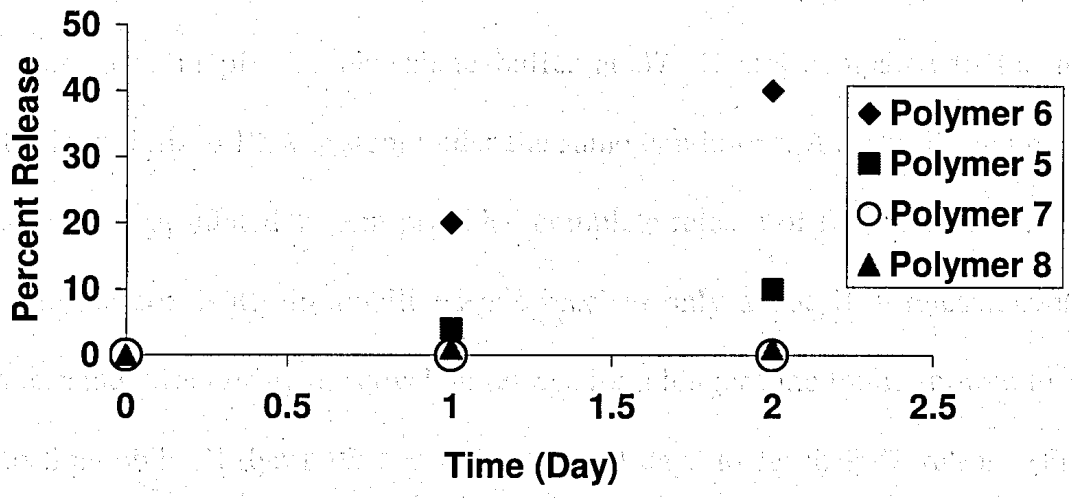

Figure 2.11: Effect of polymer choice on release rates of covalently immobilized Rhodamine.

2.2.5 *Characterization and Application of the Nanoparticles*

Through UV-Vis measurements it was found that 41% of the pendant aspartic acid handles on polymer **6** were conjugated with the Rhodamine derivative, corresponding to a drug loading of 7% (mass of dye/mass of nanoparticles). In order to compare how effectively the immobilization reduces the rate of drug release a control with physically encapsulated Rhodamine was made. Rather than immobilizing the Rhodamine on the polymer, the model drug was added to the organic phase during NP formation where it will accumulate in the NP center. The driving force for forming a concentration gradient is lowering the overall energy of the system by minimizing unfavorable polar/non-polar interactions between the Rhodamine and water and increasing favorable non-polar/non-polar interactions with the polymer core. In this case, there is no covalent bond anchoring the model drug to the NP, so the release profile may

be diffusional and display a burst. Release studies on the physically encapsulated control were done in pH 7.4 phosphate buffer at 37 °C and compared to the novel covalently immobilized PEA system under the same conditions. As seen in Figure 2.12, the physically encapsulated system provided complete release of Rhodamine in about 9 hours while the covalently immobilized one reached only about 10% release over the same time frame. Monitoring the covalent release for a longer time frame showed that the covalently immobilized dye took approximately 20 days to reach 90% release (Figure 2.13). This result shows the utility of the PEA's functional handles for covalent immobilization and the system's ability to control release rates. The model drug was released in a time frame that is considered therapeutically relevant,[22,30,41-44] making it a promising candidate for future applications.

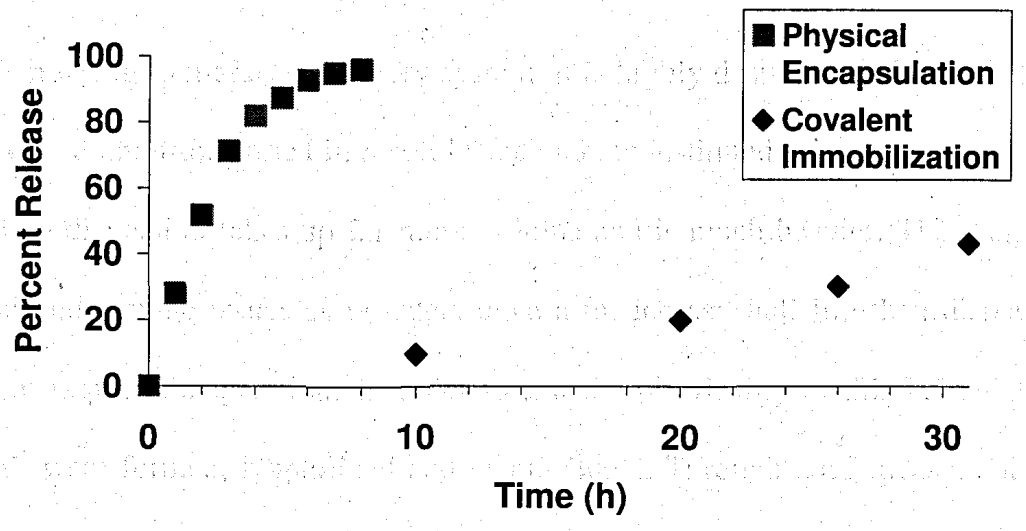

Figure 2.12: Comparing the release of physically encapsulated vs. covalently immobilized Rhodamine. The covalently immobilized drug released much more slowly

than the non-covalently immobilized drug, indicating that hydrolysis rather than diffusion is the rate limiting step in the drug release.

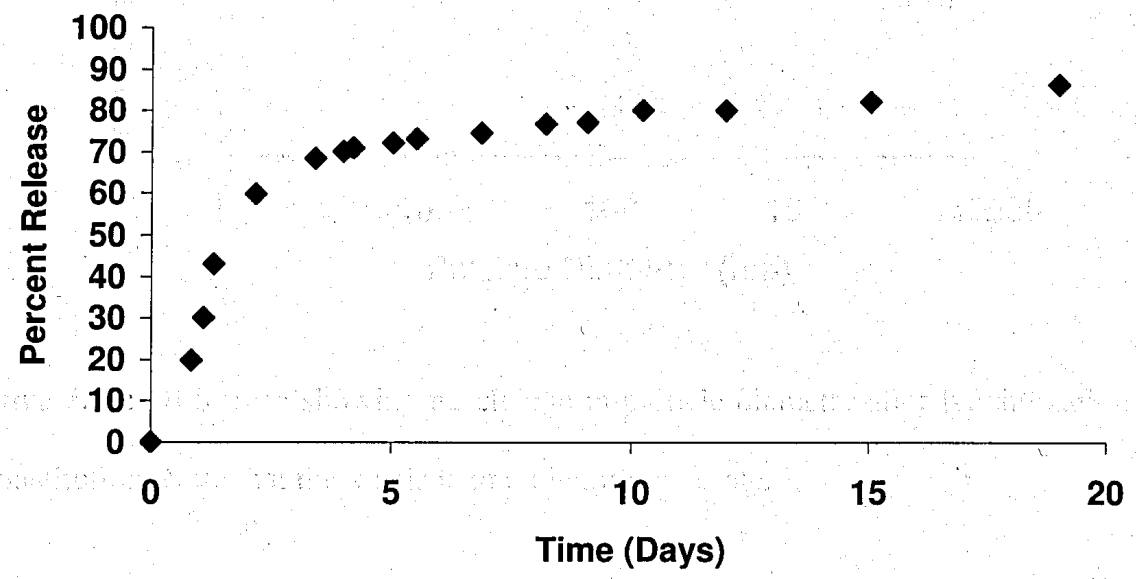

Figure 2.13: Long time frame release of covalently immobilized Rhodamine.

When trying to market a delivery system, it is highly desired that the formulation can be packaged and transported in a solid state and reconstituted prior to injection since the water in a dispersion takes up far more volume and is much heavier. There are also degradation and storage issues as powders have a far longer shelf life than dispersions and may not require refrigeration. In order to test the practicality of this PEA delivery system, NPs were formed, lyophilized and reconstituted. Through DLS measurements it was found that there was no change in NP diameter upon reconstitution (Figure 2.14). Hydrodynamic diameter and polydispersity were actually slightly smaller upon reconstitution, probably because the DLS measurement was taken directly after sonication while the pre-lyophilization measurement was done after only stirring.

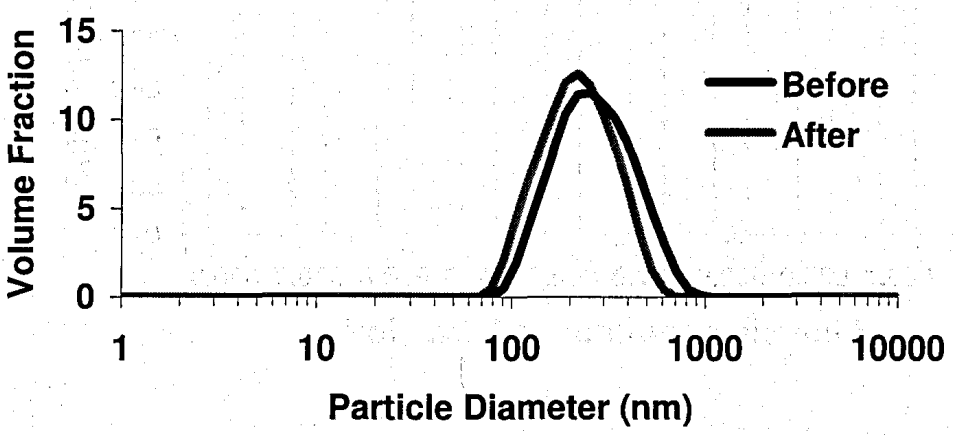

Figure 2.14: DLS trace showing no change in particle diameter after lyophilization and reconstitution. Note that the x axis is in a logarithmic scale.

In order to assess the toxicity of the NP, an MTT assay was run. In an MTT assay, 3-(4,5-Dimethylthiazol-2-yl)-2,5-diphenyltetrazolium bromide (MTT) is reduced to a purple formazan by living cells. This formazan is insoluble so a solubilizing solution is used to create a solution that can be measured using UV-Vis spectroscopy. Since the reduction is done by living cells, the absorbance of formazan will be proportional to the cell viability.[45] Over the course of 48 hours, it was found that at concentrations up to 2 mg/mL, the highest concentration investigated, the NP exhibited very low toxicity (Figure 2.15). Rough calculations predict that a therapeutically useful delivery system based on PEA NPs and dactinomycin would have a NP concentration between 0.125 and 0.25 mg/mL. This calculation assumed no change in drug loading and administration through an IV.

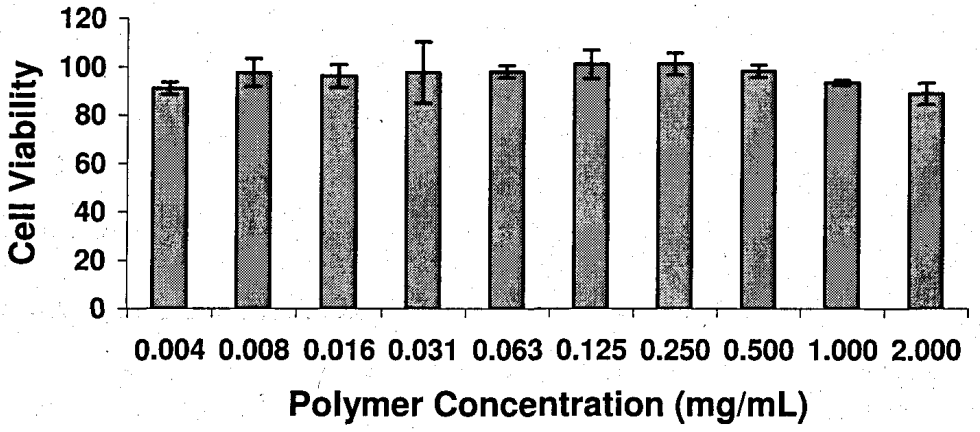

Figure 2.15: MTT assay displaying low PEA NP toxicity.

2.3 Conclusions

By employing a more powerful sonication method and running a series of optimization experiments, the procedure for creating PEA nanoparticles was significantly improved relative to previous reports,[33] resulting in the formation of nanoparticles of appropriate size to circulate in vivo. In addition, our synthetic approach for the preparation of PEAs containing pendant carboxylic acids was used to prepare nanoparticles from these functional polymers. An alcohol functionalized Rhodamine B derivative was chosen as a model drug and was coupled to the PEA prior to NP synthesis. It was found that the covalently immobilized model drug was released far slower than a traditional physically encapsulated control. In addition, this system is potentially capable of delivering a wide range of therapeutics, can be dried and reconstituted for convenient storage and transport, and the remaining pendant carboxylic acids can potentially be further conjugated with targeting ligands or dyes for imaging. This covalently

immobilized nanocarrier displays great promise for applications in sustained release drug delivery.

2.4 Experimental

2.4.0 General Procedure and Methods

Solvents were purchased from Caledon Labs (Georgetown, ON). All other chemicals were purchased from Sigma Aldrich (Milwaukee, WI) or Alfa Aesar (Ward Hill, MA). Unless noted otherwise, all chemicals were used as received. Anhydrous dichloromethane and *N,N*-dimethylacetamide (DMA) were distilled over CaH_2. Tetrahydrofuran (THF) was obtained from a solvent purification system. Infrared (IR) spectra were obtained using a Bruker Tensor 27 instrument as films from dichloromethane on NaCl plates. ^{1}H NMR spectra were obtained at 400 MHz on a Varian Mercury 400 Spectrometer. Chemical shifts are reported in ppm and are calibrated against residual solvent signals of $CDCl_3$ (δ7.27) or dimethylsulfoxide (DMSO-d_6) (δ2.54). All coupling constants (J) are reported in Hz. Gel permeation chromatography data were obtained using a Waters 2695 separations module equipped with a Waters 2414 refractive index detector (Waters Limited, Mississauga, ON) and two PLgel 5 μm mixed-D (300 mm x 7.5 mm) columns connected in series (Varian Canada). Samples (5 mg/mL) dissolved in the eluent, which comprised 10 mM LiBr and 1% (v/v) NEt_3 in DMF at 85 °C were injected (100 μL) at a flow rate of 1 mL/min and calibrated against either poly(styrene) or poly(ethylene glycol) standards. Molecular weights are reported in grams/mol (g/mol).

2.4.1 *Procedure for Solution Polymerizations of Poly(ester amide)s without Pendant Functional Groups*

2.4.1.1 Synthesis of Polymer **1**

A di-*p*-nitrophenyl succinate monomer (1.5 g, 3.3 mmol, 1.0 equiv.) and a di-*p*-toluenesulfonic acid salt monomer from alanine and octanediol (2.0 g, 3.3 mmol, 1.0 equiv.) were combined in a round bottom flask, evacuated and purged with argon. Distilled DMA (4.0 mL) was added to these monomers and the resulting mixture was heated to 60°C. Triethylamine (1.0 mL, 7.3 mmol, 2.2 equiv.) was then added dropwise to the solution and the temperature was raised to 70°C. The reaction mixture was maintained at this temperature for 48 h. The solution was then precipitated in cold ethyl acetate (250 mL) and further purified through Soxhlet extraction with ethyl acetate for 48 h to provide pure polymer **1**. Yield: 69%. Spectral data agreed with that previously reported.[40] GPC: M_n = 29000, M_w = 45000, PDI = 1.7.

2.4.2 *Procedure for Interfacial Polymerizations of Poly(ester amide)s without Pendant Functional Groups*

2.4.2.1 Synthesis of Polymer **2**

Sebacoyl chloride (1.1 mL, 5.0 mmol, 1.0 equiv.) was added to anhydrous dichloromethane (30 mL), and added dropwise over 30 min to an aqueous solution (30

mL) containing a di-*p*-toluenesulfonic acid salt monomer from alanine and octanediol (3.2 g, 5.0 mmol, 1.0 equiv.) and sodium carbonate (1.1 g, 10 mmol, 2.0 equiv.) and allowed to react for 12 h. Upon completion of the reaction, the solvent was removed *in vacuo*. The polymer was then washed with water prior to purification via Soxhlet extraction with ethyl acetate for 48 h and dried *in vacuo* yielding polymer **2**. Yield: 68%. Spectral data agreed with those previously reported.[28] GPC: M_n = 45000, M_w = 63000, PDI = 1.38.

2.4.2.2 Synthesis of Polymer **3**

The same procedure for preparing polymer **2** was used except a di-*p*-toluenesulfonic acid salt monomer from phenylalanine and butanediol (3.6 g, 5.0 mmol, 1.0 equiv.) was used instead. Yield: 78%. Spectral data agreed with those previously reported.[28] GPC: M_n = 63000, M_w = 168000, PDI = 2.65.

2.4.2.3 Synthesis of Polymer **4**

The same procedure for preparing polymer **2** was used except di-*p*-toluenesulfonic acid salt monomer from phenylalanine and octanediol (3.9 g, 5.0 mmol, 1.0 equiv.) was used instead. Yield: 60%. Spectral data agreed with those previously reported.[28] GPC: M_n = 63000, M_w = 130000, PDI = 2.14.

2.4.3 Procedure for Solution Polymerizations of Functional Poly(ester amide)s

2.4.3.1 Synthesis of Polymer **5**

A di-*p*-nitrophenyl succinate monomer (1.05 g, 2.9 mmol, 1.0 equiv.), a di-*p*-toluenesulfonic acid salt monomer from alanine and octanediol (1.66 g, 2.6 mmol, 0.9 equiv.), and a hydrogenated Asp(OtBu)-butanediol monomer (0.13 g, 0.29 mmol, 0.1 equiv) were combined in a round bottom flask, evacuated and purged with argon. Distilled DMA (5.0 mL) was added to these monomers and the resulting mixture was heated to 60°C. Distilled triethylamine (0.9 mL, 6.4 mmol, 2.2 equiv.) was then added dropwise to the solution and the temperature was raised to 70°C. The reaction mixture was maintained at this temperature for 48 h. The solution was then precipitated in cold ethyl acetate (250 mL) and collected. The crude product was redissolved in DMF and dialyzed for at least 8 h twice. The solvent was removed *in vacuo* before dissolution in 4 mL of 1:1 trifluoroacetic acid:dichloromethane. This solution was stirred for 2 h in a flame dried flask under an argon atmosphere. The solvent was removed under a stream of air with 3 washes of 15 mL of toluene to introduce an azeotrope. Residual solvent was removed *in vacuo* resulting in a brown solid, polymer **5**. Yield: 71%. Spectral data agreed with those previously reported.[40] GPC: M_n = 6600, M_w = 7700, PDI = 1.17.

2.4.3.2 Synthesis of Polymer **6**

The same procedure as polymer **5** was followed except that a di-*p*-toluenesulfonic acid salt monomer from phenylalanine and butanediol (1.8 g, 2.6 mmol, 0.9 equiv.) was

used and after the reaction, the solution was diluted with dichloromethane and washed with 1 M $KHSO_4$ (2 x 75 mL) followed by 10% Na_2CO_3 (3 x 75 mL). The organic phase was dried over $MgSO_4$, filtered before trifluoroacetic acid deprotection. Yield: 62%. Spectral data agreed with those previously reported.[40] GPC: M_n = 15000, M_w = 20000, PDI = 1.33

2.4.4 Procedure for Interfacial Polymerizations of Functional Poly(ester amide)s

2.4.4.1 Synthesis of Polymer **7**

A di-*p*-toluenesulfonic acid salt monomer from alanine and octanediol (2.3 g, 3.6 mmol, 0.9 equiv.) and sodium carbonate (0.85 g, 8.0 mmol, 2.0 equiv.) were dissolved in distilled water (30 mL). A diamine made from deprotected aspartic acid and butanediol (0.17 g, 0.4 mmol, 0.1 equiv.) was dissolved in dichloromethane (15 mL) and added to the aqueous phase and allowed to mix for 30 min. Sebacoyl chloride (1.0 mL, 4.0 mmol, 1.0 equiv.) diluted in anhydrous dichloromethane (15 mL), was added dropwise over 30 min to the biphasic solution and was allowed to react for 24 h. Upon completion of the reaction, solvent was removed *in vacuo*. The functional poly(ester amide) was redissolved in DMF permitting filtration of the insoluble salts. The filtrate was then dialyzed against DMF for at least 8 h twice. The solvent was removed *in vacuo* before dissolution in 4 mL of 1:1 trifluoroacetic acid:dichloromethane. This solution was stirred for 2 h in a flame dried flask under an argon atmosphere. The solvent was removed under a stream of air with 3 washes of 15 mL of toluene to introduce an azeotrope. Residual solvent was removed *in vacuo* resulting in a brown solid, polymer **7**. Yield:

86%. ^{1}H NMR (400 MHz, $CDCl_3$): δ 6.17 (d, 2H, J = 7.4, -N*H*-CO-), 4.59 (m, 2H, -C$_\alpha$*H*), 4.18-4.08 (m, 4H, -C(O)O-C*H*$_2$-), 2.23-2.17 (m, 4H, -NH-C(O)-C*H*$_2$-), 1.69-1.58 (m, 8H, -C(O)O-CH$_2$-C*H*$_2$-, -NH-C(O)-CH$_2$-C*H*$_2$-), 1.43 (s, 1.8H, -C(O)O-C(CH$_3$)$_3$, 1.40-1.27 (m, 22H, -C$_\alpha$H-C*H*$_3$, -C(O)O-CH$_2$-CH$_2$-(C*H*$_2$)$_4$-, -NH-C(O)-CH$_2$-CH$_2$-(C*H*$_2$)$_4$-). GPC: M_n = 18000, M_w = 32000, PDI = 1.8.

2.4.4.2 Synthesis of Polymer **8**

The same procedure for the synthesis of polymer 7 was used, except that a di-p-toluenesulfonic acid salt monomer from phenylalanine and butanediol (2.6 g, 3.6 mmol, 0.9 equiv.) was used instead. Yield: 74% 1H NMR (400 MHz, CDCl3): δ 7.33-7.07 (m, 10H, Ph), 6.03 (d, 2H, J = 7.8, -NH-CO-), 4.92-4.83 (m, 2H, -CαH), 4.17-3.98 (m, 4H, -C(O)O-CH2-), 3.17-3.03 (m, 4H, -CαH-CH2-Ph), 2.16 (t, 4H, J = 7.4, -NH-C(O)-CH2-), 1.66-1.50 (m, 8H, -C(O)O-CH2-CH2-, -NH-C(O)-CH2-CH2-), 1.43 (s, 1.8H, -C(O)O-C(CH$_3$)$_3$ 1.33-1.19 (m, 8H, -NH-C(O)-CH2-CH2-(CH2-)4. GPC: Mn = 43000, Mw = 101000, PDI = 2.4.

2.4.5 General Procedure for Rhodamine Derivative Coupling to PEAs

2.4.5.1 Rhodamine Dye Coupling to Polymer **5**

Polymer **5** (0.01 g, 27 μmol), DPTS (0.006 g, 20.5 μmol, 5 equiv. relative to the number of pendant carboxylic acids), DMAP (0.003 g, 20.5 μmol, 5 equiv. relative to the number of pendant carboxylic acids) and the Rhodamine derivative (0.021 g, 41.0 μmol,

10 equiv. relative to the number of pendant carboxylic acids) were combined in a round bottom flask, evacuated and purged with argon. Distilled CH_2Cl_2 (4 mL) was added and the mixture was allowed to stir. Upon complete dissolution, DCC (0.017 g, 82.0 µmol, 20 equiv. relative to the number of pendant carboxylic acids) was added and the solution was covered in aluminum foil and allowed to stir overnight. The solvent was removed *in vacuo* and the dark pink product was dialyzed against DMF with molecular weight cut off (MWCO) 12-14 kg/mol for 24 hours with changing of the dialysate every 8 hours (dialysis beaker covered in aluminum foil to prevent photo-bleaching). The solvent was removed *in vacuo* yielding a dark pink solid. Yield: 90%.

2.4.5.2 Rhodamine Dye Coupling to Polymer **6**

The same procedure for the coupling to polymer **5** was used except polymer **6** (0.01 g, 21 µmol) was used instead. Yield: 91%.

2.4.5.3 Rhodamine Dye Coupling to Polymer **7**

The same procedure for the coupling to polymer **5** was used except polymer **7** (0.01 g, 16 µmol) was used instead. Yield: 89%.

2.4.5.4 Rhodamine Dye Coupling to Polymer **8**

The same procedure for the coupling to polymer **5** was used except polymer **8** (0.01 g, 18 µmol) was used instead. Yield: 87%.

2.4.6 *Nanoparticle Formation Procedure*

Poly(vinyl alcohol) with a MW of 33 kg/mol and 87-89% hydrolyzed (0.2 g, 6.1 μmol) was dissolved in 10 mL of distilled water with heavy sonication (but no heating as heating would cause precipitation of polymer prior to NP formation). The chosen polymer (5 mg) was put in a 5 dram vial and 0.5 mL of chloroform was added. Upon dissolution, the PVA solution was added and the two phase mixture was sonicated with a Branson Digital Sonifier. The probe tip was kept 1.5 cm from the vial bottom and the amplitude was set to 25%. The mixture was sonicated for 2 minutes with pulses of 30 seconds on and 10 seconds off. Once sonicated, the latex was stirred overnight to remove the chloroform. The dispersion was put in an ultrafiltration apparatus with a membrane MWCO of 500000 g/mol. The dispersion was diluted and filtered a total of four times.

2.4.7 *Determination of Dye Loading*

Dye coupled polymer (0.015 g) was dissolved in 2 mL of THF and 4 mL of 1 M KOH was added. After stirring for 48 hours, while covered with aluminum foil, 0.2 mL of the solution was removed and diluted with 2.5 mL of distilled water. UV-Vis measurements were performed using a molar absorptivity of 76470 $M^{-1}cm^{-1}$.

2.4.8 Covalently Immobilized Nanoparticle Release Study Procedure

The same nanoparticle formation procedure was followed using dye-conjugated PEA but afterwards the dispersion was placed in a Slide-A-Lyzer dialysis cassette and kept at 37 °C in pH 7.4 phosphate buffer. UV-Vis measurements were taken of the internal volume and therefore the absorbance measured includes light scattering from the particles. For every measurement, a power curve was fitted to the scattering and subtracted from the measured data in order to decouple the absorbance. Each fitted curve had an R^2 value of at least 0.98.

2.4.9 Physically Encapsulated Nanoparticle Release Study Procedure

The same procedure for the covalently immobilized release study was used however non-dye-conjugated PEA was used and 0.0025 g of Rhodamine derivative was dissolved in the organic phase prior to sonication.

2.5 References

(1) Riehemann, K.; Schneider, S. W.; Luger, T. A.; Godin, B.; Ferrari, M.; Fuchs, H. *Angew. Chem., Int. Ed.* **2009**, *48*, 872.

(2) Theis, T.; Parr, D.; Binks, P.; Ying, J.; Drexler, K. E.; Schepers, E.; Mullis, K.; Bai, C. L.; Boland, J. J.; Langer, R.; Dobson, P.; Rao, C. N. R.; Ferrari, M. *Nat. Nanotechnol.* **2006**, *1*, 8.

(3) Bhardwaj, V.; Ankola, D. D.; Gupta, S. C.; Schneider, M.; Lehr, C. M.; Kumar, M. N. V. R. *Pharm. Res.* **2009**, *26*, 2495.

(4) Kalaria, D. R.; Sharma, G.; Beniwal, V.; Kumar, M. N. V. R. *Pharm. Res.* **2009**, *26*, 492.

(5) Hariharan, S.; Bhardwaj, V.; Bala, I.; Sitterberg, J.; Bakowsky, U.; Kumar, M. *Pharm. Res.* **2006**, *23*, 184.

(6) Mittal, G.; Sahana, D. K.; Bhardwaj, V.; Kumar, M. N. V. R. *J. Controlled Release* **2007**, *119*, 77.

(7) Italia, J. L.; Yahya, M. M.; Singh, D.; Kumar, M. N. V. R. *Pharm. Res.* **2009**, *26*, 1324.

(8) Italia, J. L.; Bhatt, D. K.; Bhardwaj, V.; Tikoo, K.; Kumar, M. N. V. R. *J. Controlled Release* **2007**, *119*, 197.

(9) Meena, A. K.; Ratnam, D. V.; Chandraiah, G.; Ankola, D. D.; Rao, P. R.; Kumar, M. N. V. R. *Lipids* **2008**, *43*, 231.

(10) Wu, Y.; Yang, W. L.; Wang, C. C.; Hu, J. H.; Fu, S. K. *Int. J. Pharm.* **2005**, *295*, 235.

(11) Colonna, C.; Conti, B.; Perugini, P.; Pavanetto, F.; Modena, T.; Dorati, R.; Genta, I. *J. Microencapsulation* **2007**, *24*, 553.

(12) Ma, Z. S.; Yeoh, H. H.; Lim, L. Y. *J. Pharm. Sci.* **2002**, *91*, 1396.

(13) Janes, K. A.; Fresneau, M. P.; Marazuela, A.; Fabra, A.; Alonso, M. J. *J. Controlled Release* **2001**, *73*, 255.

(14) Chawla, J. S.; Amiji, M. M. *Int. J. Pharm.* **2002**, *249*, 127.

(15) Shim, J.; Kang, H. S.; Park, W. S.; Han, S. H.; Kim, J.; Chang, I. S. *J. Controlled Release* **2004**, *97*, 477.

(16) Alvarez-Roman, R.; Naik, A.; Kalia, Y. N.; Guy, R. H.; Fessi, H. *Pharm. Res.* **2004**, *21*, 1818.

(17) Cai, X. J.; Xu, Y. Y. *Cytotechnology* **2011**, *63*, 319.

(18) Ferrari, M. *Nat. Rev. Cancer* **2005**, *5*, 161.

(19) Yeo, Y.; Baek, N.; Park, K. *Biotechnol. Bioprocess Eng.* **2001**, *6*, 213.

(20) Caliceti, P.; Veronese, F. M. *Adv. Drug Delivery Rev.* **2003**, *55*, 1261.

(21) Moghimi, S. M.; Davis, S. S. *Crit. Rev. Ther. Drug Carrier Syst.* **1994**, *11*, 31.

(22) Huang, X.; Brazel, C. S. *J. Controlled Release* **2001**, *73*, 121.

(23) Rizi, K.; Green, R. J.; Khutoryanskaya, O.; Donaldson, M.; Williams, A. C. *J. Pharm. Pharmacol.* **2011**, *63*, 1141.

(24) Cheng, Y. Y.; Xu, T. W. *Eur. J. Med. Chem.* **2008**, *43*, 2291.

(25) Patri, A. K.; Kukowska-Latallo, J. F.; Baker, J. R. *Adv. Drug Delivery Rev.* **2005**, *57*, 2203.

(26) Jokhadze, G.; Machaidze, M.; Panosyan, H.; Chu, C. C.; Katsarava, R. *J. Biomater. Sci., Polym. Ed.* **2007**, *18*, 411.

(27) Lee, S. H.; Szinai, I.; Carpenter, K.; Katsarava, R.; Jokhadze, G.; Chu, C.-C.; Huang, Y.; Verbeken, E.; Bramwell, O.; De Scheerder, I.; Hong, M. K. *Coron. Artery Dis.* **2002**, *13*, 237.

(28) Knight, D. K.; Gillies, E. R.; Mequanint, K. *Biomacromolecules* **2011**, *12*, 2475.

(29) Del Valle, L. J.; Roca, D.; Franco, L.; Puiggalí, J.; Rodríguez-Galán, A. *J. Appl. Polym. Sci.* **2011**, *122*, 1953.

(30) Guo, K.; Chu, C. C. *J. Biomater. Sci., Polym. Ed.* **2007**, *18*, 489.

(31) Guo, K.; Chu, C. C. *Biomaterials* **2007**, *28*, 3284.

(32) Pang, X. A.; Chu, C. C. *Polymer* **2010**, *51*, 4200.

(33) Guo, K.; Chu, C. C. *J. Biomed. Mater. Res. B Appl. Biomater.* **2009**, *89B*, 491.

(34) Vera, M.; Puiggali, J.; Coudane, J. *J. Microencapsulation* **2006**, *23*, 686.

(35) Iyer, A. K.; Khaled, G.; Fang, J.; Maeda, H. *Drug Discov. Today* **2006**, *11*, 812.

(36) Liversidge, G. G.; Cundy, K. C. *Int. J. Pharm.* **1995**, *125*, 91.

(37) Sandhiya, S.; Dkhar, S. A.; Surendiran, A. *Fundam. Clin. Pharmacol.* **2009**, *23*, 263.

(38) Tsitlanadze, G.; Machaidze, M.; Kviria, T.; Djavakhishvili, N.; Chu, C. C.; Katsarava, R. *J. Biomater. Sci., Polym. Ed.* **2004**, *15*, 1.

(39) Lee, S.; Yang, S. C.; Heffernan, M. J.; Taylor, W. R.; Murthy, N. *Bioconjugate Chem.* **2007**, *18*, 4.

(40) Atkins, K. M.; Lopez, D.; Knight, D. K.; Mequanint, K.; Gillies, E. R. *J. Polym. Sci., Part A: Polym. Chem.* **2009**, *47*, 3757.

(41) Blanco, E.; Hsiao, A.; Mann, A. P.; Landry, M. G.; Meric-Bernstam, F.; Ferrari, M. *Cancer Sci.* **2011**, *102*, 1247.

(42) Gillies, E. R.; Frechet, J. M. J. *Bioconjugate Chem.* **2005**, *16*, 361.

(43) Preiss, M. R.; Bothun, G. D. *Expert Opin. Drug Deliv.* **2011**, *8*, 1025.

(44) Yokoyama, M.; Okano, T.; Sakurai, Y.; Kataoka, K. *J. Controlled Release* **1994**, *32*, 269.

(45) Mosmann, T. *J. Immunol. Methods* **1983**, *65*, 55.

Chapter Three:

Development of Poly(ethylene oxide)-Poly(ester amide) Graft Copolymers for Micellar Drug Delivery Vehicles

3.1 Introduction

Among the various polymer nanocarriers that have been investigated,[1-4] polymer micelles are attractive due to their ease of synthesis and their ability to be tuned.[1] Polymeric micelles are colloidal dispersions of amphiphilic polymers that can be used to increase the solubility and bioavailability of poorly soluble drugs as well as increase the *in vivo* circulation time due to nanoscale particle diameters and hydrophilic outer shells that inhibit phagocytic and renal clearance.[3] The extended circulation time leads to selective tumour accumulation via the enhanced permeability and retention (EPR) effect.[2-4]

One limitation of the delivery system discussed in Chapter 2 is that relatively large amounts of poly(vinyl alcohol) (PVA) are required in order to obtain nanoparticles (NPs) small enough to remain in circulation. While PVA is approved by the Food and Drug Administration for many applications, coating the nanoparticle surface may mask the properties of the poly(ester amide) (PEA), slowing its biodegradation, and preventing the conjugation of targeting moieties to the PEA's pendant functional groups. In addition, certain molecules were found to interact non-specifically with the surfactant layer, which impeded diffusion from the nanoparticle. Finally, the PVA layer may impede diffusion

from the nanoparticle and may increase the minimum particle diameter by increasing external phase viscosity at higher concentrations.[5]

In order to address these issues, poly(ethylene oxide) (PEO)-PEA graft copolymers were proposed. Such graft copolymers could be prepared by the conjugation of PEO to the pendant amine groups of PEAs previously reported by our group.[6,7] PEO was chosen for the hydrophilic block due to its strong hydrophilic properties as well as its capability for masking the presence of circulating foreign substances by shielding antigenic and immunogenic epitopes as well as preventing receptor-mediated uptake by the RES.[6] While the PEA backbone is quite hydrophobic, PEO is a well known hydrophilic polymer and by imparting amphiphilic properties to the PEA itself, the need for surfactant should be eliminated. The resulting copolymer should self assemble in aqueous media into micelles in the absence of surfactant addition.

Described here is the preparation of PEO-PEA graft copolymers and the study of their assembly into micelles. These micelles are very promising biomaterials due to their biodegradability. Under physiological conditions, the ester bonds in the backbone can be cleaved hydrolytically, while the amide bonds can potentially be cleaved enzymatically.[7-9] This biodegradation would ultimately result in the release of individual PEO chains that can be readily excreted from the body. In addition, while the conjugation of PEO would consume some pendant amine groups of the polymer, the remainder could be used to covalently immobilize drug molecules in order to control their release as described in Chapter 2. In addition, while one terminus of the PEO would be conjugated to the PEA, the other terminus could be used to conjugate bioactive moieties to target the micelles to

selective tissues, such as tumours. To the best of our knowledge, this work is the first example of polymeric micelles based on PEAs.

3.2 Results and Discussion

3.2.1 Synthesis of PEO-PEA graft copolymers

A PEA having pendant amine functional groups (Figure 3.1) was synthesized according to the previously published method.[9] Briefly, as shown in Scheme 3.1, an interfacial polymerization was performed using 1.0 equivalents of sebacoyl chloride **1**, 0.90 equivalents of the phenylalanine-based diamine **2**, and 0.1 equivalents of the lysine-based diamine **3**. The interfacial polymerization was performed with the diamines in the aqueous phase and the diacid chlorides in the dichloromethane organic phase. As shown in Scheme 3.2, the BOC protecting group was removed using trifluoroacetic acid (TFA). NMR spectroscopic characterization agreed with the previously published results[6,7] with the M_n and PDI of the polymer being 48000 g/mol and 1.5 respectively.

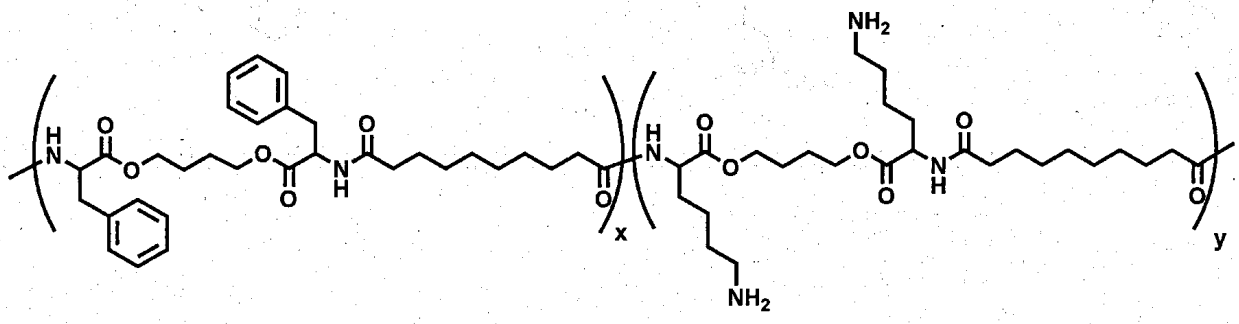

Figure 3.1: Structure of PEA with pendant amines.

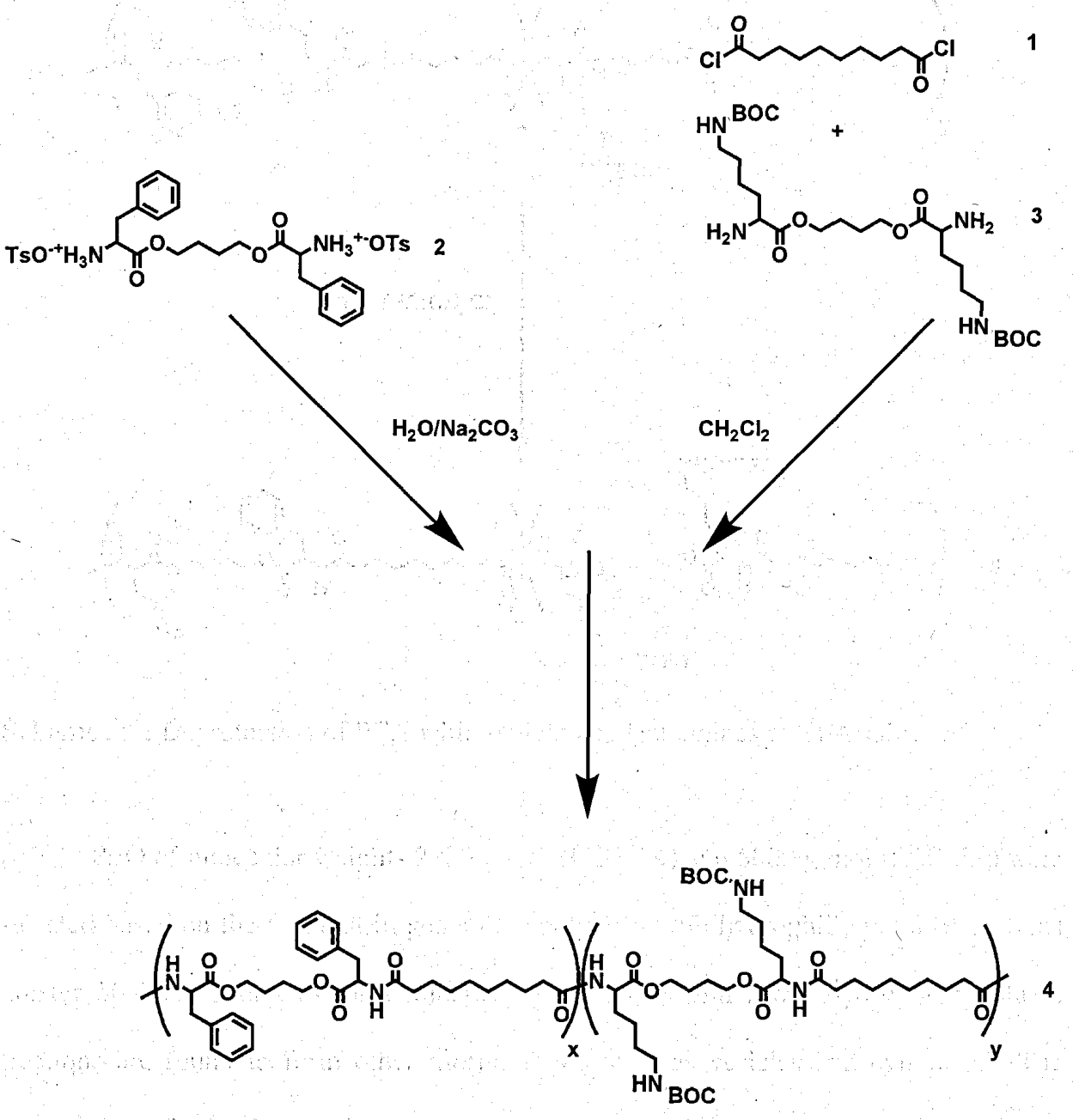

Scheme 3.1: Interfacial polymerization reaction conditions. Note that **x**:**y** = 9:1.

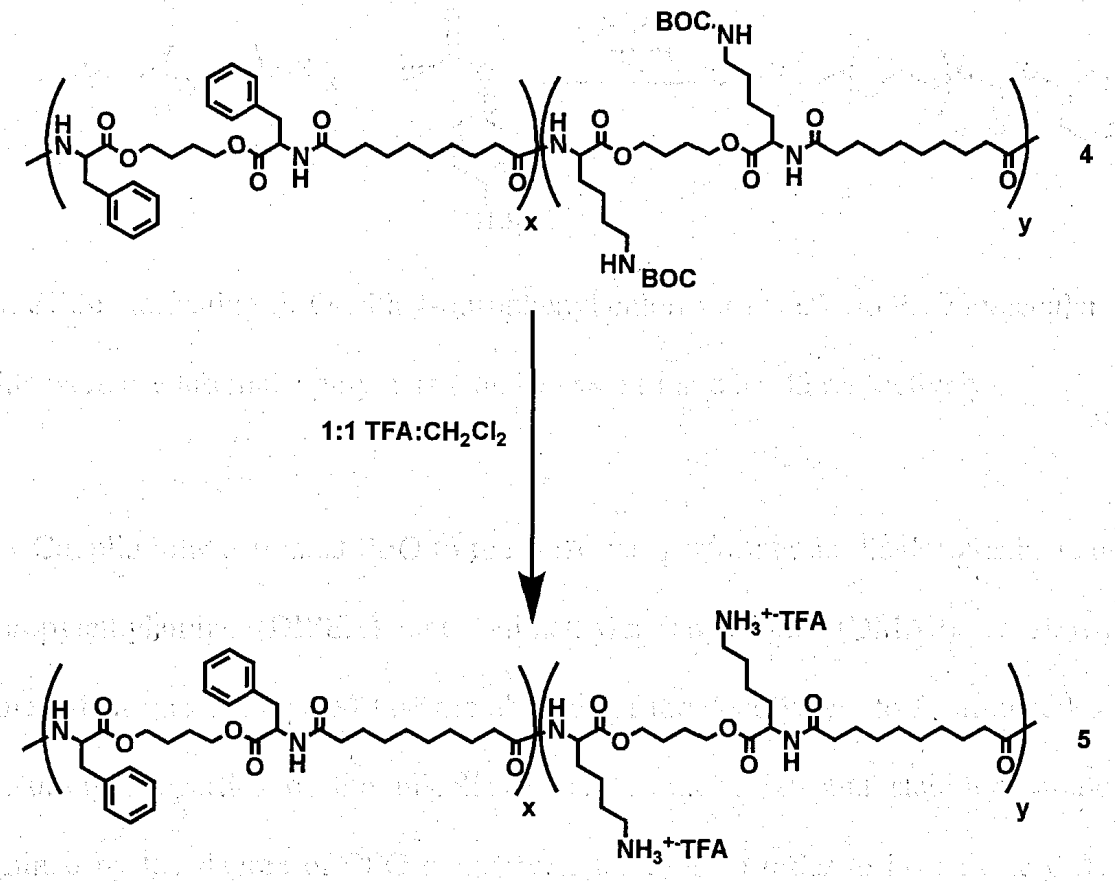

Scheme 3.2: Deprotection of PEA with to yield pendant amines as TFA salts.

PEO of molecular weights 2000 g/mol (PEO 2K) and 5000 g/mol (PEO 5K) were selected based on the fact that in general, copolymers with hydrophilic volume fractions greater 50% are found to form micelles, while those with lower hydrophilic volume fractions are found to form other morphologies such as vesicles and cylinders.[10] The conjugation of PEO 2K to 100% of the amines would provide a PEO weight content of 41% while the conjugation of PEO 5K to 100% of the pendant amines would provide a weight content of 64%. The conjugation reaction conditions can be adjusted to give fine control over the weight content of PEO in the copolymer. The conjugation reaction required activated PEOs which were synthesized by the reaction of PEO and 4-nitrophenyl chloroformate as shown in Scheme 3.3.

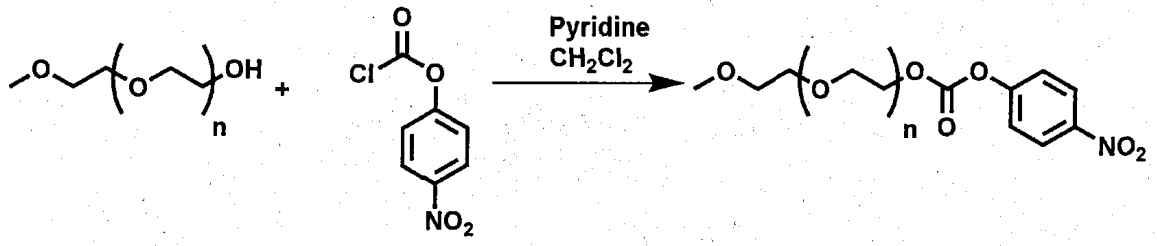

Scheme 3.3: Activating PEO with 4-nitrophenyl chloroformate. Two PEO molecular weights were used to make polymers **6** and **7** (n= 114 and n= 45 respectively).

Coupling the activated PEO to the PEA was performed in dichloromethane using diisopropylethylamine (DIPEA) and 4-dimethylaminopyridine (DMAP), as shown in Scheme 3.4. It was anticipated that the abilities of the copolymers to form micelles and the resulting properties of the micelles, such as their size and stability, would be determined by the degree of PEO coupling. Therefore, in order to investigate different PEO contents, either 0.85, 1.2, or 3 equivalents of PEO 5K relative to the number of pendant amines were used in the coupling to provide graft copolymers **8**, **9**, and **10** respectively. The coupling with PEO 2K was performed using 1.2 equivalents to provide graft copolymer **11**.

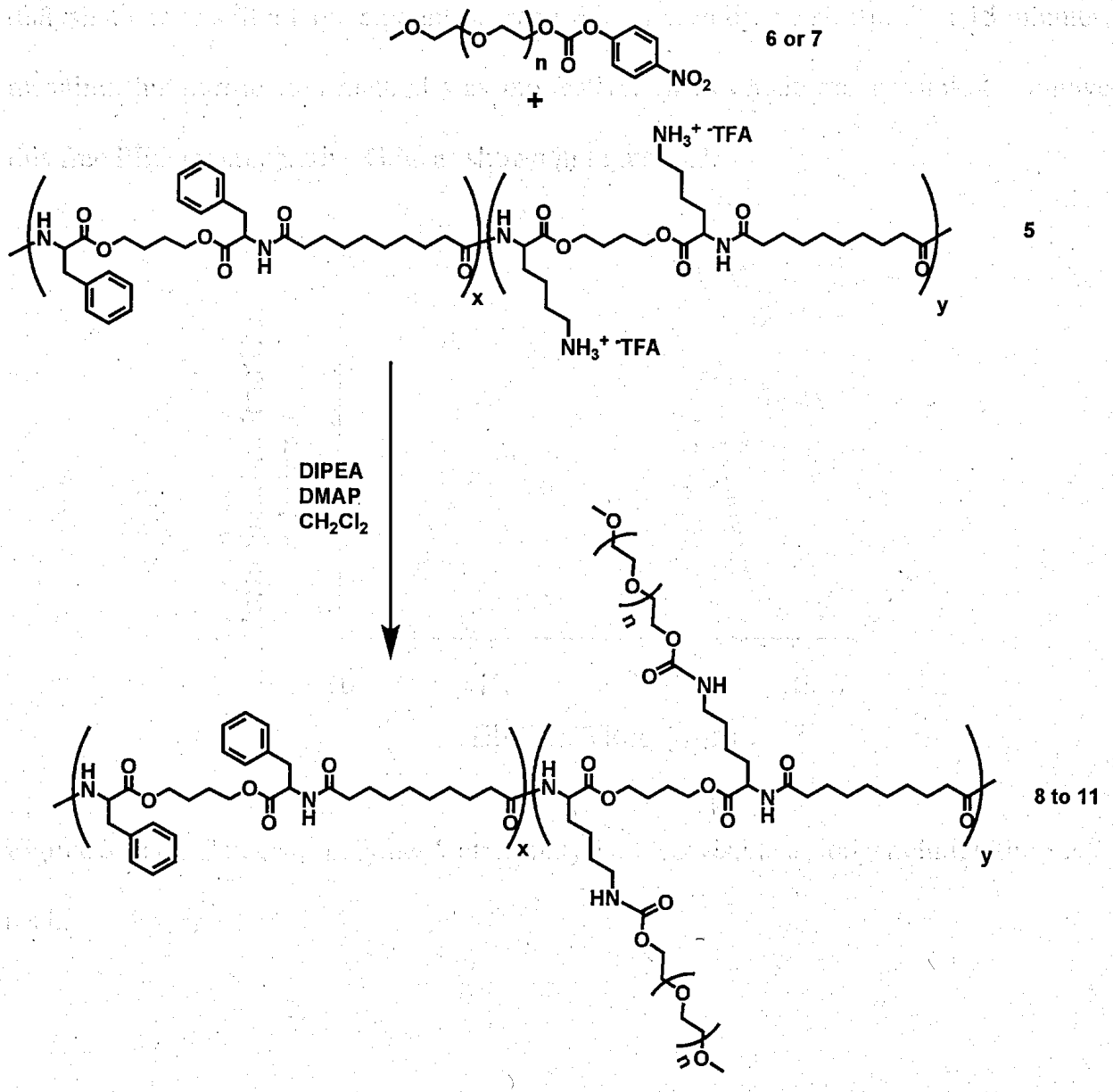

Scheme 3.4: Synthesis of PEO-PEA graft copolymers. Varying the MW and loading of PEO affords copolymer **8** through **11**.

Following the evaporation of the reaction solvent, the removal of free PEO was challenging. First, dialysis in water using a membrane with a 50000 g/mol molecular weight cut off (MWCO) was attempted. The dialysate was changed twice a day over the course of one week. The polymer suspension inside the dialysis bag was recovered and

dried *in vacuo*. The GPC chromatograph shown in Figure 3.2, indicates that after dialysis there is still a large amount of free PEO, as seen by the side peak at 15 minutes, meaning this purification method was ineffective. However, it was possible to remove this free PEO by preparative GPC as shown in Figure 3.3.

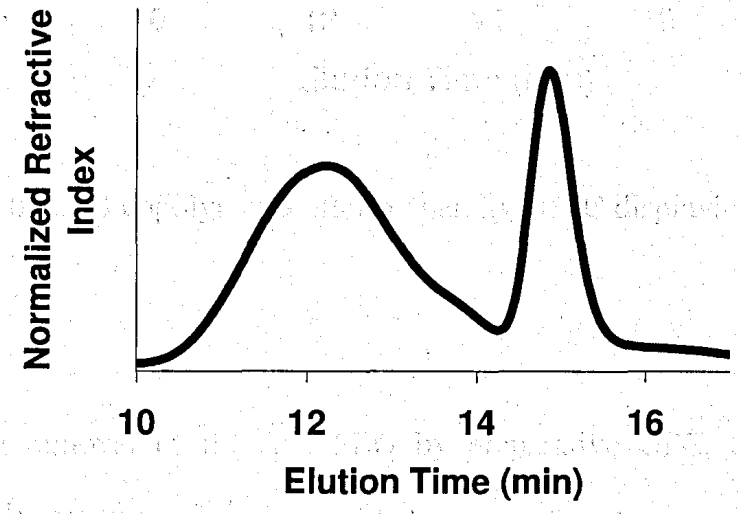

Figure 3.2: GPC trace of polymer **9** after dialysis. PEO visible as longer elution time side peak.

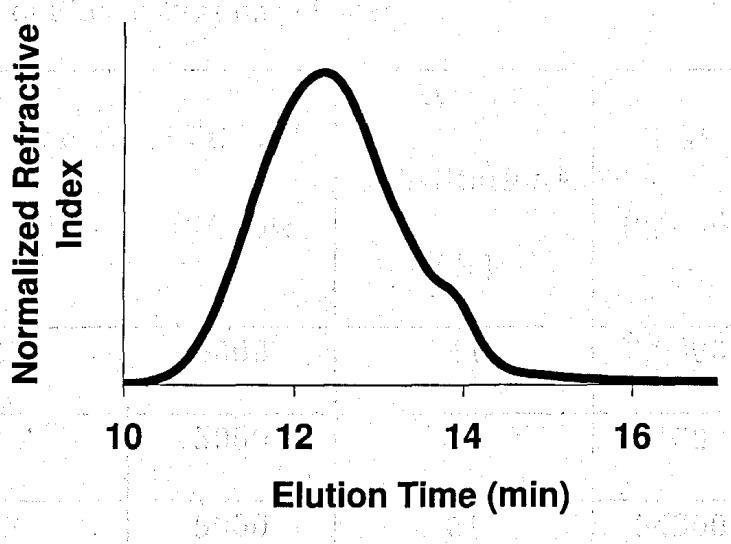

Figure 3.3: GPC trace of copolymer 9 after preparative GPC displaying effective removal of PEO.

Following removal of the free PEO by preparative GPC, the polymers were characterized by ^{1}H NMR spectroscopy and size exclusion chromatography. The results are summarized in Table 3.1. When 0.85 equivalents of PEO relative to the pendant amines were used, 41% of the amine groups were functionalized with PEO based on NMR analysis. Increasing the number of PEO equivalents to 1.2 led to an increase in the degree of functionalization to 50%, while using 3 equivalents provided 61% functionalization. Using PEO 2K, 1.2 equivalents provided a graft copolymer in which 53% of the amines were functionalized. As expected, the M_ns of the polymers increased with the degree of PEO functionalization as well as PEO MW.

Table 3.1: Effect of PEO loading on polymer

Polymer	Equivalents of PEO [a]	PEO MW (g/mol)	Lysine Substitution [b] (%)	M_n [c] (g/mol)	PDI
8	0.85	5000	41	30000	1.5
9	1.2	5000	50	31000	1.6
10	3	5000	61	34300	1.2
11	1.2	2000	53	24000	1.4

[a] During synthesis- relative to the number of lysine residues

[b] According to NMR integration

[c] Relative to poly(ethylene oxide)

3.2.2 Preparation of micelles

Multiple methods of micelle formation were investigated and compared using dynamic light scattering (DLS). Syringe nanoprecipitation, solvent exchange, thin film rehydration and chloroform emulsion evaporation were evaluated for their ability to produce small micelles of low polydispersity. It was found that syringe nanoprecipitation best met these criteria and was chosen as the standard procedure. In short, a dilute solution of copolymer in tetrahydrofuran (THF) was stirred rapidly. To this solution, distilled water was added dropwise and the THF was removed by dialysis against water. Once prepared, micelles were characterized by DLS and transmission electron microscopy (TEM). The results are summarized in Table 2.

Table 3.2: Effect of PEO loading on micelles

Polymer	Micelle Diameter [a] (nm)	Micelle PDI
8	Bimodal: 37.2, 172.3	0.30
9	64.7	0.40
10	123.8	0.15
11	Bimodal: 38.1, 184.0	0.44

[a] Z-average diameter determined by DLS

3.2.3 Effect of PEO Loading on Micelle Formation

As shown in Figure 3.4, DLS analysis of micelles formed from polymer **8** exhibited a bimodal size distribution. It is likely that this results from aggregation of individual micelles due to insufficient PEO. This hypothesis is supported by TEM imaging (Figure 3.5) where it appears there are multiple particles adhered to one other. Overall, this ratio of PEO does not produce particles of narrow enough polydispersity to be useful clinically.

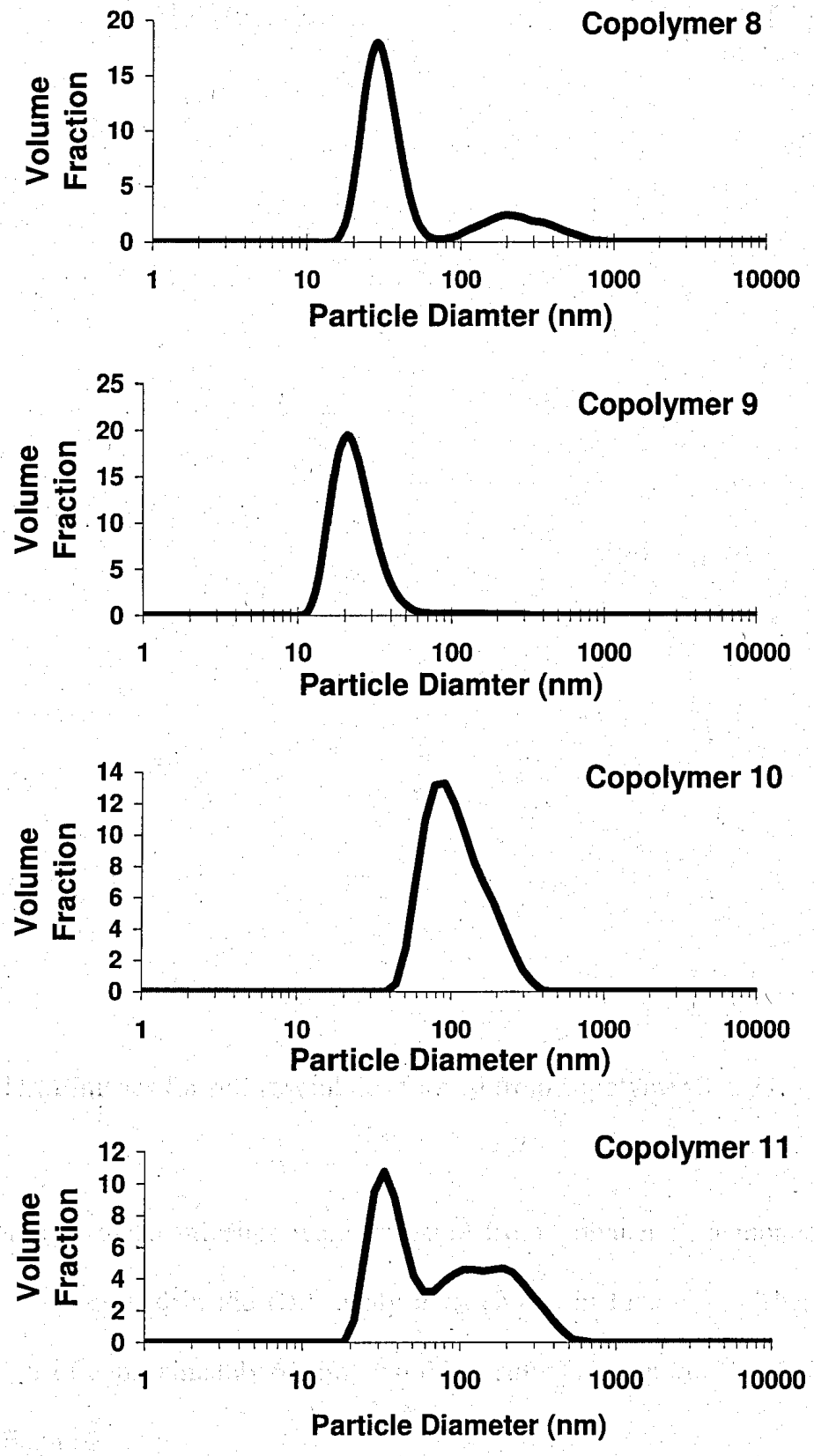

Figure 3.4: DLS traces for self assemblies formed from copolymers **8** to **11**.

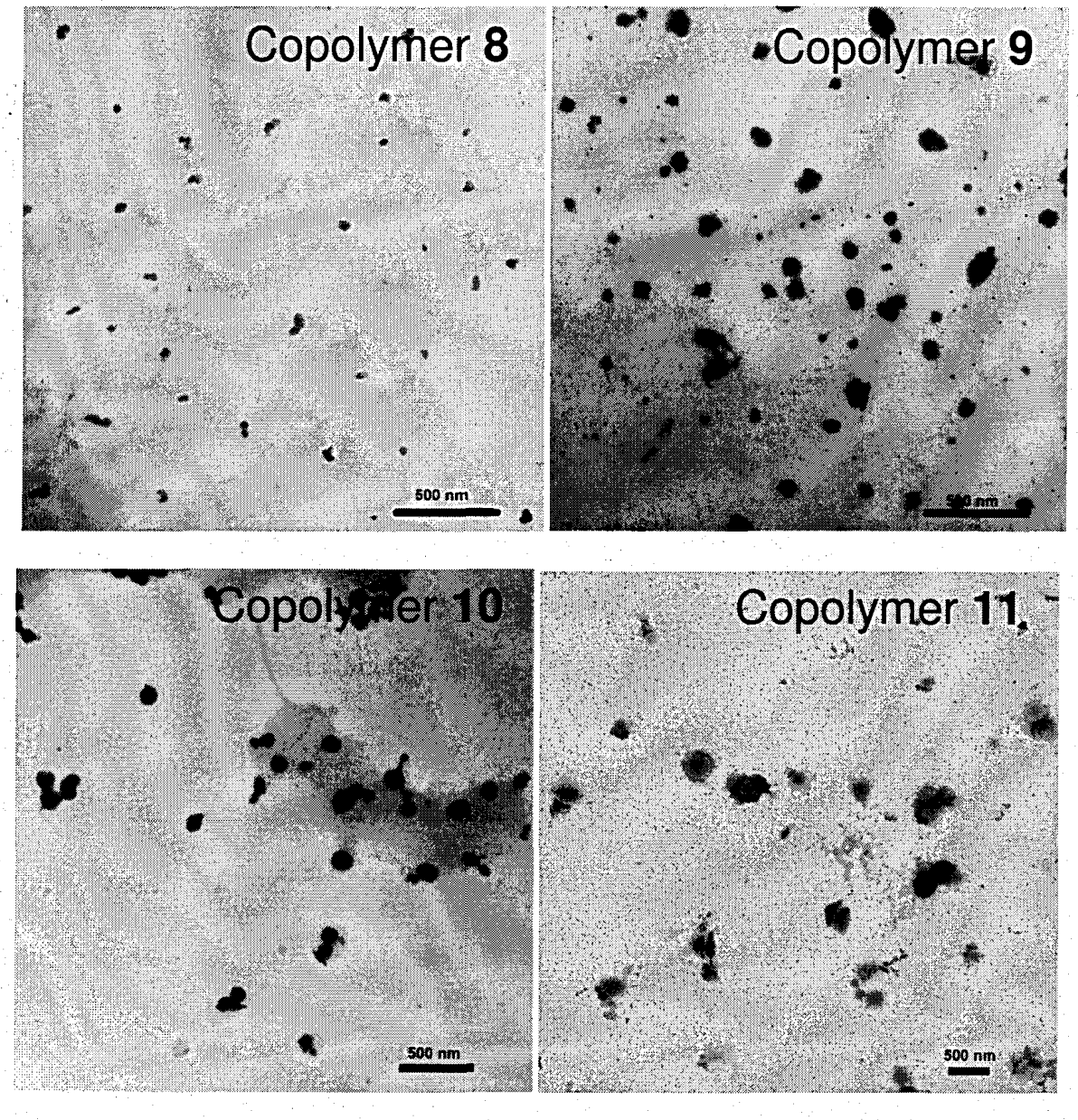

Figure 3.5: TEM images for self assemblies formed from copolymer **8** to **11**.

In contrast, when micelles were prepared from polymer **9**, a monomodal size distribution was observed in the DLS analysis as shown in Figure 3.4. These micelles have a diameter of approximately 65 nm, and this result was supported by TEM analysis as shown in Figure 3.5.

When micelle formation with polymer **10** was investigated, DLS analysis indicated that micelles increased in diameter to approximately 130 nm as shown in Figure 3.4. TEM imaging corroborates the size increase as shown in Figure 3.5.

DLS analysis of the micelles formed from polymer **11** revealed aggregation of the micelles as shown in Figure 3.4. A TEM image of these micelles is shown in Figure 3.5. These results show that the content of PEO obtained from conjugating PEO 2K is insufficient to prevent the aggregation of the micelles.

Based on conjugation ratios, as well as, the ability to produce small, narrowly dispersed micelles, 1.2 equivalents of PEO 5K was the ideal ratio. The small gain in conjugation yield obtained from using 3 equivalents of PEO 5K does not compensate for the increased difficulty of purification by preparative GPC. In addition, the sizes of the micelles formed from polymer **9** are ideal for circulation in vivo.[11-13] Since 50% of the pendant amines are uncoupled, there is the possibility of conjugation of imaging agents or for the covalent immobilization of drug molecules. Thus, further studies were carried out using polymer **9**.

3.2.4 Further Characterization and Release

3.2.4.1 Critical Aggregation Concentration

The critical aggregation concentration (CAC) is the concentration at which an amphiphilic polymer forms aggregates in solution.[11] Nile Red, a hydrophobic dye shown in Figure 3.6, was equilibrated with varying concentrations of micelles and the fluorescence was measured. Nile Red is not soluble in water; therefore, it will not

. fluoresce in aqueous media. It will, however, exhibit fluorescence upon encapsulation within the hydrophobic core of a micelle.[12] By investigasting a series of increasingly dilute samples, the CAC can be determined as the point where the concentration is too low to form micelles and therefore Nile Red will not fluoresce. The range of polymer concentrations under study was chosen by looking at previously published work of similar systems.[2,11,12] According to Figure 3.7, all concentrations produced fluorescence, which implies that at low concentrations, the micelles are likely unimolecular.[2]

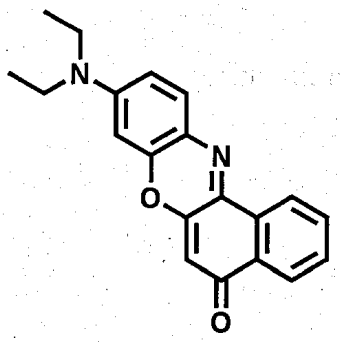

Figure 3.6: Structure of the chosen model drug, Nile Red.

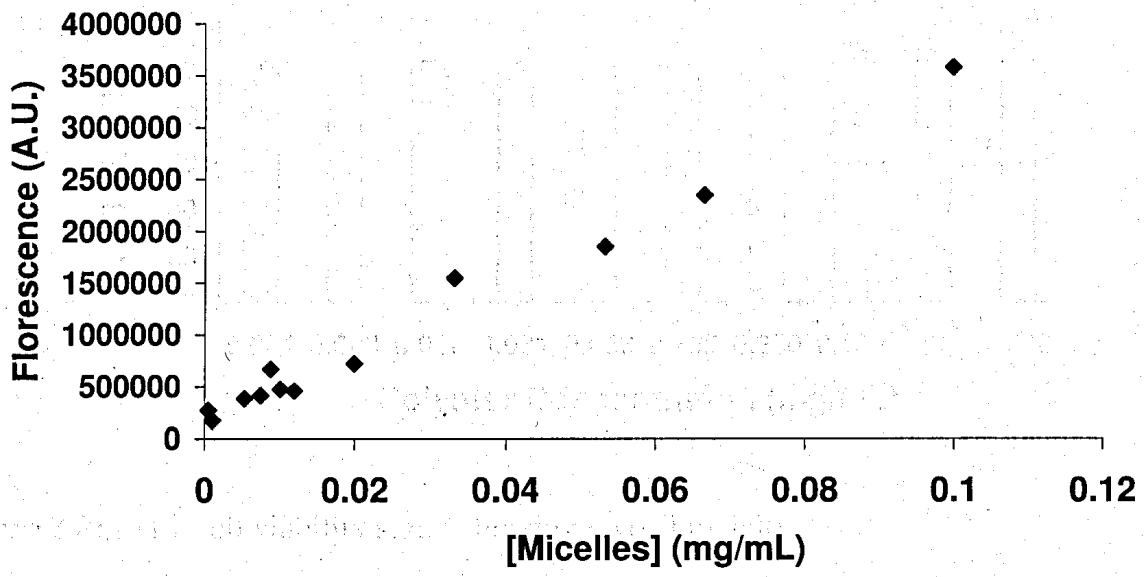

Figure 3.7: Graph displaying results of CAC experiment. Florescence was observed at all concentrations.

3.2.4.2 MTT Assay

In order to assess the toxicity of the micelles formed from copolymer **9**, an MTT Assay was run. In an MTT Assay, 3-(4,5-Dimethylthiazol-2-yl)-2,5-diphenyltetrazolium bromide (MTT) is reduced to purple formazan by living cells. Purple formazan is insoluble, so a solubilizing solution is used to create a solution that can be measured using UV-Vis spectroscopy. Since the reduction is done by living cells, the absorbance of formazan will be proportional to the cell viability.[13] It was found that at concentrations up to 2 mg/mL, the highest concentration investigated, the micelles produced no toxicity (Figure 3.8).

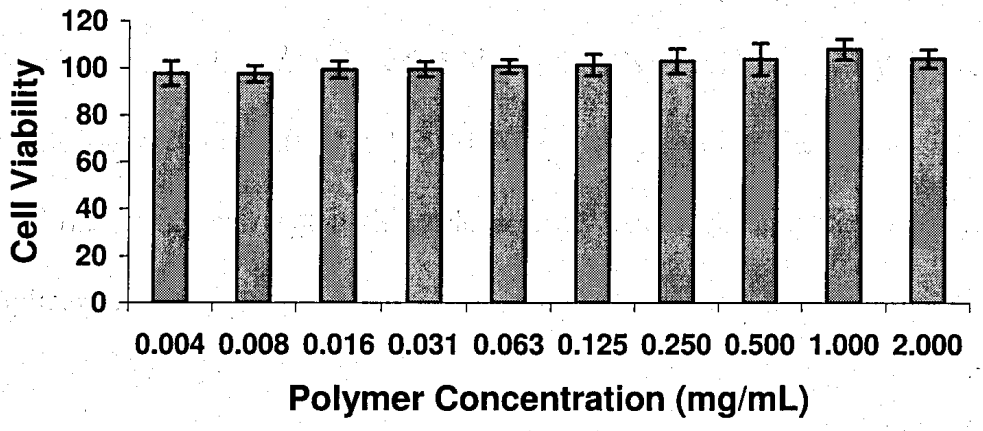

Figure 3.8: MTT cell viability study showing no cell toxicity.

3.2.4.3 Nile Red Release

In order to test the release kinetics of the micelles, a model drug, Nile Red, was loaded and released. In order to load the micelles, Nile Red was dissolved in the initial THF solution. Water was added dropwise with stirring and the THF was removed by dialysis against water. Once all of the THF was removed, centrifugation was used to remove any precipitated Nile Red. The micelle suspension was placed in a Slide-A-Lyzer dialysis cassette and kept at 37 °C in pH 7.4 or 6.0 phosphate buffer or pH 5.0 citric acid/phosphate buffer. The internal solution was measured in a fluorometer every hour and was compared to a standard of Nile Red in THF that was kept in the fridge. The results are summarized in Figure 3.9. The release in pH 5.0 and 6.0 are very similar, achieving almost total release in 13 hours while the release took approximately 20 hours in pH 7.4. It is hypothesized that the difference in release rates is due to the protonation of the aniline nitrogens in Nile Red, which would facilitate its migration into the external aqueous environment by increasing the polarity of Nile Red. It is predicted that the pK_a

of the aniline nitrogens is between 5 and 6. Methyl Red, a dye with aniline nitrogens in a similar environment, has a pK_a of 5.3[14] and Advanced Chemistry Development (ACD/Labs) Software V11.02 (© 1994-2011 ACD/Labs) predicts the pK_a as 5.4. Overall, the results of this study show that this release rate would be suitable for *in vivo* drug delivery applications.[18,19]

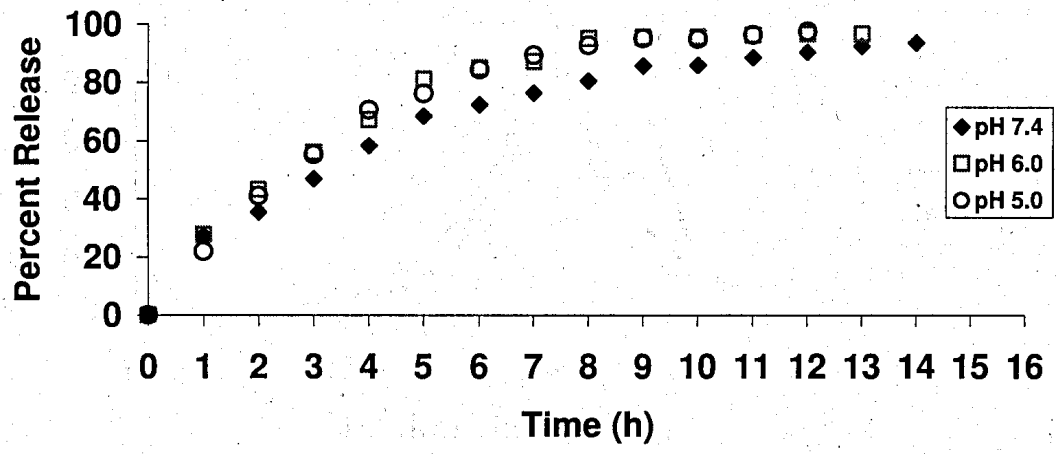

Figure 3.9: Comparing Nile Red release from micelles at varying pHs.

3.2.4.4 Hydrolytic Degradation

As described above, as the PEA backbone contains hydrolysable linkages, the polymer can be cleaved under physiological conditions to release smaller polymers. The advantage of the degradation is that the higher MW polymer can be broken down into smaller components that may eventually be excreted, rather than remain circulating in the body. To examine the kinetics of this degradation, a study was performed. The micelles were incubated in pH 7.4 phosphate buffer at 37 °C. At various time points, aliquots of

the solution were removed, dried, and analyzed by GPC. As shown in Figure 3.10, a side peak gradually appeared in the chromatogram suggesting the breakdown of the polymer backbone which releases lower MW polymers over the time period of this study. This study suggests that over time the micelles will break down *in vivo*, thus providing an efficient means of leaving the body.

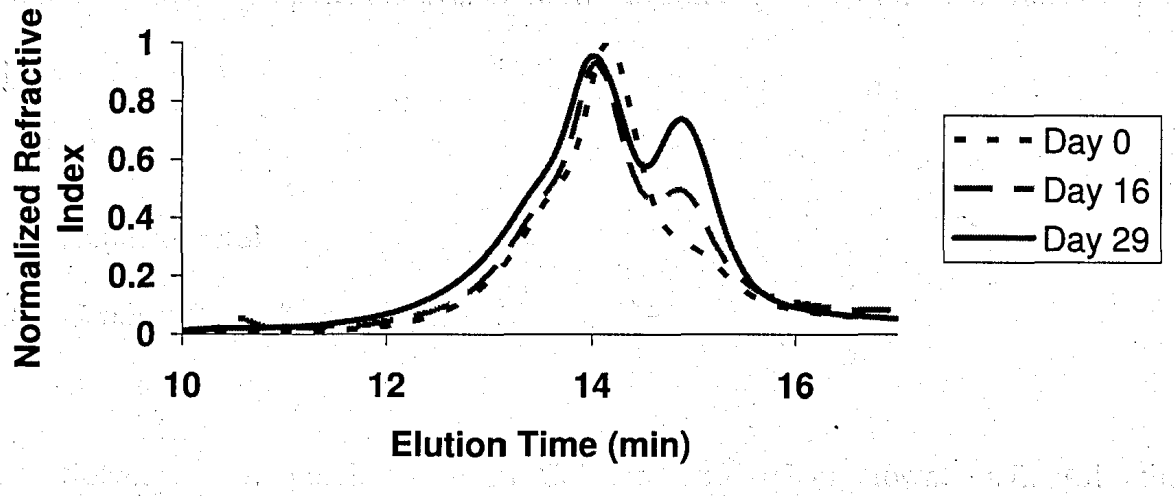

Figure 3.10: GPC micelle degradation study indicating that the copolymer breaks down under physiological conditions.

3.3 Conclusions

A PEA containing pendant amine groups was synthesized as previously reported and was reacted with activated PEO to produce novel PEO-PEA copolymers. Various equivalents of PEO were investigated in this coupling and the micelles formed from the resulting polymers were studied by DLS and TEM. The copolymer synthesis was optimized to produce the smallest micelles with lowest polydispersities. It was found that

using 1.2 equivalents of PEO 5K relative to the pendant amines provided unimolecular micelles of mean diameter 62 nm could be produced. The micelles were capable of encapsulating and releasing hydrophobic compounds as exemplified by the model drug Nile Red. The release occurs on a pharmacologically relevant time scale, with full release occurring after approximately 20 hours in physiological conditions (pH 7.4 and 37 °C). A degradation studied revealed that the polymer degraded gradually under physiological conditions, providing a potential avenue for the eventual release of the materials from the body.

3.4 Experimental

3.4.0 General Procedure and Methods

Solvents were purchased from Caledon Labs (Georgetown, ON). All other chemicals were purchased from Sigma Aldrich (Milwaukee, WI) or Alfa Aesar (Ward Hill, MA). Unless noted otherwise, all chemicals were used as received. Anhydrous dichloromethane was distilled over CaH_2. Infrared (IR) spectra were obtained using a Bruker Tensor 27 instrument as films from dichloromethane on NaCl plates. ^1H NMR spectra were obtained at 400 MHz on a Varian Mercury 400 Spectrometer. Chemical shifts are reported in ppm and are calibrated against residual solvent signals of $CDCl_3$ (δ7.27). All coupling constants (J) are reported in Hz. Gel permeation chromatography data were obtained using a Waters 2695 separations module equipped with a Waters 2414 refractive index detector (Waters Limited, Mississauga, ON) and two PLgel 5 μm mixed-D (300 mm x 7.5 mm) columns connected in series (Varian Canada). Samples (5 mg/mL)

dissolved in the eluent, which comprised 10 mM LiBr and 1% (v/v) NEt_3 in DMF at 85 °C were injected (100 μL) at a flow rate of 1 mL/min and calibrated against either poly(styrene) or poly(ethylene glycol) standards.. Molecular weights are reported in grams/mol (g/mol). Preparative GPC was equipped with a Waters 515 High performance liquid chromatography (HPLC) pump set at a flow rate of 3mL/min. Separation was achieved with two consecutively connected columns, a PLgel 10 μm 100 A (600x25 mm) followed by a PLgel 10 μm 500 A (600x25 mm) and a preceding PLgel Prep Guard column (25x25mm). Detection was obtained with a Wyatt Optilab Rex Refractive Index detector. HPLC grade dimethylformamide with 1% triethylamine solvent was prepared and filtered before eluting through columns. Dialysis was performed with Spectra/Por 6 dialysis tubing (Spectrum Laboratories, Rancho Dominguez, CA).

3.4.1 Synthesis of Polymer ***4***

The di-*p*-toluenesulfonic acid salt monomer **1** (1.7 g, 2.3 mmol, 0.9 equiv.) and sodium carbonate (0.54 g, 5.1 mmol, 2.0 equiv.) were dissolved in distilled water (30 mL). Diester **3** (0.14 g, 0.25 mmol, 0.1 equiv.) was dissolved in dichloromethane (15 mL) and added to the aqueous phase and allowed to mix for 30 min. Sebacoyl chloride (0.55 mL, 2.6 mmol, 1.0 equiv.) diluted in anhydrous dichloromethane (15 mL), was added dropwise over 30 min to the biphasic solution and was allowed to react for 24 h. Upon completion of the reaction, solvent was removed *in vacuo*. The functional poly(ester amide) was redissolved in DMF permitting filtration of the insoluble salts. The filtrate was then dialyzed against DMF for at least 8 h twice and then dried *in vacuo*

providing polymer **4** as a sticky solid. Yield: 60%. Spectral data agreed with those previously reported.[7,8] GPC (relative to PS standards): M_n = 48000, M_w = 73900, PDI = 1.5.

3.4.2 Synthesis of Polymer 5

Polymer **4** (0.1 g, 0.18 mmol, 1.0 equiv.) was dissolved in 4 mL of 1:1 trifluoroacetic acid:dichloromethane in a flame dried flask and the reaction mixture was stirred for 2 h under an argon atmosphere. The solvent was removed under a stream of air with 3 washes of 15 mL of toluene to introduce an azeotrope. Residual solvent was removed *in vacuo* resulting in a brown solid, polymer **5**. Yield: 99%. Spectral data agreed with those previously reported.[8,9] GPC (relative to PS standards): M_n = 30400, M_w = 40600, PDI = 1.3.

3.4.3 Synthesis of Activated Poly(ethylene oxide) (MW=5,000 g/mol) 6

5,000 g/mol poly(ethylene oxide) (10 g, 2.0 mmol, 1 eq) and 4-nitrophenyl chloroformate (0.81 g, 4.0 mmol, 2.0 eq) were dissolved in dichloromethane (5 mL). To this solution, pyridine (0.9mL, 8.0 mmol, 4.0 eq) was added dropwise and the reaction was stirred overnight. The reaction was precipitated in cold ethyl ether (250 mL). The precipitate was recovered, dried *in vacuo*, dissolved in dichloromethane and washed twice in 1 M HCl. Yield: 92%. ^{1}H NMR (400 MHz, $CDCl_3$): δ8.30-8.28 (d, 2H, Ar-*H* ortho to NO_2), δ7.40-7.39 (d, 2H, Ar-*H* meta to NO_2), 4.46-4.44 (-C*H*$_2$-O-C(O)-O-), 3.65

(br s, 449H, -O-CH_2-CH_2-O-), 3.39 (s, 3H,-O-CH_3). FTIR (cm^{-1}): 2880 (sp^3 C-H stretch), 1765 (C=O stretch), 1526 (CH_2 bend, C=C ring stretch), 1462 (CH_3 bend, C=C ring stetch), 1380 (symetic Ar-NO_2 stretch), 1259 (Ar-O stretch), 1111 (assymetric C-O-C stretch), 847 (out of plane C-H on Ar bending). GPC (relative to PEO standards): M_n = 4500, M_w = 4600, PDI = 1.08.

3.4.4 Synthesis of Activated Poly(ethylene oxide) (MW=2000 g/mol) 7

The same procedure for the synthesis of polymer **6** was used except that 2000 g/mol poly(ethylene glycol) (4 g, 2.0 mmol, 1.0 eq) was used instead. Yield: 75%. ^{1}H NMR (400 MHz, $CDCl_3$): δ8.28-8.25 (d, 2H, Ar-*H* ortho to NO_2), δ7.39-7.37 (d, 2H, Ar-*H* meta to NO_2), 4.45-4.43 (-CH_2-O-C(O)-O-), 3.62 (br s, 449H, -O-CH_2-CH_2-O-), 3.36 (s, 3H,-O-CH_3). FTIR (cm^{-1}): 2883 (sp^3 C-H stretch), 1769 (C=O stretch), 1526 (CH_2 bend, C=C ring stretch), 1468 (CH_3 bend, C=C ring stetch), 1360 (symetic Ar-NO_2 stretch), 1280 (Ar-O stretch), 1115 (assymetric C-O-C stretch), 843 (out of plane C-H on Ar bending). GPC (relative to PEG standards): M_n = 1700, M_w = 1800, PDI = 1.1.

3.4.5 Synthesis of PEO-PEA Copolymer 8

The *p*-nitrophenyl functionalized 5000 g/mol poly(ethylene glycol), **6**, (0.0653 g, 0.01 mmol, 0.85 eq relative to the number of lysine residues), deprotected lysine PEA, **5**, (0.0526 g, 0.01 mmol), and 4-(dimethylamino)pyridine (DMAP) (0.4 mg, 2.98 μmol, 0.2 eq relative to the number of lysine residues) were added to a flame dried flask in an argon

atmosphere. Dichloromethane (4 mL) was added to dissolve the solids. Upon dissolution, diisopropylethylamine (DIPEA) (0.004 g, 0.03 mmol, 2 eq relative to the number of lysine residues) was added dropwise. The reaction mixture was allowed to stir overnight. The solvent was removed *in vacuo* and the product was dialyzed against DMF using a membrane with a with MWCO 25,000 g/mol. The solvent was removed *in vacuo* and the off-white solid was separated from any uncoupled PEG through preparative GPC. The solvent was removed *in vacuo* yielding polymer **8**. Yield: 25%. ^{1}H NMR (400 MHz, $CDCl_3$): δ7.26-7.05 (m, 9H, Ph), 6.00-5.94 (br m, 1.8H, -C(O)-N*H*-C_αH-CH_2-Ph), 4.86-4.79 (m, 1.8, -C_α*H*-CH_2-Ph), 4.50 (br m, 0.2H, -N*H*-C(O)-O-), 4.12-3.97 (m, 4H, -C(O)O-C*H*$_2$-), 3.65 (br m, 24H,-O-C*H*$_2$-C*H*$_2$-O-), 3.37 (s, 0.2H, -O-C*H*$_3$), 3.09-3.00 (m, 3.8H, -C_αH-C*H*$_2$-Ph), 2.13-2.09 (m, 4H, -NH-C(O)-C*H*$_2$-), 1.55-1.50 (m, 8H, -C(O)O-CH_2-C*H*$_2$-, -NH-C(O)-CH_2-C*H*$_2$-),1.23-1.19 (m, 8H, -NH-C(O)-CH_2-CH_2-(C*H*$_2$)$_4$). FTIR (cm^{-1}): 3100 (N-H stretch), 3030 (sp^2 C-H stretch), 2883 (sp^3 C-H stretch), 1745 (C=O etser stretch), 1690 (C=O amide stretch), 1550 (N-H bending), 1526 (CH_2 bend, C=C ring stretch), 1468 (CH_3 bend, C=C ring stetch), 1400 (C-N stretch), 1115 (assymetric C-O-C stretch), 999 (C-O stretch), 850 (symmetric C-O-C stretching), 843 (out of plane C-H on Ar bending), 750 (monosubstituted Ar C-H bending) 690 (monosubstituted Ar C-H bending). GPC (relative to PEO standards): M_n = 30000, M_w = 45700, PDI = 1.5.

3.4.6 Synthesis of PEO-PEA Copolymer 9

The same procedure described above for polymer **8** was used except that 1.2 equivalents of *p*-nitrophenyl carbonate activated PEO 5K relative to the number of lysine

residues was used. Yield: 27%. ^{1}H NMR (400 MHz, $CDCl_3$): δ7.28-7.09 (m, 9H, Ph), 6.28 (br m, 0.2H, -C(O)-N*H*-C_αH-$(CH_2)_4$-NH-C(O)-O-) 6.01-6.00 (br m, 1.8H, -C(O)-N*H*-C_αH-CH_2-Ph), 4.88-4.84 (m, 1.8, -C_α*H*-CH_2-Ph), 4.54 (br m, 0.2H, -N*H*-C(O)-O-), 4.12-4.01 (m, 4H, -C(O)O-C*H*$_2$-), 3.65 (br m, 45H,-O-C*H*$_2$-C*H*$_2$-O-), 3.37 (s, 0.3H, -O-C*H*$_3$), 3.12-3.03 (m, 3.8H, -C_αH-C*H*$_2$-Ph), 2.18-2.12 (m, 4H, -NH-C(O)-C*H*$_2$-), 1.57-1.52 (m, 8H, -C(O)O-CH_2-C*H*$_2$-, -NH-C(O)-CH_2-C*H*$_2$-),1.28-1.22 (m, 8H, -NH-C(O)-CH_2-CH_2-(C*H*$_2$)$_4$). FTIR (cm^{-1}): 3110 (N-H stretch), 3032 (sp^2 C-H stretch), 2886 (sp^3 C-H stretch), 1755 (C=O etser stretch), 1696 (C=O amide stretch), 1551 (N-H bending), 1528 (CH_2 bend, C=C ring stretch), 1468 (CH_3 bend, C=C ring stetch), 1405 (C-N stretch), 1114 (assymetric C-O-C stretch), 979 (C-O stretch), 853 (symmetric C-O-C stretching), 843 (out of plane C-H on Ar bending), 737 (monosubstituted Ar C-H bending) 692 (monosubstituted Ar C-H bending). GPC (relative to PEO standards): M_n = 31000, M_w = 48600, PDI = 1.6.

3.4.7 Poly(ester amide)-co-poly(ethylene glycol) using 3.0 eq of 5000 g/mol PEG, ***10***

The same procedure described above for polymer **8** was used except that 3.0 equivalents of *p*-nitrophenyl carbonate activated PEO 5K relative to the number of lysine residues was used. Yield: 30%. ^{1}H NMR (400 MHz, $CDCl_3$): δ7.30-7.10 (m, 9H, Ph), 6.06-6.04 (br m, 1.8H, -C(O)-N*H*-C_αH-CH_2-Ph), 4.88-4.86 (m, 1.8, -C_α*H*-CH_2-Ph), 4.13-4.02 (m, 4H, -C(O)O-C*H*$_2$-), 3.65 (br m, 56H,-O-C*H*$_2$-C*H*$_2$-O-), 3.39 (s, 0.4H, -O-C*H*$_3$), 3.11-3.08 (m, 3.8H, -C_αH-C*H*$_2$-Ph), 2.22-2.14 (m, 4H, -NH-C(O)-C*H*$_2$-), 1.89-1.69 (m, 8H, -C(O)O-CH_2-C*H*$_2$-, -NH-C(O)-CH_2-C*H*$_2$-), 1.28-1.26 (m, 8.4H, -NH-C(O)-CH_2-CH_2-

-(CH_2)$_4$). FTIR (cm^{-1}): 3110 (N-H stretch), 3061 (sp^2 C-H stretch), 2881 (sp^3 C-H stretch), 1746 (C=O etser stretch), 1678 (C=O amide stretch), 1523 (N-H bending), 1523 (CH_2 bend, C=C ring stretch), 1476 (CH_3 bend, C=C ring stetch), 1369 (C-N stretch), 1119 (assymetric C-O-C stretch), 1001 (C-O stretch), 851 (symmetric C-O-C stretching), 853 (out of plane C-H on Ar bending), 751 (monosubstituted Ar C-H bending) 694 (monosubstituted Ar C-H bending). GPC (relative to PEO standards): M_n = 34000, M_w = 42000, PDI = 1.2.

*3.4.8 Poly(ester amide)-co-poly(ethylene glycol) using 1.2 eq of 2000g/mol PEG, **11***

The same procedure described above for polymer **8** was used except that 1.2 equivalents of *p*-nitrophenyl carbonate activated PEO 2K relative to the number of lysine residues was used. Yield: 28%. ^{1}H NMR (400 MHz, $CDCl_3$): δ7.28-7.10 (m, 9H, Ph), 6.29 (br m, 0.2H, -C(O)-N*H*-C$_\alpha$H-(CH_2)$_4$-NH-C(O)-O-) 6.01-6.00 (br m, 1.8H, -C(O)-N*H*-C$_\alpha$H-CH_2-Ph), 4.88-4.85 (m, 1.8, -C$_\alpha$*H*-CH_2-Ph), 4.54 (br m, 0.2H, -N*H*-C(O)-O-), 4.12-4.01 (m, 4H, -C(O)O-C*H*$_2$-), 3.65 (br m, 19H,-O-C*H*$_2$-C*H*$_2$-O-), 3.38 (s, 0.3H, -O-C*H*$_3$), 3.15-3.05 (m, 3.8H, -C$_\alpha$H-C*H*$_2$-Ph), 2.21-2.12 (m, 4H, -NH-C(O)-C*H*$_2$-), 1.57-1.55 (m, 8H, -C(O)O-CH_2-C*H*$_2$-, -NH-C(O)-CH_2-C*H*$_2$-),1.26-1.22 (m, 8.4H, -NH-C(O)-CH_2-CH_2-(CH_2)$_4$). FTIR (cm^{-1}): 3099 (N-H stretch), 3022 (sp^2 C-H stretch), 2880 (sp^3 C-H stretch), 1749 (C=O etser stretch), 1693 (C=O amide stretch), 1556 (N-H bending), 1527 (CH_2 bend, C=C ring stretch), 1468 (CH_3 bend, C=C ring stetch), 1429 (C-N stretch), 1107 (assymetric C-O-C stretch), 992 (C-O stretch), 851 (symmetric C-O-C stretching), 832 (out of plane C-H on Ar bending), 758 (monosubstituted Ar C-H bending) 687

(monosubstituted Ar C-H bending). GPC (relative to PEO standards): M_n = 24000, M_w = 34000, PDI = 1.4.

3.4.9 Micelle Formation

The PEA-PEG copolymer, one of **8-11** (2.5 mg), was dissolved in 0.5 mL of THF and was stirred rapidly. To this solution, 2 mL of distilled water was added dropwise. The THF was removed by dialysis against water with a regenerated cellulose membrane of MWCO 12-14 kg/mol for 24 hours with the dialysate being replaced every 8 hours.

3.4.10 Determination of CAC

The PEA-PEG copolymer, **9** (2.5 mg), was dissolved in 0.5 mL of THF and stirred rapidly. To this solution, 2 mL of distilled water was added dropwise. The THF was removed by dialysis against water with a regenerated cellulose membrane of MWCO 12-14 kg/mol for 24 hours with the dialysate being replaced every 8 hours. Nile Red (0.94 mg, 3.0 μmol) was dissolved in 9 mL of CH_2Cl_2 and 0.1 mL of this solution was added to a series of 12 vials. The CH_2Cl_2 was removed under a stream of air. A series of concentrations of the micelle dispersion ranging from to 0.0005 mg/mL to 1 mg/mL was made by dilution with pH 7.4, 100 mM phosphate buffer. The dilute dispersions were added to the vials containing Nile Red and were allowed to equilibrate with stirring for 40 hours. The fluorescence spectra were obtained on a QM-4 SE spectrometer from Photon Technology International (PTI), equipped with double excitation and emission

monochromators. An excitation wavelength of 550 nm was used for Nile Red and the emission spectra were recorded from 565 and 700 nm. The maximum emission intensity was obtained for each micelle concentration.

3.4.11 MTT Procedure

Proliferation of HeLa cells were measured by an MTT assay. [19] Cells were seeded into 88 wells of a 96-well plate (Nunclon TC treated) at a density of $2x10^3$ cells per well in a final volume of 100 µL of Dulbecco's Modified Eagle Medium (DMEM) containing 10% serum and 1% antibiotics. Cells were allowed to adhere for 24 hours at 37 °C in a humidified incubator with 5% CO_2. After 24 hours the growth media was aspirated. Control cells were grown in growth media alone while nanoparticle samples were incubated in two-fold decreasing concentrations from 2 mg/ml to 0.0039 mg/mL in growth media with 8 replicates at each concentration for 48 hours. All media was aspirated then 100 µL of fresh media and 10 µL of MTT solution (5 mg/mL) was added to each well and incubated for another 4 hours. The media was aspirated and the formazan product was solubilized by addition of 50 µL DMSO to each well. Absorbance of each well was measured at 540 nm using a plate reader (Tecan Safire).

3.4.12 Encapsulation and Release of Nile Red

The PEA-PEG copolymer, 10 (2.5 mg), and Nile Red (0.5 mg, 1.6 µmol) were dissolved in 0.5 mL of THF and stirred rapidly. To this solution, 2 mL of distilled water

was added dropwise. The THF was removed by dialysis against water with a regenerated cellulose membrane of MWCO 12-14 kg/mol for 24 hours with the dialysate being replaced every 8 hours. Once all of the THF was removed, centrifugation (6000 rpm for 30 min) was used to remove any precipitated Nile Red. The micelle suspension was placed in a Slide-A-Lyzer dialysis cassette and kept at 37°C in either pH 7.4 or 6.0, 100 mM phosphate buffer or pH 5.0, 100 mM citric acid/phosphate buffer. The fluorescence spectra were obtained on a QM-4 SE spectrometer from Photon Technology International (PTI), equipped with double excitation and emission monochromators. An excitation wavelength of 550 nm was used for Nile Red and the emission spectra were recorded from 565 and 700 nm. A measurement was obtained every hour and was compared to a standard of Nile Red in THF which was covered in aluminum foil and kept in fridge.

3.4.13 Hydrolytic Degradation of Micelles

The PEA-PEG copolymer **10** (39 mg) was dissolved in 4 mL of THF and stirred rapidly. To this solution, 16 mL of distilled water was added dropwise. The THF was removed by dialysis against water with a regenerated cellulose membrane of MWCO 12-14 kg/mol for 24 hours with the dialysate being replaced every 8 hours. The dispersion was concentrated to 3 mL using a stream of air and was then placed in a Slide-A-Lyzer dialysis cassette with a MWCO of 3,500 g/mol. The cassette was kept in pH 7.4 100 mM phosphate buffer at 37 °C with stirring. Samples were removed periodically from the internal solution and lyophilized before analysis by GPC.

3.4.14 TEM Sample Preparation

A micelle solution of 0.2 mg/mL was prepared and 20 µL of this was placed on a copper TEM grid and allowed to dry overnight. Transmission electron microscopy (TEM) was carried out using a carbon Formvar grid and a Phillips CM10 microscope operating at 80 kV with a 40 μm aperture.

3.5 References

(1) Jain, A. K.; Das, M.; Swarnakar, N. K.; Jain, S. *Crit. Rev. Ther. Drug Carrier Syst.* **2011**, *28*, 1.

(2) Park, J.; Moon, M.; Seo, M.; Choi, H.; Kim, S. Y. *Macromolecules* **2010**, *43*, 8304.

(3) Sandhiya, S.; Dkhar, S. A.; Surendiran, A. *Fundam. Clin. Pharmacol.* **2009**, *23*, 263.

(4) Shi, M.; Lu, J.; Shoichet, M. S. *J. Mater. Chem.* **2009**, *19*, 5485.

(5) Wei, Y.; Wang, Y.; Wang, L.; Hao, D.; Ma, G. *COLLOID SURFACE B* **2011**, *87*, 399.

(6) Manjappa, A. S.; Chaudhari, K. R.; Venkataraju, M. P.; Dantuluri, P.; Nanda, B.; Sidda, C.; Sawant, K. K.; Murthy, R. S. R. *J. Controlled Release* **2011**, *150*, 2.

(7) Atkins, K. M.; Lopez, D.; Knight, D. K.; Mequanint, K.; Gillies, E. R. *J. Polym. Sci., Part A: Polym. Chem.* **2009**, *47*, 3757.

(8) De Wit, M. A.; Wang, Z. X.; Atkins, K. M.; Mequanint, K.; Gillies, E. R. *J. Polym. Sci., Part A: Polym. Chem.* **2008**, *46*, 6376.

(9) Knight, D. K.; Gillies, E. R.; Mequanint, K. *Biomacromolecules* **2011**, *12*, 2475.

(10) Ahmed, F.; Photos, P. J.; Discher, D. E. *Drug Dev. Res.* **2006**, *67*, 4.

(11) Capek, I. *Adv. Colloid Interface Sci.* **2002**, *97*, 91.

(12) Gillies, E. R.; Goodwin, A. P.; Frechet, J. M. J. *Bioconjugate Chem.* **2004**, *15*, 1254.

(13) Mosmann, T. *J. Immunol. Methods* **1983**, *65*, 55.

(14) de Oliveira, H. P. *Microchem. J.* **2008**, *88*, 32.

Chapter Four:

Conclusion

4.1 Thesis Summary

In the first part of this thesis, the use of poly(ester amide)s (PEA)s containing pendant functional groups for the preparation of drug delivery nanoparticles (NP)s was explored. By employing a more powerful emulsifying method and running a series of optimization experiments, the procedure for preparing nanoparticles based on PEAs was significantly improved relative to previously reported routes[1,2] by providing nanosized particles with low polydispersity indices. In addition, it was possible for the first time, to prepare these particles from PEAs with carboxylic acid functional handles. To investigate the potential use of these functional handles for the covalent immobilization of drug molecules, an alcohol functionalized Rhodamine B derivative was chosen as a model drug and was coupled to the PEA via an ester linkage prior to nanoparticle preparation. It was found that the covalently immobilized model drug was released much more slowly than a physically encapsulated control. While the physically encapsulated Rhodamine was completely released in 9 hours, only approximately 10% of the covalently bound drug was released in the same time frame. This result suggests that the covalently bound system would be effective as a sustained delivery vehicle, avoiding the undesirable burst release seen in currently used chemotherapy systems.[3-5] In addition, this system can be dried and reconstituted for convenient storage and transport. Overall, this nanocarrier displays great promise for applications in sustained release drug delivery.

The covalently immobilized system did have a drawback in that relatively large amounts of poly(vinyl alcohol) (PVA) were required in order to obtain NPs small enough

. to remain circulating for extended periods as well as extravasate into cancerous tissue. Problems may arise as PVA may mask the desirable properties of the PEA such as slowing its biodegradation, and preventing the conjugation of targeting molecules to the PEA's pendant functional groups. The PVA layer may also impede diffusion from the nanoparticle and may increase the minimum particle diameter by increasing external phase viscosity at higher concentrations.[6]

In order to overcome these issues, novel poly(ethylene oxide)-poly(ester amide) (PEO-PEA) copolymers were synthesized. By imparting amphiphilic properties to the PEA, the need for surfactant was eliminated and the resulting copolymer self-assembled into micelles in aqueous media. The micelle formation procedure was optimized to produce micelles less than 100 nm in diameter with low polydispersities. By characterization with dynamic light scattering and transmission electron microscopy it was found that micelles of mean diameter 62 nm could be produced with a PDI of 0.4. The micelles were capable of encapsulating and releasing hydrophobic compounds as exemplified by the encapsulation and release of Nile Red. The release occurs on a pharmacologically relevant time scale, with full release occurring after approximately 20 hours under physiological conditions. The release rate increased at lower pH, such as would be found in the acidic environment of a tumour cell; however, it was hypothesized that the change in release was due to protonation of the Nile Red and not due to pH sensitivity of the copolymer. The degradation of the micelles in phosphate buffer was studied by gel permeation chromatography and it was found that the polymer degraded gradually, suggesting that the copolymers would be hydrolyzed in vivo, providing a route for the eventual excretion of the polymers from the body. Overall, these results suggest

that micelles derived from PEO-PEA copolymers are promising materials for drug delivery applications.

PEAs offer several properties superior to currently used systems such as fewer acidic degradation products and functional handles for the conjugation of bioactive molecules. Though still in the early phase of evaluation, through characterization and release studies, PEAs are being revealed as promising drug delivery vehicles. Overall, the results obtained in this thesis suggest that PEAs are excellent biomaterials, capable of delivering therapeutics and potentially overcoming many of the deficiencies found in current delivery systems.

4.2 Future Work

4.2.1 Covalent Immobilization of Drug Molecules in Poly(ester amide) Nanoparticles

A variety of drugs should be coupled to the PEA to establish the versatility of this drug delivery system. Biological assays should be performed to determine cell uptake and *in vitro* toxicity of both the empty and drug loaded NP. If these results are promising, the carriers should then be evaluated *in vivo* to determine their biocompatibility, biodistribution behavior and therapeutic efficacy. Eventually, targeting ligands could be incorporated in order to increase the specificity of the system for disease targets such as cancerous tumours.

4.2.2 Development of Poly(ethylene oxide)-Poly(ester amide) Graft Copolymers for Micellar Drug Delivery Vehicles

Clinically used drugs should be encapsulated within micelles and their release properties investigated in order to determine behavior and the versatility of the nanocarrier system. Biological assays should be performed to determine the cell uptake, intracellular localization, and toxicities of these systems, while *in vivo* studies will reveal their therapeutic potential. In the longer term, the addition of targeting groups to the terminus of the PEO chain may lead to improvements in the system's efficacy.

4.2.3 Combination of Projects

It is intended that aspects of the two delivery systems be combined. For example, drugs can be covalently bound to the interior of a micelle, where they will be well protected from the *in vivo* environment but will still degrade in a sustained release fashion. The projects were kept separate in this thesis in order to develop the methods and to elucidate the properties of each system, but in the future it should be possible to combine the developed methods to attain the best properties of each system.

4.3 References

(1) Guo, K.; Chu, C. C. *J. Biomed. Mater. Res. B Appl. Biomater.* **2009**, *89B*, 491.

(2) Vera, M.; Puiggali, J.; Coudane, J. *J. Microencapsulation* **2006**, *23*, 686.

(3) Guo, K.; Chu, C. C. *J. Biomater. Sci., Polym. Ed.* **2007**, *18*, 489.

(4) Huang, X.; Brazel, C. S. *J. Controlled Release* **2001**, *73*, 121.

(5) Rizi, K.; Green, R. J.; Khutoryanskaya, O.; Donaldson, M.; Williams, A. C. *J. Pharm. Pharmacol.* **2011**, *63*, 1141.

(6) Wei, Y.; Wang, Y.; Wang, L.; Hao, D.; Ma, G. *COLLOID SURFACE B* **2011**, *87*, 399.